

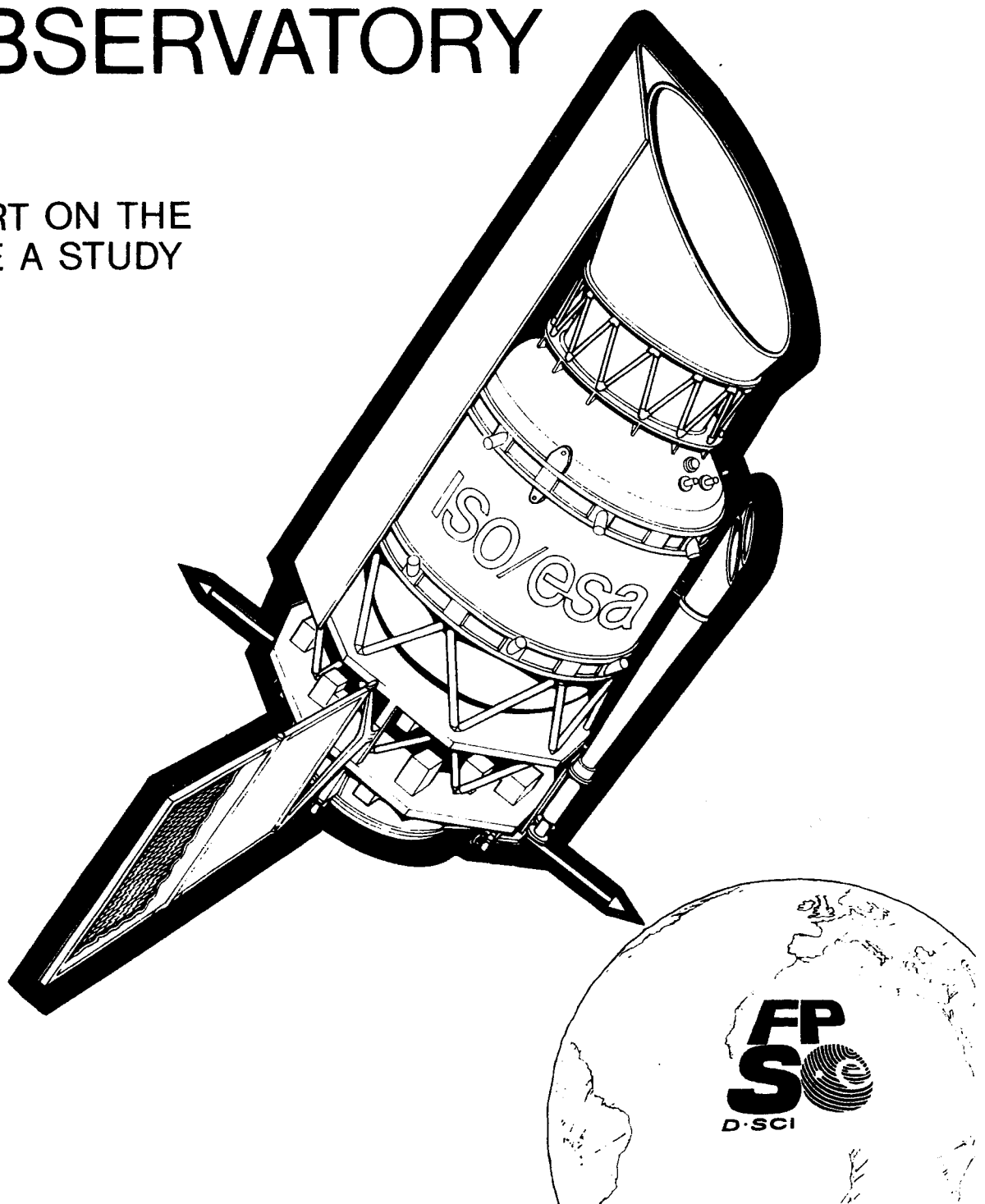


european space agency

SCI (82)6
November 1982

INFRARED SPACE OBSERVATORY

REPORT ON THE
PHASE A STUDY



Foreword

A proposal for an Infrared Space Observatory (ISO) was submitted to ESA in response to an announcement of a new planning cycle issued in November 1978.

The original proposal, made by Van Duinen (NL), Courtin (F), Fitton (ESA), de Graauw (ESA), Harries (UK), Jennings (UK), Künzi (CH), Magun (CH), Moorwood (ESO), Salinari (I) and Wrixon (Eire), called for a 1 m cryogenically cooled telescope containing focal plane instruments for infrared and sub-millimeter heterodyne astronomy and, possibly, atmospheric research. After evaluation of all the proposals received in response to the above-mentioned announcement, the Astronomy Working Group (AWG) recommended this proposal for an assessment study. This recommendation was subsequently endorsed by the Science Advisory Committee (SAC).

In November 1979, the assessment study of the mission (reported in document SCI(79)6) was presented to the scientific community. Subsequently, the AWG and SAC recommended this mission for further study and, in particular, demonstration of the feasibility of a cryogenic system for long-operation flights. The results of this pre-phase A study were presented at a Workshop held at ESTEC on 28-29 May 1980 and in a report issued in November 1980 (Document SCI(80)9).

This led to the recommendation of a Phase A study for ISO, which was confirmed by the SPC in November 1980. Following further industrial supportive studies relating to cryogenics, the industrial Phase A was started in September 1981 and completed at the end of October 1982. During this study, as in the earlier work, ESA was supported by a Science Working Team (SWT).

The present document summarises the results of the scientific and technical Phase A study activities. The scientific part of this document was prepared by the SWT working in close collaboration with the Study Scientist from Space Science Department, ESTEC. The technical part was prepared by the Future Projects Study Office, ESTEC with the support of specialists from the Directorate of Operations and the Technical Directorate.

The members of the SWT were:

Dr. W. Aalders/Dr. J. Wijnbergen, University of Groningen (NL)
 Dr. R. D. Joseph, University of London (GB)
 Dr. R. Katterloher, MPI Garching (D)
 Dr. D. Lemke, MPI Heidelberg (D)
 Dr. L. Nordh/Dr G. Olofsson, Stockholm Observatory (S)
 Dr. P. Salinari, Obs. Astro. de Arcetri (I)
 Dr. F. Sibille, Observatoire de Lyon (F)

Later in the study, SWT support was given by Prof. C B Cosmovici, DFVLR (D), Dr. C. Cesarsky and Dr M Gorisse, CEN-Saclay (F). Valuable contributions and comments on the Science Objectives were also given by:

Dr. S. Drapatz, MPI Garching (D)
 Dr. A. Moorwood, ESO, Garching (D)
 Dr. L. Woltjer, ESO, Garching (D)
 Dr. G. Gahm, Stockholm Observatory (S)
 Prof. I. Appenzeller, Landessternwarte, Heidelberg (D)
 Prof. P. Mezger, MPI Bonn (D)
 Prof. M. Longair, ROE Scotland (GB)
 Prof. P. Encrenaz, Observatoire de Meudon (F)
 Dr. H. Habing/Dr. G. Miley/Dr. L. Allamandola, Sterrewacht Leiden (NL)
 Dr. Th. Encrenaz, Observatoire de Meudon (F)

The ESA personnel from the Directorate of Science who were responsible for the study were:

R. J. Emery Study Scientist, Space Science Department
 C. Burgio Study Manager, Future Projects Study Office

The industrial Phase A of this mission was carried out by MBB, Ottobrunn in the period between October 1981 and November 1982 with the support of the following sub-contractors:

- Optical subsystem : Carl Zeiss (D)
- Cryogenic subsystem: Linde (D)
- Attitude and orbit control subsystem; solar arrays: Fokker (NL)
- Power subsystem: Etca (B)
- Data handling and telecommunication subsystems: Selenia (I)
- Cost and schedule analyses: Aerospatiale (F)

Requests for further information or for additional copies of this report may be made either of the above at the following addresses:

R J Emery	C Burgio
Space Science Department	Future Projects Study Office
Scientific Programme Directorate	Scientific Programme Directorate
ESTEC, Postbus 299	ESTEC, Postbus 299
2200 AG Noordwijk	2200 AG Noordwijk
The Netherlands	The Netherlands

or to the secretary of the Astronomy Working Group:

Dr H Olthof
 Scientific Programme Directorate
 European Space Agency
 8-10, rue Mario Nikis
 75738 Paris Cédex 15
 France

I S OTable of contents

	<u>Page</u>
Foreword	
1. <u>SUMMARY</u>	1
2. <u>INSTRUMENTAL BACKGROUND</u>	5
2.1 Present Facilities	5
2.2 Capabilities of a cooled telescope in space	7
3. <u>MISSION TIMING</u>	9
4. <u>SCIENTIFIC OBJECTIVES</u>	10
4.1 Planets, Asteroids and Comets	10
4.2 Stellar Studies	13
4.3 Interstellar matter	18
4.4 Galaxies	24
4.5 Cosmology	30
5. <u>SCIENCE REQUIREMENTS ON THE TELESCOPE FACILITY</u>	33
5.1 Mission lifetime	33
5.2 Observational modes	33
5.3 Optics temperature	33
5.4 Telescope size	34
5.5 Operating wavelength range	34
5.6 Orbit/Integration time	34
5.7 Telescope pointing accuracy and stability	34
5.8 Telescope baffling	35
5.9 Sky cover	35
6. <u>THE INSTRUMENT PAYLOAD</u>	36
6.1 Selection of a model instrument payload	36
6.2 Michelson interferometers	38
6.3 Photometer	42
6.4 Near IR camera	44
6.5 Detectors	47
6.6 Model payload accommodation & interface requirements	48
7. <u>ISO SYSTEM DESIGN</u>	50
7.1 Design Philosophy	50
7.2 System Configuration Description	53
7.3 System Functional Description	61

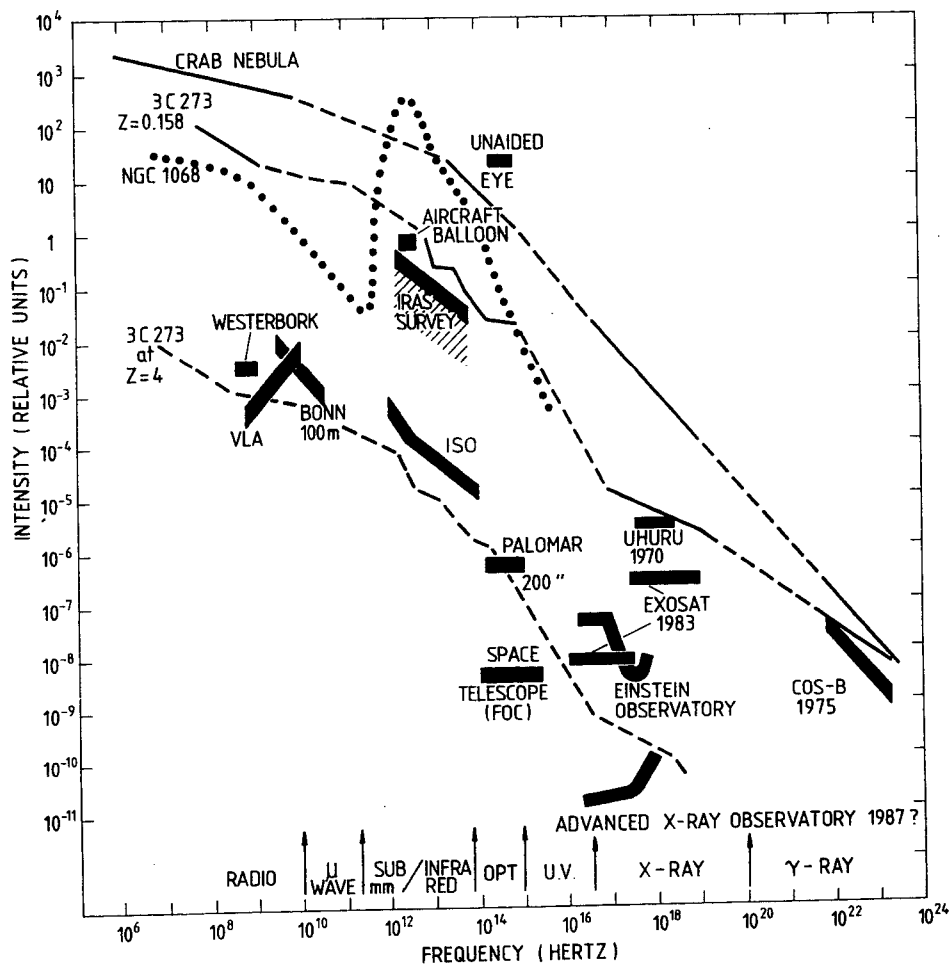
	<u>Page</u>
8. <u>LAUNCH and ORBIT ANALYSIS</u>	66
8.1 Orbit trade-off	66
8.2 Launch vehicle selection	66
8.3 ISO operational orbit	67
8.4 Launch window	67
8.5 Drift orbit	68
8.6 The sky Coverage	68
9. <u>SUBSYSTEM DESIGN and PERFORMANCE</u>	72
9.1 The structure subsystem	72
9.2 The thermal control subsystem	74
9.3 Attitude/Orbit control and measurement subsystem	82
9.4 Optical subsystem	90
9.5 The electrical subsystem	97
9.6 The on-board data handling subsystem	99
9.7 Telecommunication subsystems	101
10. <u>SYSTEM BUDGETS and PERFORMANCES</u>	102
10.1 ISO system budgets	102
10.2 ISO facility performance summary	105
10.3 System margins and confidence in the design	105
11. <u>SPECIAL ASPECTS</u>	108
11.1 Contamination	108
11.2 Safety considerations	109
11.3 Particle radiation	109
11.4 New developments	110
12. <u>ISO OPERATIONS</u>	111
12.1 Pre-Launch activities	111
12.2 Launch and early orbit phase	111
12.3 On-orbit operations	115
13. <u>MANAGEMENT</u>	120
13.1 Procurement policy	120
13.2 Scientific management	120
13.3 The verification approach	121
13.4 The ISO programme planning	121

1. Summary

The enormous wealth of astronomy awaiting the development of a high sensitivity infrared observatory can be judged from the major contributions that infrared astronomy has already made with very limited performance. These include observations on all scales ranging from extragalactic systems, galactic structure, molecular clouds and star formation regions, down to stars and studies of planets and comets. These contributions have been made despite the severe limitations imposed on observations by atmospheric effects and the thermal emission from uncooled optical systems. In order to reduce these limitations, infrared telescopes have been used on board aircraft and balloons, but these measures have only partially alleviated the problem. Improvements in infrared detectors lead now to a situation where only by cooling a telescope to around 20 K and placing it outside the Earth's atmosphere can the technological advantages be fully exploited. This will provide an increase in sensitivity of several orders of magnitude, bringing infrared observations roughly to the level of sensitivity achievable at most other wavelengths.

The present gap in sensitivity covering infrared/submillimetre wavelengths is demonstrated in figure 1.01, where comparison is made with facilities available for observing over the electromagnetic spectrum. Shown also are the equivalent spectra, either known or expected, of a number of important astronomical objects.

Figure 1.01 - Sensitivities for astronomical observations



The 1980's will see IR astronomy step across the atmospheric barrier with a number of infrared space missions, and the impact of that transition will doubtless be of the same order as was made when UV and X-ray astronomy took that same step. A photometric survey of the IR sky in 4 wavelength bands will be carried out by the US-UK-NL Infrared Astronomy Satellite (IRAS) to be launched early in 1983. The Spacelab 2 mission will contain a small liquid helium cooled telescope to study Galactic regions at low spatial resolution. The development of infrared technology has continued in Europe with the German Infrared Laboratory (GIRL) which will perform photometric and spectroscopic studies from Spacelab. This presents the timely opportunity for the Infrared Space Observatory (ISO) to follow up these measurements with an observatory range of infrared instruments, including high resolution spectrometers. The orbit proposed for ISO will allow integration times of hours to achieve the highest level of sensitivity for selected small regions of sky. The planned ISO mission lifetime of 1½ years will enable it to be used for the study of a whole range of astrophysical objects at an unequalled sensitivity.

ISO consists of a cooled 0.6m diameter telescope in a 3-axis stabilised spacecraft. The telescope and scientific instruments are cooled by a dual cryogen system involving liquid helium and liquid hydrogen. Studies have shown that the proposed system can provide a 1½ year lifetime with generous margins. The cryostat initially contains 100 kg of superfluid helium to provide a range of temperatures down to 3K, and 50kg of liquid hydrogen to provide the bulk of the total cooling which is required for the cryostat vapour cooled shields. A number of instruments can be accommodated, consistent with the concept of an infrared astronomy observatory. For this phase A study, a model instrument payload represents a selection from a range of possible instruments to establish realistic mechanical, electrical and thermal interfaces and requirements. The model payload consists of a near infrared camera, two Michelson interferometers with spectral resolving powers up to 10^5 and a multi-band photometer, and is well matched to investigate the scientific objectives.

The IR/submillimetre wavelength range, identified in Figure 1.01 as falling well behind in the sensitivity of available observing facilities, covers about 10 octaves in wavelength. This large range cannot be covered optimally by a single facility, and so emphasis has been placed on the IR from consideration of the following points:

- . The scientific interest in this wavelength regime, which is particularly rich in molecular, atomic, ionic and solid state transitions, a study of which provides insight into a whole range of astrophysical phenomena.
- . To obtain very high sensitivity to continuum radiation over this wavelength range a cooled telescope with low background photoconductive detectors (covering $1\mu\text{m}$ to about $180\mu\text{m}$) is required. This arrangement allows for efficient observations over a wavelength range of 7.5 octaves, particularly for spectroscopic explorations using multiplexing spectrometers. The need to cool the telescope dictates a moderate sized telescope which will have good spatial resolution over the IR range. For some measurements, this telescope

system, used with other detectors, will have many advantages for operation out to much longer wavelengths but will be limited for spatial resolution and collecting area by the moderate telescope size. A facility optimised for the longer wavelengths would not be able to offer equivalent performance for IR measurements.

- . The recognition that, in the Space Telescope era, extragalactic studies are likely to have particular prominence. IR measurements with ISO offer a direct continuation of these studies to longer wavelengths.

The situation now is that a space infrared telescope cooled to $T \sim 20K$ and coupled to modern photoconductor detectors will give a sensitivity which is approaching the natural limit set by the zodiacal light background. This would, for example, mean that for the photometry of normal galaxies, the sensitivity would be comparable to that of existing optical photographic sky surveys. This enormous gain in sensitivity has occurred at the same time as the development of two dimensional detector arrays which will allow imaging at the same high sensitivity.

ISO is planned as an observatory open to the whole community, operating as far as possible in real-time, and is intended to be used in a similar way to IUE by astronomers with observing proposals which have been accepted by an ESA Selection Committee. It will differ from IUE in two respects. First, the scientific payload will be designed and built by national groups. Consequently, a period will be required not only for commissioning the spacecraft and instruments, but also to provide an immediate return to those groups who have contributed to this hardware development. Some PI group involvement in operations will also be essential during the remainder of the mission lifetime in order to ensure efficient operation of the instrument and will require a concomitant assignment of observing time. The second difference from IUE is the use of a 12 hour orbit requiring two ground stations, a prime and a slave station.

Of the many possible scientific areas where ISO will have an important impact, the field of extragalactic astronomy is expected to be one of particular importance. Estimates of the number of IR excess galaxies to be detected by IRAS suggest a figure of at least 2,000. Detailed observation by ISO of a selection of these, particularly involving spectroscopy of the brighter galaxies, will enormously enhance the astrophysical information derived from these detections. The fact that ISO will be able to integrate on weak sources for hours means that it will in practice achieve considerably improved sensitivity, and hence see much further. This will be particularly valuable to such extragalactic observations. The mapping, classification, total luminosity and continuum energy distribution measurements of galaxies will be basic ISO photometric measurements, as will studies of time variations in active galaxies. In the near infrared, spectroscopic observations of the CO and H₂O bands can give information on stellar populations in galaxies (and possibly QSO's) and provide evidence of evolution as a function of redshift. Apart from these basic observations, more speculative studies are likely, such as the presence of cool low mass stars in haloes around galaxies.

ISO should make significant contributions to cosmology. It may be possible to define infrared galaxies as standard candles for calibrating the distance scale of the Universe. Study of the evolution of infrared properties of galaxies may help to resolve whether the Universe is open or closed. The high sensitivity of ISO will permit deep searches for galaxies forming out of the primeval fluid.

Studies of star formation processes in our own galaxy and in other nearby galaxies are likely to be very productive. The energy balance of molecular clouds and the shape of the mass spectrum of stars can be investigated on the basis of IR photometric observations. The processes that trigger star formation, and the role played by density waves, are best studied by detailed IR photometric mapping of nearby galaxies. Near-infrared spectroscopy will provide information on the gas dynamics of star forming regions allowing the study of collapse, fragmentation and shock fronts. Analysis of recombination lines and forbidden fine-structure lines of the ionised gas in HII regions, ranging from ultra-compact to well-developed, will result in the determination of the ionising fluxes of massive stars, of chemical abundances in the gas and of chemical abundance gradients in our own galaxy and other nearby galaxies. Spectroscopic studies of more evolved objects, ranging from cool giant stars and planetary nebulae to globular clusters, will contribute significantly to our knowledge of the chemical abundances and the dynamical evolution of these objects.

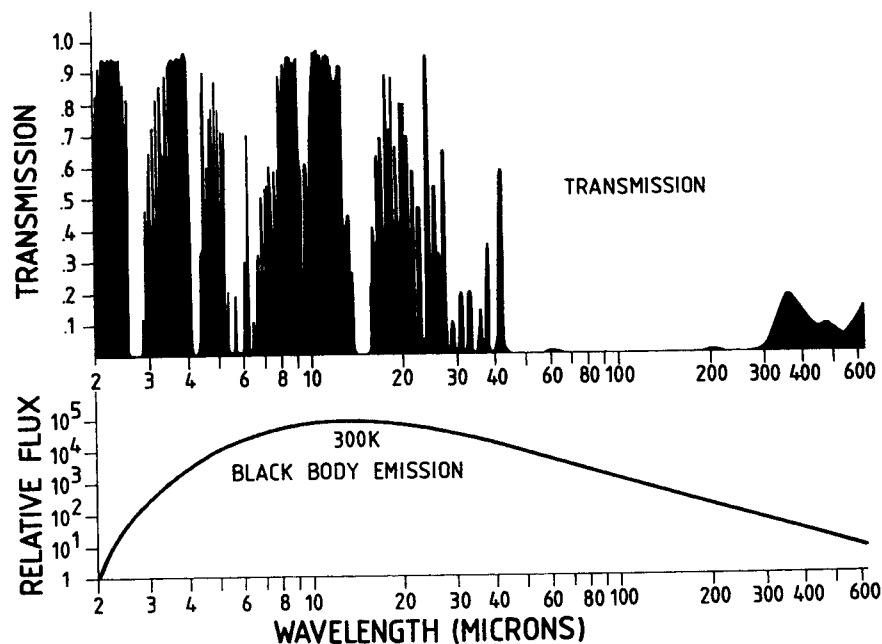
ISO will be offering high sensitivity observing facilities for a large region of the electromagnetic spectrum which is relatively unexplored for astronomy. It can be expected that proposals from the science community for its use will cover a very wide range of subject areas relating to almost all aspects of astronomy. The operation of ISO as an observatory, together with the wide range performance possible for the payload instruments when used with a cooled telescope, is well matched to this situation.

2. Instrumental Background

2.1 Present facilities

The atmosphere of the earth is opaque through most of the ten octaves of the infrared electromagnetic spectrum from 1 μ to 1mm wavelength, as seen in Figure 2.1.1. There are several narrow "windows" of varying degrees of transparency at the shorter wavelengths, but in general atmosphere absorption and emission place very severe constraints on both the wavelength range and the sensitivity of ground based IR astronomy measurements. At airplane and balloon altitudes the atmospheric transmission is improved, allowing a greater wavelength coverage. Observations are, however, still limited by the remnant atmosphere, since the dominant noise source arises from the large fluctuations in its thermal emission. Consequently it is not possible to take full advantage of the new generation of very high sensitivity IR photoconductor detectors which are available for wavelengths less than $\sim 180\mu\text{m}$.

Figure 2.1.1 - Atmospheric absorption and 300K emission



Apart from the atmospheric absorption problem, thermal emission of the atmosphere, warm optics and instrument imposes a fundamental sensitivity limit on the detector. As an example, Figure 2.1.2 shows the value of this limit, in terms of noise equivalent power (NEP), for a diffraction limited observation using optics at the various temperatures noted, plotted against wavelength. The spectral bandwidth is 10% and the total effective emissivity is taken as 4%. This shows the factor of around 100 improvement in NEP which may be gained by cooling the telescope when in the space environment. The performance of aircraft IR observations is shown in figure 1.0.1. Figures 2.2.2 and 2.2.3 include the limiting sensitivities of various facilities such as a large telescope at a high mountain site, at those wavelengths where there is an atmospheric window.

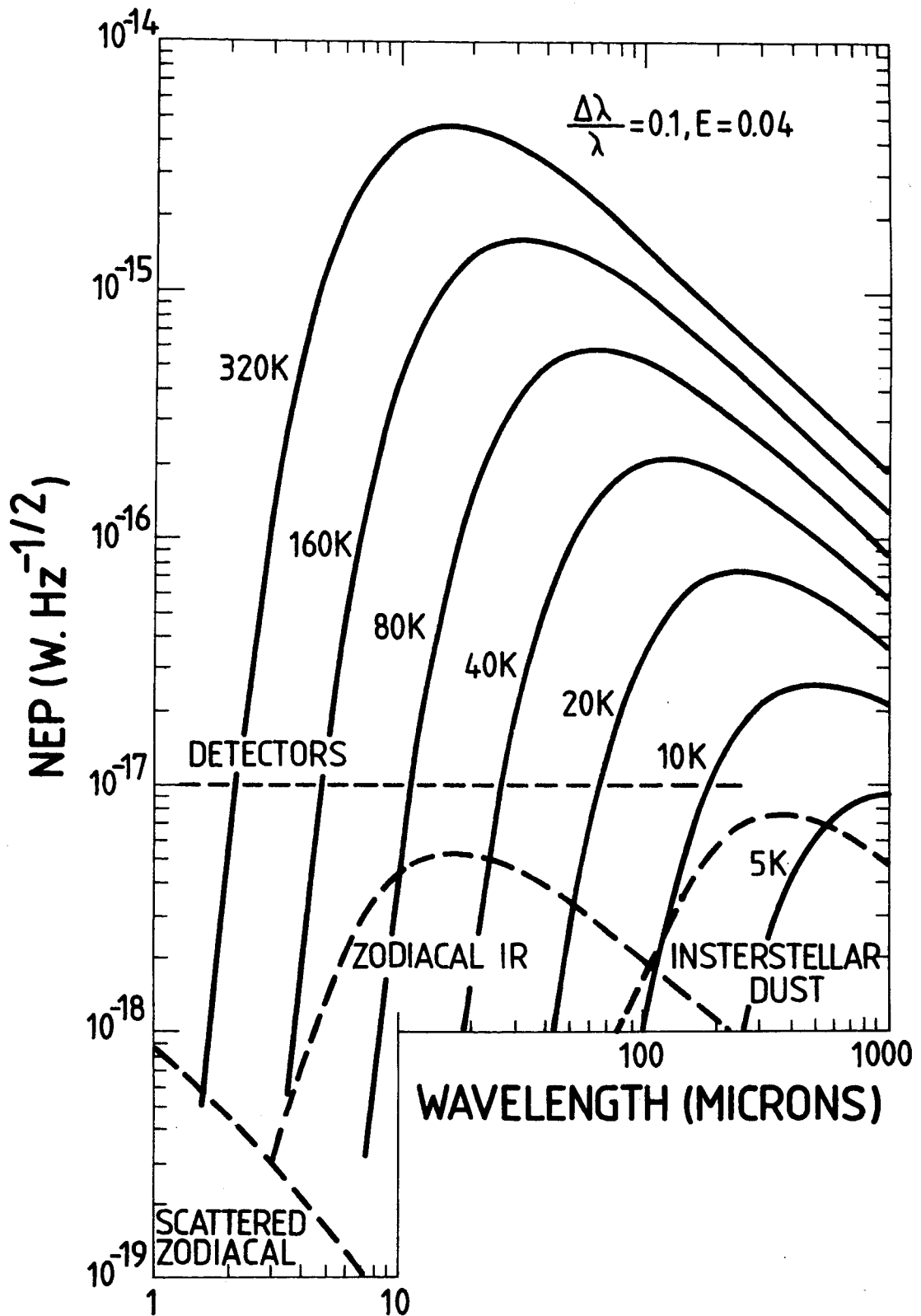


Figure 2.1.2 - Sensitivity limits due to thermal background of a telescope operated at its diffraction limit

Note - NEP is a parameter used to give the sensitivity of an IR detector, being the signal power required on the detector to give unit signal-noise with one second integration time.

2.2 Capabilities of a cooled telescope in space

Figure 2.1.2 shows the sensitivity limit of an IR telescope due to the background radiation on the detector. Zodiacal emission, scattered solar radiation and the emission of interstellar dust establish a natural low limit which varies considerably over the wavelength range. The objective in this study is to provide a telescope facility which approaches this natural limit by reducing the photon background to a level equivalent to a detector NEP of $1 \times 10^{-17} \text{ W Hz}^{-\frac{1}{2}}$. Figure 2.1.2 shows that a temperature of around 10K is required to achieve this for wavelengths out to around $200 \mu\text{m}$, the present limits of low background photoconductive detector technology.

The sensitivity improvement in using a cooled telescope in space, varies considerably with the observation wavelength, the bandpass of the instrument and the field of view. Figure 2.2.1 shows the integration time required by a one metre warm telescope (balloon-borne) to achieve various flux levels at $80 \mu\text{m}$ wavelength, compared with a cold telescope. Atmospheric absorption or fluctuations are ignored, so the warm telescope should really be considered to be in space.

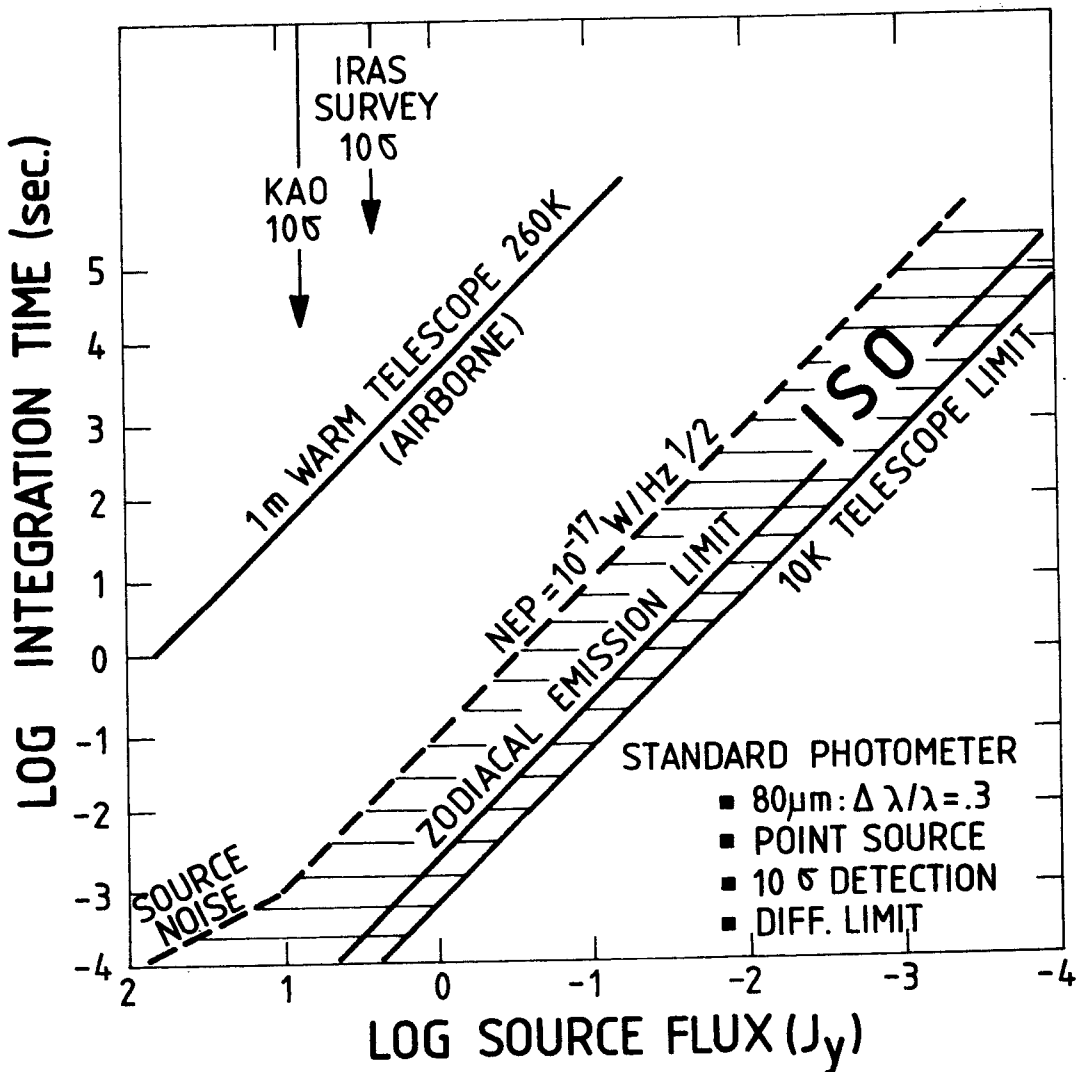


Figure 2.2.1 - Sensitivity of a cooled 60cm diameter telescope in space

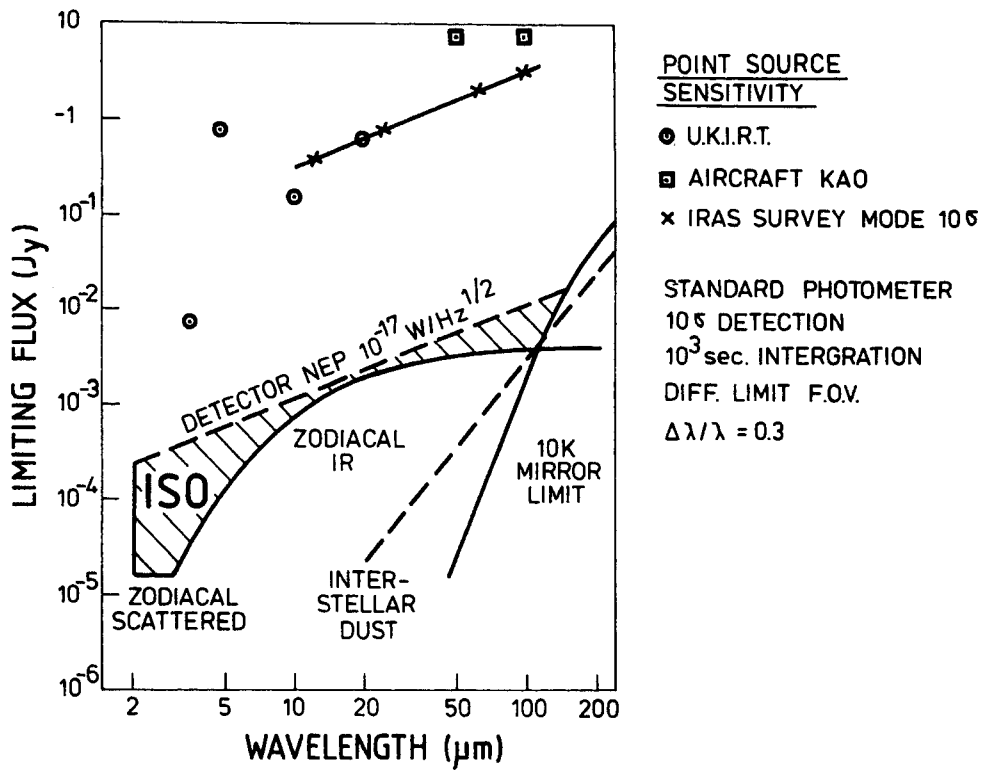


Figure 2.2.2 - Sensitivity of a cooled telescope to point sources

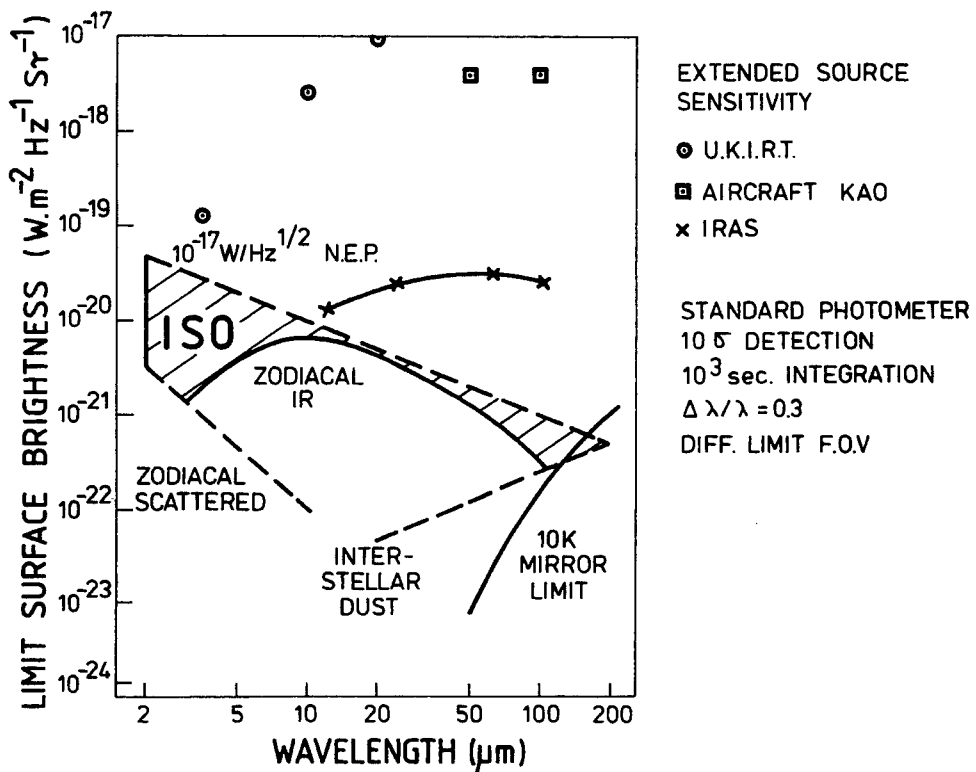


Figure 2.2.3 - Sensitivity of a cooled telescope to surface brightness measurements (Note - the IRAS FOV is about 10 x the diffraction limit)

3. Mission Timing

While the breakthrough achievable in sensitivity establishes the technical advantages of an infrared space observatory, the timeliness of such a mission is also very important. In the past few years, infrared astronomy has proven its scientific potential in many fields in astrophysics. Many of these achievements have been obtained through the deployment of rather modest instruments in aircraft and balloon gondola. Early in 1983, the first infrared space mission IRAS will be launched, which is of an exploratory nature. For the first time the full potential of cryogenic telescopes in space will be applied to observations in the infrared. The next step which is needed in the development of infrared astronomy is an observatory type space mission: ISO. The science objectives outlined in Section 4 show something of the broad range of observation and astrophysics which are likely to be accomplished by ISO. Technically, infrared astronomy has also reached a level of development that warrants investment in such a mission. The recent improvements in IR detectors by two orders of magnitude in sensitivity, supported by developments in cryogenic technology for space, lead to a performance for ISO which is nearly equal to the fundamental limit set by the photon shot noise from zodiacal emission. Similarly, considerable experience has been gained in applicable infrared photometric and spectroscopic instrumentation, a particularly relevant technique being that of Fourier Transform spectroscopy.

The timing of an infrared space observatory mission in the 1980's is also ideal in the context of space astronomy in general. With the launch of IRAS providing the first high sensitivity infrared all-sky survey, the next infrared space mission needed will be one to follow up with a detailed study of the host of new objects discovered. Clearly, it should have a sensitivity and angular resolution, at least equal to IRAS and it must also be provided with a complement of instrumentation designed for these more refined studies. ISO is designed to meet these requirements. Two other space infrared projects are in the planning, SIRTf (USA), or development, GIRL (Germany), phase. Using a cryogenic telescope of a size similar to that of ISO, they will be flown on Spacelab for limited flight durations of 7 to 30 days. The 1½ year mission of ISO has the enormous advantage that it will allow adequate time and an improved environment to fully utilise the gains that a cooled telescope in space offers to observations in this wavelength range. (GIRL) is an important precursor to an IR observatory, particularly for the preceding development and experience in many areas of space cryogenic technology and instrumentation. The timing of the proposed ISO mission, its duration and the observatory concept have each been established with due consideration of the Space Telescope era. The ST observations will undoubtedly have a significant bias towards extragalactic objects. Spectroscopic observations by ISO of highly red-shifted objects at near infrared wavelengths and high sensitivity photometry at longer wavelengths are foreseen as important complementary measurements to the ST observations.

4. Scientific Objectives

Infrared astronomy has made a major impact on the study of extragalactic objects and to our ability to observe the elusive locations of star formation in the galaxy. Yet these discoveries have been made with infrared astronomy still confined to the use of modest instruments on aircraft, balloon gondolas and ground-based telescopes, all suffering from the presence of the atmosphere. The step into space, permitting the use of cooled telescopes of unprecedented sensitivity, will no doubt give rise to the observations of a whole range of new phenomena. In what follows, the main emphasis will be on those areas of infrared astronomy that have already proven to be extremely fruitful. We have avoided extensive speculation about new classes of objects and phenomena that may very well be within the horizon of the extremely sensitive cooled space infrared telescopes.

4.1 Planets, Asteroids and Comets

Among the various objects of the Solar System, the giant planets, the asteroids and the comets are of special interest since they are expected to be witnesses, partly or completely, of the physical and chemical conditions of the Primordial Solar Nebula. The small bodies, asteroids and comets, have encountered little or no evolution since their origin, due to their small sizes and low temperature; the giant planets have kept most of their original reducing atmosphere, basically composed of hydrogen and helium with traces of other elements in a reduced form (CH_4 , NH_3 , H_2O etc). The determination of elemental and isotopic ratios (H/He , D/H , C/H , $^{12}\text{C}/^{13}\text{C}$) is a basic tool in cosmogonical and cosmological studies. The infrared range is well suited to studying these objects since the planets, asteroids and comets are cold, and therefore radiate most of their energy in the infrared. Moreover, all the molecular species which may be formed on these objects have spectral signatures (rotation or vibration-rotation transitions) between $1\mu\text{m}$ and 1mm . For these reasons, understanding of the chemical composition of the giant planets has benefited enormously from the development of IR astronomy; a dozen molecules have been identified on Jupiter since 1970, mostly from IR observations, while before that date only three molecules (H_2 , CH_4 and NH_3) had been definitely detected.

Up to now, however, the IR study of the giant planets has been limited either by the spectral resolution or the sensitivity of the airborne or space experiments. For instance, the Voyager IRIS observations of Jupiter, Saturn and Titan, which made many exciting new discoveries, were still limited to a spectral resolution of 4.3 cm^{-1} . In the case of Uranus and Neptune, only broadband or low resolution measurements exist from ground-based or airborne experiments in the infrared. For asteroids, very little is known about their spectrum above $5\mu\text{m}$ and in the case of comets, only few measurements exist from ground-based IR experiments. Clearly these studies would benefit enormously from both the high spectral resolution and very high sensitivity of an infrared instrument operating outside the Earth's atmosphere.

4.1.1 Jupiter and Saturn

The remarkable results obtained by the Voyager IRIS experiment on Jupiter and Saturn have firmly underlined the value of infrared observations. Since we know now that organic and prebiotic molecules can be found in the atmospheres of the giant planets, the need to observe them at high spectral resolution is established. The discovery of HCN on Jupiter illustrates this need when the constituent is present in only small amounts. Among the possible candidates on Jupiter and Saturn we find H_2S , HF, H_2CO , CH_3CN , AsH_3 , C_3H_4 , C_2H_4 and CH_3NH_2 . Obviously such an observation has to be made from outside the Earth's atmosphere, and a Fourier Transform Spectrometer (FTS) on ISO would be an ideal instrument since it has the required spectral range, spectral resolution and sensitivity.

4.1.2 Uranus and Neptune

Due to their large distance from the Earth, Uranus and Neptune are still poorly known in terms of atmospheric composition. This situation will be improved with Voyager's fly-by (1986 for Uranus and 1989 for Neptune). However, apart from H_2/He , there is little hope in obtaining the same information as on Jupiter and Saturn (C/H, D/H, P/H, $^{12}\text{C}/^{13}\text{C}$).

Again, an FTS on ISO would be very well adapted to a study of Uranus and Neptune in the IR bands of CH_4 (7.7 μm) and CH_3D (8.5 μm) from which the C/H and D/H ratios can be derived. Using the high sensitivity of ISO the same type of study performed with IRIS on Jupiter and Saturn, could be performed on Uranus and Neptune, with the advantage of a much higher spectral resolution. It should be noted that for these abundance ratio determinations, as well as for the search for minor species on Jupiter and Saturn, the lack of spatial resolution is not a critical factor (apart from the dilution factor on Uranus and Neptune). Molecules such as H_2 , He, CH_4 , CH_3D , $^{13}\text{CH}_4$, are expected to be uniformly spread over the planetary disk.

4.1.3 Titan

Since the recent discovery of complex molecules in its atmosphere (C_3H_4 , C_3H_8 , HCN, C_2N_2 , HC_3N) Titan has become one of the most fascinating objects of the Solar System. Indeed, the presence of both a solid (or liquid) surface and a reducing atmosphere could lead to the early states of life development on Titan. Thus, the search for new complex molecules on Titan is of particular importance, and the results obtained with the Voyager IRIS at medium resolution are a good indication of the scientific value to be derived from measurements at much higher spectral resolution. Again, ISO's FTS has the spectral range, sensitivity and the spectral resolution for detecting minor species; possible candidates include CH_3OH , CH_3NH_2 , $\text{C}_2\text{H}_5\text{OH}$, CH_3CN , H_2CO , which all exhibit strong vibration-rotation transitions between 3 and 15 μm .

4.1.4 Asteroids

Because of their small size and low temperature, asteroids are difficult to observe and poorly understood. However, these two factors - small size and low temperature - are their most interesting aspects because in most cases they prevent differentiation and therefore keep the asteroids close to their initial conditions. The 1-5 μ m spectrum of asteroids is specially interesting for a determination of their surface composition. Some ground-based data exists for the largest asteroids and a 1-5 μ m camera array aboard ISO could substantially improve this data by extending the spectral range into the regions of earth-atmospheric opacity and by increasing the number of samples. Broad-band photometry longward of 10 μ m permits a determination of diameters and albedo. ISO could make such measurements for a large number of asteroids.

4.1.5 Comets

Comets are known to be the most primitive objects of the Solar System. As in the case of asteroids, our knowledge of these objects is still very poor. The determination of their chemical composition would be of outstanding importance for the study of the chemical composition of the primordial nebula, as well as the study of the early stages of accretion processes. Up to now, we know some of the secondary products of comets (radicals and ionized species) but no parent molecules have been firmly identified.

The infrared appears specially useful for observing cometary parent molecules. The 2-20 μ m range is rich in spectral signatures of almost all the possible candidates and it is also the range of maximum emission when the comet approaches the sun at a distance of about 1 AU. Calculations show that parent molecules are expected to be very difficult to observe from the Earth. However, in some cases, due to the peculiar distributions within the energy levels expected in comets (very different from the Boltzmann distribution), some discrete transitions may become observable. For such an observation, a high spectral resolution is required. Possible candidates are H₂O (2.7 μ m, 6.2 μ m), CO (4.5 μ m), CO₂ (4 μ m), CH₄ (3.3 μ m, 7.7 μ m), NH₃ (10.5 μ m), N₂H₄ (10-12 μ m) and OH (3 μ m). An FTS on ISO, with its spectral range, spectral resolution and sensitivity could perform this experiment. Its field of view is also very well adapted, since a 1 arc min FOV corresponds to the diameter of the inner coma (40,000 km) where parent molecules are expected to be found.

4.2 Stellar Studies

Infrared observations are particularly relevant for elucidating the physics and nature of cooler stars, those stars that are heavily obscured by dust and star formation regions. IRAS will detect a very large number of such objects, but for only a small fraction of these will it be possible to determine fundamental details such as their evolutionary stage. ISO will have the capability to do this, and so can provide a detailed follow-up of these earlier detections.

4.2.1 Star Formation

Although the subject of star formation has been of considerable theoretical interest for many years, it is only since the relatively recent advent of radio and infrared astronomies that a substantial body of observations could be assembled to confront theoretical ideas. As a result, a host of new and fundamental questions have appeared, and concurrently, we have also become aware of a variety of fascinating new astronomical objects, such as molecular clouds, maser sources and cocoon stars. Infrared observations have already proved to be extremely powerful in the study of these dense complexes of dust and gas, and observations using ISO can play a central role in enlarging our understanding of the many facets of astrophysics associated with star-forming regions.

Observations so far available suggest that star formation takes place almost exclusively in molecular clouds where the gas density is sufficiently high and the temperature is sufficiently low to allow the gravitational collapse of stellar mass portions. The details of this process are, however, still poorly understood. For instance, the mass spectrum of stars at birth is virtually unknown. Do stars of all masses form simultaneously? Alternatively, are low-mass stars formed continuously in a quiescent way in molecular clouds, while massive stars are created only occasionally, possibly triggered by compression of the cloud? If so, what are the compression mechanisms and their relative importance? Are spiral density waves the only way to induce star formation or do shock fronts from expanding H II regions or supernova explosions also play an important role? To study these questions, infrared photometric mapping of molecular clouds is needed. This requires rapid - and therefore very sensitive - source detection so that areas typically of about 100 square arc minutes may be mapped reasonably quickly with diffraction-limited angular resolution.

Sensitive broad-band photometry of star formation regions will provide information on the overall energetics of molecular clouds and will allow identification of the most luminous newly formed stars and their contribution to the total heating of the clouds. Because heavy stars produce much more luminosity per unit mass than low-mass stars (lex M⁴) the energetics of molecular clouds is dominated by stars larger than 10 solar masses, in spite of the fact that many more lower mass stars are born simultaneously. The mass spectrum of stars at birth can be studied with the near-IR camera which, due to its good spatial resolution, allows the observation of the spatial distribution of less luminous stars (clusters) in the range 1 to 10 solar masses in nearby molecular clouds.

Operating at high spectral resolution, an FTS on ISO is very well suited to observe and map strong lines in distant molecular clouds with embedded OB stars, and to detect weak lines in the nearest clouds. The excitation state of the cloud can be determined from the emission lines observed and their relative strength, as well as from the distribution and temperature of the associated dust.

4.2.2 Early Stages of Stellar Development

When newly formed massive stars or protostars are still embedded in their dust cocoons, observations of near-IR hydrogen recombination lines (Brackett and Pfund series) allow a determination of the electron density and the size of the ultracompact H II region inside the cocoon. The extinction in the cocoon can be derived from the line ratios. The circumstellar molecular gas can also be probed by observing near-IR vibration-rotation lines in absorption against the protostellar continuum. Lines of CO have been observed in this way. The motion, expansion or inflow of the gas can be determined from the observed radial velocities. Such observations are the only reliable way of identifying bright low radio-flux IR sources as massive protostars (which have inflowing envelopes) or as heavily obscured newly formed O-stars (which have expanding envelopes). From the determination of vibrational and rotational temperatures, conclusions can be drawn about the origin of the molecular excitation.

Young stars, of both high and low mass, are often associated with strong stellar winds having velocities in the range 10-200 km/s. These winds are evident through their interaction with the surrounding molecular cloud, causing velocity broadened and shock-heated emission lines. Such emission around 2 μ m wavelength from vibration-rotation lines of hot H₂ (T = 1000-2000K) has been observed. Highly excited pure rotational lines of H₂ and CO have also been detected at wavelengths in the range 5 to 150 μ m. Spectroscopic instruments with ISO will allow these winds, and the mechanisms causing them, to be studied in detail for a large number of objects. It may also be possible to observe hydrogen recombination lines from ionized parts of the wind. The question of the ionization mechanism can also be addressed. This is of special interest for some stars which display stellar winds but are of such low mass that their ultraviolet continuum may not be sufficiently strong for pure radiative ionization.

Observation shows that in many cases the stellar winds are bi-polar in structure. This has prompted the speculation that the stellar object is surrounded by a thick disc, and that the wind is preferentially blowing in directions perpendicular to the plane of the disc. Figure 4.2.1 shows a simple picture for such an object, together with a later stage when a "classical" ionized region has formed, but which is still embedded in the parent molecular cloud. Polarization measurements with ISO could be especially effective in probing these interesting regions. Herbig-Haro objects and cometary nebulae may also be manifestations of stellar winds from nearby young stars. Spectroscopy with ISO on the nebulosities and the surrounding, presumably shocked, cloud material could contribute directly to the understanding of these stars.

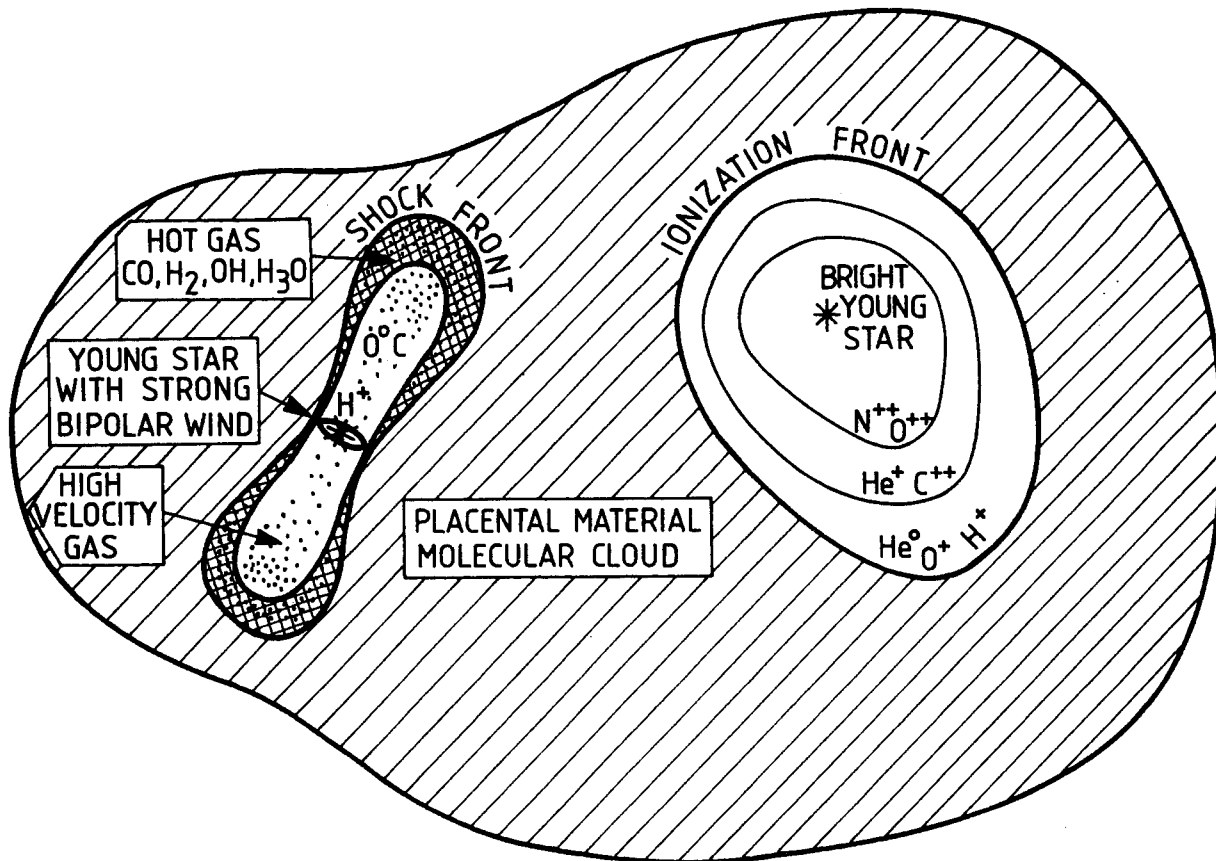


Figure 4.2.1 - Models for stages in the development of a new star

Many young stars of low mass are known to have a strong infrared excess. The general belief is that this excess comes from cold circumstellar material, presumably at large distances from the stars. Very recently, however, it was shown that the infrared excess of T Tauri is in fact almost entirely due to a cold companion, separated about 0.7 arcsec away. It is postulated that this cold companion may be a pre-solar nebula. A high sensitivity search for appropriate spectral signatures from dust and molecules at IR wavelengths would be extremely valuable for developing this study of T Tauri. ISO could also extend this search to other stars showing infrared excess. Generally these observations could be used to derive an age sequence for the youngest stars, and would greatly help our understanding of the formation of low mass stars like our sun.

4.2.3 Studies of obscured stars

There are many stars, which, in spite of high photospheric temperatures, cannot be observed at visible wavelengths due to obscuration by interstellar or circumstellar dust. Examples of such objects are protostars, cocoon stars, OH-IR sources, and heavily obscured members of young stellar clusters in the galactic plane or near the galactic centre. Some stars, like cool supergiants or even hot high-luminosity stars (like eta Car or the star R 66 in the LMC), produce dust in their outermost layers and may become obscured by their own ejected material. For all such objects, which are unobservable or strongly weakened at visible wavelengths, the best way to determine their physical nature is with high sensitivity infrared spectroscopy.

4.2.4 Cool Stars

Many of the infrared sources observable by ISO will be cool stars. From the theory of stellar structure, it is known that normal (non-degenerate) stars may have effective temperatures as low as about 2000 K. Such stars radiate mainly in the infrared and their spectra are dominated by molecular bands including H₂O, CO, H₂, OH, CN, HCN, C₂H₂, and other simple molecules of abundant atomic species. The most important of these molecular bands are found in the spectral range 1.6 μ m to 10 μ m. An analysis of these molecular spectral lines is the only reliable way of deriving the physical properties of the atmospheres and circumstellar envelopes of these very cool stars. In contrast to the spectral lines at visible wavelengths, these infrared features have the great advantage that they are formed under LTE conditions and the transition probabilities of many of these lines are relatively well known from laboratory and theoretical work. Also, in contrast to the visible spectrum, the IR spectral features can be used to study the very thin outermost layers of these cool stars. The high spectral resolution attainable with ISO will show line broadening and hence the velocity fields in the outer atmospheres and circumstellar envelopes. In the case of cool dwarf stars, we expect to obtain information on the transition layers to the chromosphere and corona of these objects. Studies of the infrared molecular lines will also prove particularly important for the determination of isotope ratios. These ratios provide the most direct information on the stellar evolution and the thermonuclear processes which were operating at earlier epochs in these stars.

Cool giant stars are known to be surrounded by dust shells. The position in the extended atmosphere or circumstellar envelope at which the observed dust is produced can be determined with the ISO infrared photometers. Low resolution spectroscopy will allow the chemical composition and geometrical proportions of the dust grains to be derived. Many cool giant and supergiant stars are variables. Time variations in the dust radiation could provide valuable information on the photometric phase most suitable for dust formation and thus on the details of the dust condensation process. In some cool giant stars the dust envelopes are so dense that no visible radiation can be detected (IR-OH sources). For these objects IR spectroscopy is the only means with which the physical parameters of the stellar surface layers can be defined. These totally obscured cool giants are known to be the immediate predecessors of the planetary nebulae and therefore a particularly interesting stage of stellar evolution.

Finally spectroscopic observations by ISO will be particularly useful for the detection and analysis of cool companions in binary systems where the visible light is dominated by a blue primary component.

4.2.5 Late Stages of Stellar Evolution

Probably all stars eject matter during a large fraction of their lifetime, but most prominently when they evolve away from the main sequence to the giant branch and during their red giant stage. The mass loss is gentle (flow velocities of 10 to 20 km s⁻¹) so that a dense circumstellar shell is formed. As the gas cools during the outflow, dust particles condense producing large continuum opacities at optical and

near-IR wavelengths. The lighter stars ($M \leq 4M_{\odot}$) continue to lose mass until they form a hot central core which ionises the circumstellar gas to produce a planetary nebula. More massive stars behave differently because their cores become unstable before they have shed most of their mass, resulting in a supernova. Stars in close-binary systems have a more complicated evolution because matter is being exchanged between the two stars. Novae are probably produced in this way.

Many of the infrared sources to be detected by ISO will be giant stars of late spectral type. This is because a substantial fraction of the total luminosity of these stars ($\sim 10^4 L_{\odot}$) is usually converted into infrared continuum radiation by dust particles in the circumstellar shell. Strong molecular absorption lines are also expected. Study of these lines with an FTS on ISO could provide insight into the kinematics of the expanding shell, the chemical processes and in particular the formation of dust particles in the shell. A better understanding of mass loss from late-type (super-) giant stars is of paramount importance because it recycles stellar material and thus is a significant factor in the evolution of our, as well as other, galaxies.

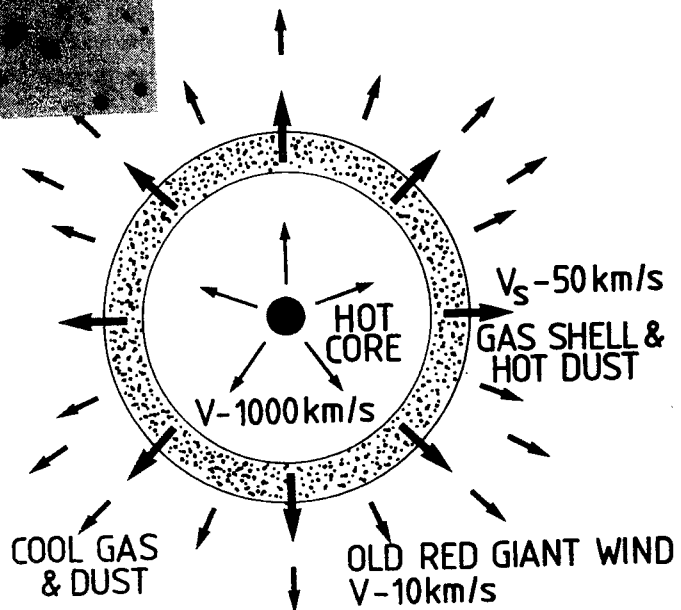
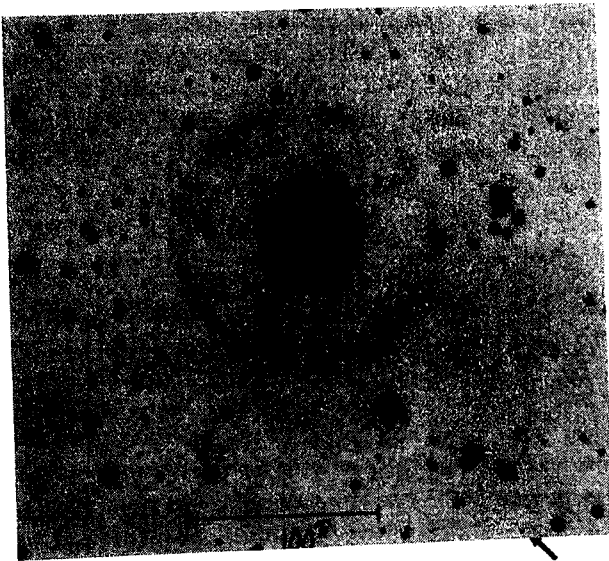


Figure 4.2.2 - Model of Planetary Nebula Formation and a picture of
NGC 6826

A special group of evolved objects are the Planetary Nebulae. The physical conditions in their ionised gas are similar to those in H II regions, but can involve higher excitation temperatures. The dust is hot, therefore the continuum IR spectrum peaks at near IR wavelengths. Giant halos surrounding several planetary nebulae have recently been found, see Figure 4.2.2. These contain several solar masses of matter deposited by stellar winds during their red giant phase. The total luminosity and dust mass of the planetaries, including these faint halos, could be derived from sensitive IR observations. These halos show that massive stars can lose several solar masses of matter by stellar winds. Therefore a better mass limit distinguishing between stars ending as supernovae or as planetary nebulae could result from measurements with ISO. The sensitivity of ISO will also enable a very large number of Planetary Nebulae to be studied. Particularly fruitful will be the study of Planetary Nebulae in the inner parts of the galaxy, because they can be used as test particles to probe the gravitational potential in the galactic centre. Like H II regions, Planetary Nebulae can also be used to study the galactic gradients of chemical abundances.

The oldest objects in the galaxy are the Globular Clusters whose infrared emission is dominated by late-type giants. The study of these objects with ISO to determine their sizes, their infrared light distributions and their dwarf-to-giant ratios (from the CO band), particularly in the galactic centre, will give information on the dynamical processes that ultimately destroy them.

4.3 Interstellar matter

The composition of the interstellar matter reflects the chemical processing that has taken place in the past, and sets the stage for the future developments. To obtain its chemical properties, a knowledge of the basic physical parameters such as temperature, density and radiation fields is needed. These are also of vital importance for a proper understanding of the interaction between stars and the interstellar medium, of the overall energetics of the interstellar medium and of the properties and implications of shocks. Only recently has it been fully realised that the interstellar matter exists in a number of different phases of widely different properties - cold molecular clouds, diffuse clouds of mostly neutral atoms, extended low-density ionized regions with temperatures typical of classical HII-regions and hot galactic clouds, or halos, that seem to reach coronal temperatures.

To be able to realistically describe the complex interstellar medium and to fully appreciate its impact on a number of issues that are central to current astronomical thinking, one needs novel and high-quality observations. As will be demonstrated below, the contribution to be expected from an infrared facility like ISO is a major step forward.

4.3.1 Neutral Clouds

It was only a few years ago that the presence of vast clouds of cold gas and dust, known as molecular clouds, was established. Subsequently it has been seen that these clouds form a large fraction of the total mass of our galaxy, and many others. Their importance has also been enhanced by the recognition of their role in the formation of new stars. The cold clouds have been shown to contain a wide range of molecules, and a substantial amount of work has been undertaken to model the cloud chemistry, particularly in relation to carbon.

High resolution infrared spectroscopy can effectively address questions concerning the heating, cooling and dynamics of the interstellar matter. The wavelengths of concern here are short enough to permit a reasonably high spatial resolution but still long enough to be essentially unaffected by interstellar extinction. As an example, the determination of the H/D ratio is of particular theoretical importance to astrophysics. The HD molecule is a very efficient cooling agent in dense molecular clouds, with temperatures in the range 50-150K, where it is in fact more important than H₂ as a coolant. Favourable conditions for the detection of the HD lines at 56.2 μ m and 37.7 μ m are found in the molecular clouds associated with the galactic centre and the 4-7 kpc molecular ring. Line emission from many other molecules residing in dense, cold molecular clouds under equilibrium conditions will probably be difficult to observe in the IR. However, observations of neutral carbon emission suggest that substantial non-equilibrium zones appropriate to IR observation can be created by mixing with material excited by radiation from an adjoining star formation region.

Observations of molecular line absorption can also be made against infrared background sources, providing a promising tool for a study of those molecules without strong transitions at microwave frequencies.

Recently, the importance and widespread occurrence of shocks within the interstellar medium caused by stellar winds, supernovae outbursts and cloud collision has been recognised. Considerable theoretical work has been devoted to a study of the energetics and chemistry of these different types of shocks. In most cases, it is found that the gas is effectively cooled by a few lines such as the [OI] line at 63.2 μ m, the rotation lines of H₂ between 28 μ m and 4 μ m and the vibration transitions of H₂ in the 2 μ m region. Observations of some of these lines exist for a handful of objects. In many shock situations, the chemistry and emission of molecules other than H₂ are important. Hot CO and OH have thus been observed from Orion with derived temperatures in the range 1000-2000K. With ISO it will be meaningful to try to observe lines from rotational levels with higher energies, and thereby sample gas with a temperature in excess of \sim 2000K. Molecular species other than CO and OH may also be important. Among the latter, H₂O plays a central role, but terrestrial absorption has so far made such observations impossible.

Closely related to shocks are ionization fronts caused by stellar winds. From such regions recombination lines from hydrogen can be observed in the near infrared as well as fine structure transitions

4.3.2 HII Regions

Most HII regions are intimately linked with molecular clouds, because they form as a result of ionisation of the gas around recently born O and B stars. The Orion nebula for example, although known and studied for many years at visible wavelengths, has turned out to be the ionised front edge of a massive molecular cloud, only recently discovered. Infrared radiation is observed from dust grains, in and around HII regions, which are heated by both stellar and nebular photons. Many HII regions, embedded in molecular clouds are completely obscured in the visible by local dust. They are usually discovered by radio techniques but they can best be studied in the infrared where they emit most of their energy.

Recombination lines of Hydrogen, Helium and forbidden lines of many ions in HII regions are powerful probes of the density, temperature and chemical abundances of ionized gas. Predicted, and in some cases measured, line fluxes for the Orion Nebula are shown in Figure 4.3.2. For many objects obscuration by dust precludes the use of optical lines, whilst certain ions do not have optical forbidden lines at all. Therefore observations of the forbidden fine-structure lines in the infrared are often the only way to study the physical conditions and in particular the chemical abundances in HII regions. Because of its high sensitivity and high spectral resolution ISO will significantly increase the number of HII regions that can be studied. This allows the possibility to determine chemical abundance gradients in our galaxy and perhaps in other nearby galaxies.

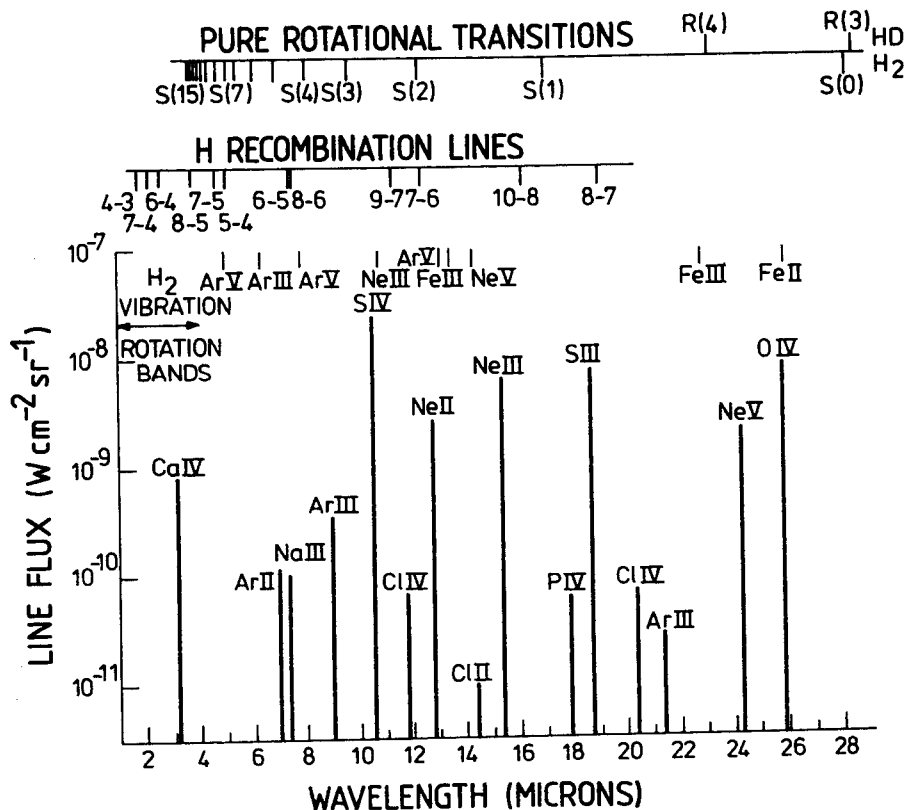


Figure 4.3.2 - Predicted line flux for the Orion Nebula together with the positions of HD and H₂ lines, and H recombination lines

4.3.3 Dust

Little is known about interstellar dust with any certainty. Formation and destruction mechanisms are largely the subject of speculation, as are the size, shape and composition of the dust. It is of major astrophysical importance, however, not only as an interstellar constituent itself, but because of the central role it plays in many other processes. Important examples of these include interstellar molecule formation and destruction, the determination of the initial mass function in star formation, cloud heating by photoelectron ejection and radiation conversion from higher energy photons into infrared photons. The role which the dust plays in these processes is determined by its precise composition which, until very recently, has been guessed at. Infrared spectroscopy of the dust is the only way to obtain this information.

Several dust-related spectral features have been observed in the infrared, although rather secure identifications exist only for three - the silicate bands at 10 and 20 μm and the iceband at 3.1 μm . Only some of the bands are observable from the ground. With ISO, all the bands would be observable together with a range of new bands which will most likely be detected. Very accurate spectral shapes could be obtained and the anticipated high sensitivity would drastically increase the number and types of regions where the bands can be observed. This would greatly facilitate the identification and interpretation of the bands by providing a full data base for use with appropriate laboratory and theoretical work.

The bandwidth of most infrared absorptions arising from molecular ices at temperatures 10K - 50K, lies in the range between 1 and 20 cm^{-1} . The substantially greater widths of the 3.1 μm ice band and the 10 and 20 μm silicate bands are obvious exceptions. These widths are due to strong coupling of the molecular vibration with other species in the solid. For example, in the case of " Si_nO_x ", this coupling is with the silicate lattice itself. Unravelling the molecular composition of the dust therefore requires a 1 cm^{-1} resolution spectrum from 2.5 to 25 μm (4000 - 400 cm^{-1}), the range in which nearly all vibrations occur for molecules composed of the most abundant elements H, O, C and N. Assignment of an IR absorption band to a particular molecule is rarely possible on the basis of one line, but generally requires the entire spectrum since most molecules possess more than one absorption in the 2.5 - 25 μm range. As a diagnostic tool, IR spectroscopy can be used to determine the composition of the dust material and the amount associated with different types of object. This bears directly on the morphological history of each region. In particular, the type of molecular ice present as a mantle on an interstellar dust grain, for a diffuse or a dense cloud, should be quite different. A schematic representation of the kinds of mantles one might expect is shown in figure 4.3.3, and each kind possesses unique spectral characteristics. In addition, precise band profile measurements should enable one to determine how much of the extinction is due solely to absorption by the molecular ices, and how much to scattering. From this, the size of the grains involved can be deduced, a very important but presently extremely uncertain piece of information.

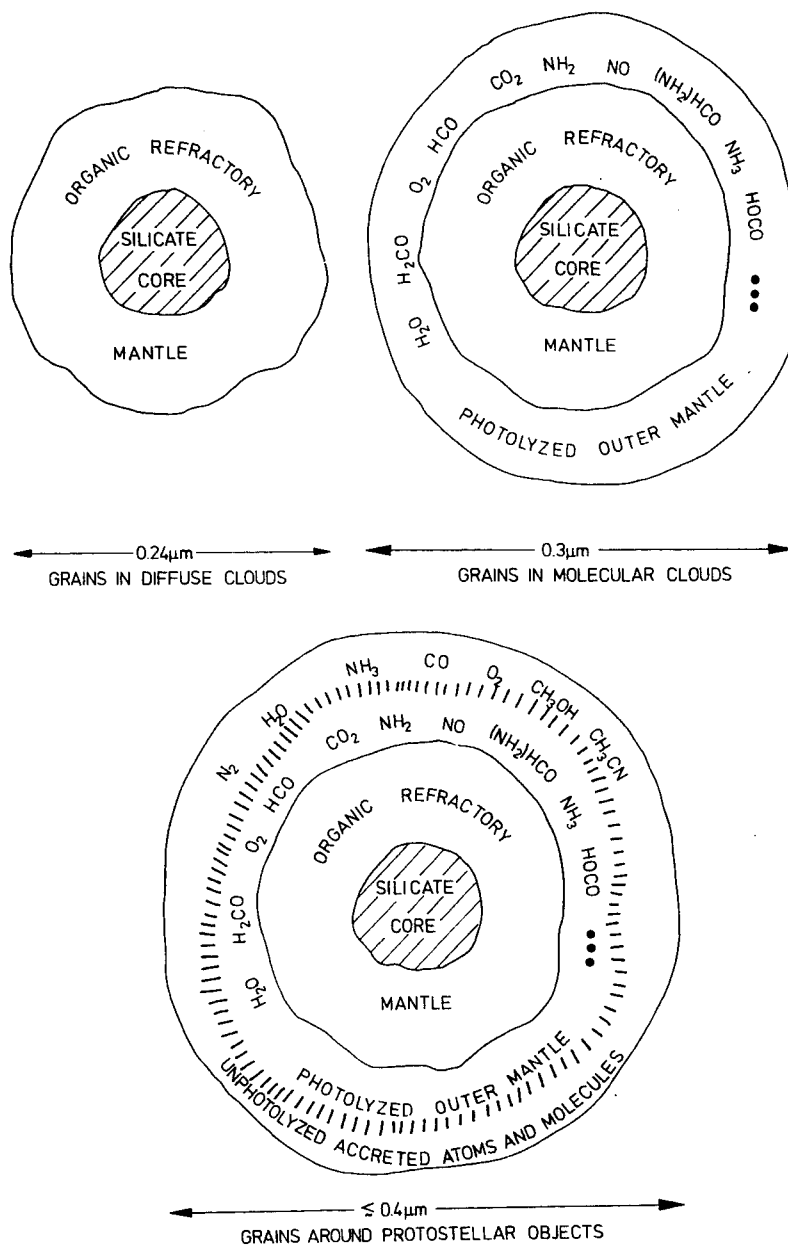


Figure 4.3.3 - Possible kinds of grain mantels

Since some of the bands, like the unidentified one at 3.28 μm, seem to require irradiation by UV light for their "excitation", mapping with high spatial resolution in these bands could serve as a method of tracing the distribution of non-ionizing UV-radiation associated with young objects deeply embedded in molecular clouds. In dense molecular clouds the energetics are controlled by the dust through its thermal emission at infrared wavelengths. A cold telescope in space is the ideal tool for a detailed study of this flow of energy, especially when combined with radio frequency molecular data of similar spatial resolution. Thermal dust emission from the shocks associated with supernova remnants interacting with dense interstellar matter may also be observable. No such high-velocity shocks have so far been identified within molecular clouds, presumably due to the large obscuration at shorter wavelengths. Observations at infrared wavelengths therefore offer unique possibilities.

4.4 Galaxies

Perhaps the single most important result to emerge from infrared astronomy to date is the discovery that many different types of galaxy are powerful infrared sources. In many sources, including our own Galactic Centre, the infrared radiation dominates the power emitted at all other wavelengths. However, difficulties in observing from the ground longward of about $10\mu\text{m}$ have prevented generalisation of this result to most objects. Clearly, in many cases the spectrum must turn over between $100\mu\text{m}$ and $1000\mu\text{m}$ to meet the observed radio spectrum, indicating the presence of a large infrared excess. In many galaxies the infrared emission is attributable to thermal re-radiation of stellar photons by dust, but in other cases, particularly quasars and BL Lac objects, non-thermal radiation is the only likely mechanism. Bursts of star formation seem adequate to explain thermal infrared emission from many galaxies, but the source of energy for the non-thermal radiation is still a mystery.

4.4.1 Normal Galaxies

ISO can be used to extend to nearby galaxies those studies of stars, star formation and the interstellar medium discussed in previous sections. Although long infrared wavelengths are practically unimpeded by interstellar absorption, solid state transitions in dust do occur (eg the $10\mu\text{m}$ "silicate" and $3\mu\text{m}$ "ice" features). It will be intriguing to see if the strength of these depends on type of galaxy or the presence of non-thermal sources, since this may enhance our understanding of dust composition and formation or destruction processes.

In general, of course, ISO will be most sensitive to the presence of the coolest stars. Because the Hayashi effect funnels evolved stars into the M giant part of the Hertzsprung-Russell diagram, these therefore are the ones seen best. These stars contain strong molecular bands of CO at $2.3\mu\text{m}$ and $4.6\mu\text{m}$ and H₂O at $2.7\mu\text{m}$ and $6.2\mu\text{m}$ which can be used for population studies and to search for evolutionary effects. These bands will also be extremely powerful probes of the presence of stars in QSO's.

The nearest members of the Local Group of Galaxies are the Magellanic clouds - about a factor of 10 further away from the sun than the galactic centre. The clouds do not have spiral arms like the galaxy, nor do they seem to contain as much dust. However, vigorous star formation occurs at various places and there are many bright HII regions. A study of the Magellanic clouds with ISO could elucidate the similarities and the differences in the star formation processes compared with our own galaxy, in particular the role played by density waves. From a comparison of our own galaxy and the Magellanic clouds one might also hope to learn something about the relation between the chemical abundances in the gas and the amount of dust.

Similar studies to map the large scale distribution of star formation in the nearest spiral galaxies, M31 and M33, can also be carried out with ISO. Because these galaxies are nearby, about 50 times further away from the sun than the galactic centre, such studies combined with the known distribution of the gas and other available information could significantly increase our knowledge of how and where stars are born in galaxies.

One interesting and particular problem which ISO will immediately solve is the question of whether the "isolated extragalactic HII regions" - dwarf galaxies containing hot stars - are young, in which case there will be few red giants, or "rejuvenated" in which many more evolved stars should be present.

A more speculative project for ISO is to attempt the detection of massive galactic haloes, composed of low-mass cool dwarf stars, which have been postulated by theorists from time to time to account for the so-called "missing mass" in galaxies.

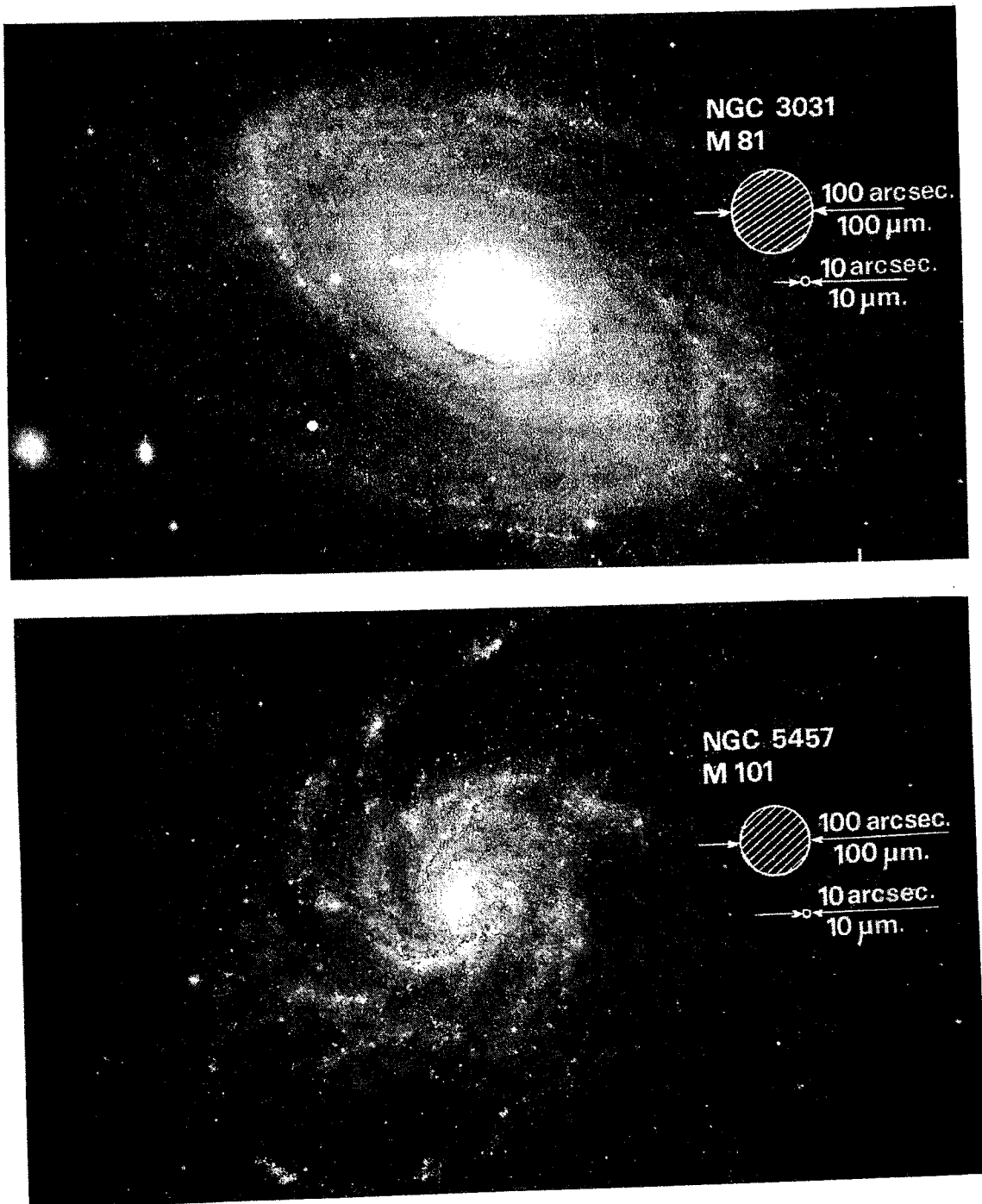


Figure 4.4.1 - Mapping of Galaxies with ISO

4.4.2 Active Galaxies

Active galaxies have attracted considerable research interest in recent years, based on observations covering a very broad range of wavelengths. Characteristically, these have shown very high luminosities from compact nuclei, with an energy peak sometimes in the radio, sometimes in the IR and sometimes in the X-ray spectral regions. Complicated spatial structure has been observed on various scales, including jets of plasma sometimes moving with apparently superluminal velocities and large scale gas movements approaching a significant fraction of the speed of light.

At the present, very little is known about the emission of these objects between $5\mu\text{m}$ and $500\mu\text{m}$. Uncertainty remains even for such basic parameters as their bolometric luminosity, by up to two orders of magnitude, because IR photometry is unavailable for more than about a dozen galaxies. This will make active galaxies (covering Seyferts, radio galaxies, quasars, blazars and BL lac objects) a very rich field of study for ISO. This critical region of the spectrum includes (i) a dramatic change in the characteristics of the nonthermal nuclear continuum, (ii) information about dust, and (iii) emission lines which can serve as unique probes of the physical conditions within the nuclear regions.

4.4.2.1 Galactic nuclei continuum

The spectral index of nonthermal emission from active galactic nuclei changes sharply in the infrared. The radio emission from most active nuclei has a flat spectrum. Towards the optical and near-IR, however, the nuclear emission falls off as $(\text{frequency})^a$ where a typically lies between -0.5 and -3. How those two regimes link up is a question of considerable importance. Figure 4.4.2 shows some examples. The broad peak of NGC 1068 at around $100\mu\text{m}$ wavelength, thought to result from thermal radiation by dust, contrasts with the spectrum of 3C 273 which rises fairly smoothly from the near IR to radio wavelength. Knowledge of the continuum spectrum in this wavelength range is essential for determining the energetics of the main energy source (or sources), and the relative prominence of the various emission mechanisms, such as thermal, synchrotron and inverse-Compton, which seem to be involved.

Specifically one might enquire whether the shape of the infrared spectrum, the infrared polarization and the variability differ for the various types of active galaxies, how these relate to activity in more normal galactic nuclei and whether there is any redshift dependence. In addition, infrared thermal emission is a unique tool for studying dust in active nuclei. Population studies between the various classes of active galaxies would yield information about this unexplored and important component. High sensitivity infrared studies could probe such questions as the absence of broadline regions in most narrow-line emission galaxies and determine if they are merely hidden from us by a nuclear fog.

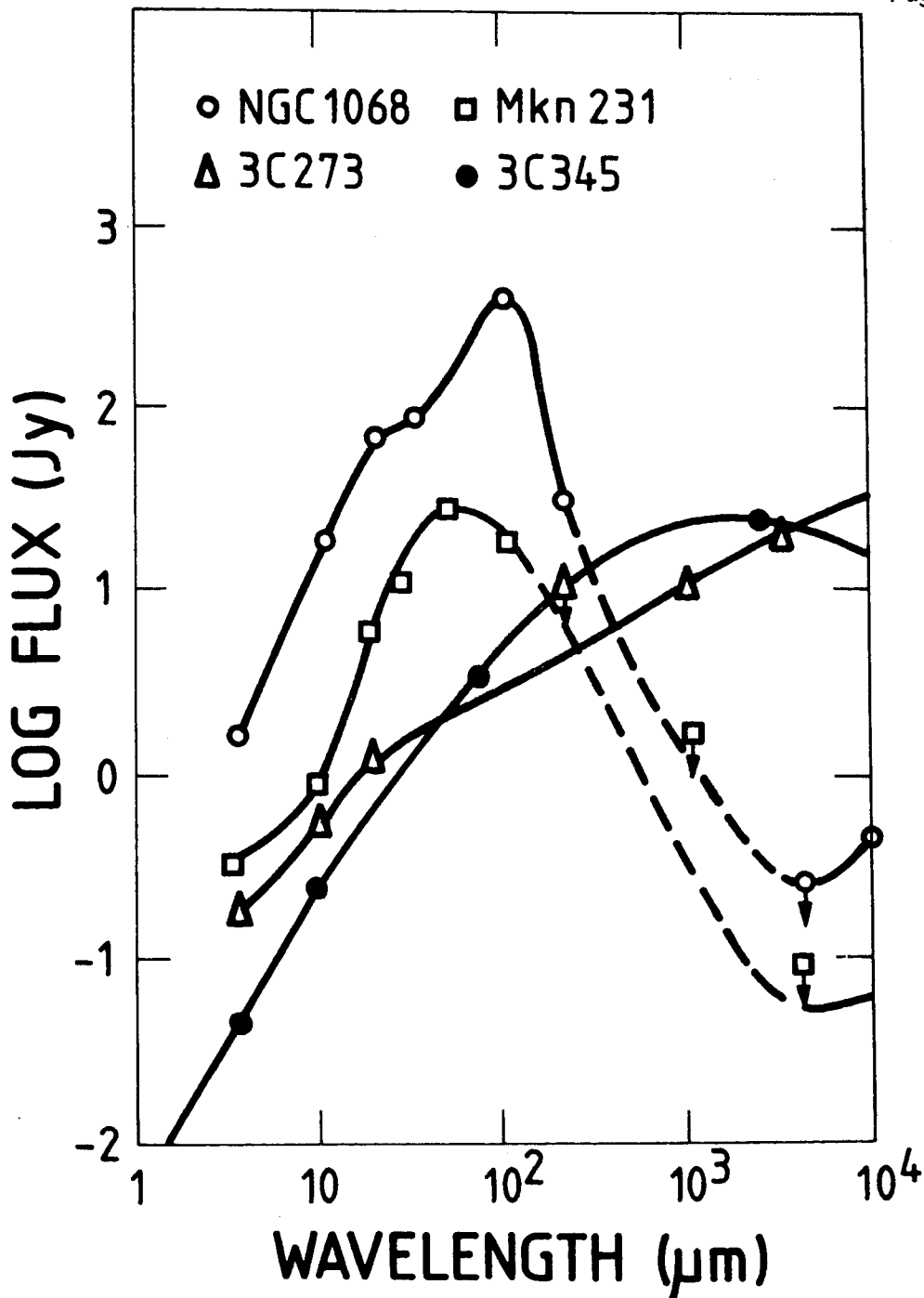


Figure 4.4.2 Continuum spectrum of some galactic nuclei

IRAS should begin these investigations of infrared nuclear emission by obtaining 4-point spectra for a few hundred active galaxies. However, the crudeness of these spectra will make the separation of the thermal and nonthermal components difficult, if not impossible. The spectroscopic and polarization capabilities of ISO should be able to impact directly on these questions as well as opening up new areas of research. It should be capable of mapping the infrared emission from narrow line regions of several active galactic nuclei. Taking a size of ~ 1 kpc, the narrow line regions should be resolvable out to a redshift of ~ 0.01 . For closer objects, it will be particularly interesting to relate the dust distribution to the geometry of various line emitting elements, and to examine the implications for the various ionization processes required.

4.4.2.2 The Extranuclear Continuum

Infrared emission from extranuclear regions of active galaxies is a fascinating field which ISO can explore. Several forms of extranuclear emission are expected. First is emission from synchrotron jets. In recent years, jet-like structures have been detected in extended radio sources and these are thought to pinpoint channels in which energy is quasi-continuously supplied to the extended radio lobes. There is considerable evidence that most of these jets are like that of M87 and have spectra which extend continuously from the radio to the optical with a (frequency)^{-0.7} spectrum. Several of these should be detectable by ISO and the results would be useful inputs to work on particle acceleration in extended radio sources. Secondly, extrapolation of the radio spectra of the lobes themselves shows that they should be detectable in the infrared by ISO in many radio sources. Comparison of the infrared and radio fluxes should yield valuable information about radiation losses in extended radio sources. Thirdly, extranuclear emission lines have been detected in many active galaxies and these are sometimes found to be morphologically closely related to extended radio emission. The connection between the radio continuum and optical line radiation is not yet understood. The sensitivity and angular resolution provided by ISO would make it fruitful to search for dust associated with these regions. A study of infrared emission from these objects would place useful constraints on models of the interaction between the line-emitting thermal gas and the radio-emitting relativistic plasma.

4.4.2.3 Spectroscopy

The capability to carry out sensitive high-resolution spectroscopy in the infrared will open several new avenues of active galaxy research. Comparison of the intensities of infrared emission lines with those of optical lines can give new information about the physical conditions within the galactic nuclei, and detailed profile studies between the various lines would yield important velocity information.

First, we may expect to detect several infrared forbidden lines from the narrow line region. Near-infrared and millimetre observations of NGC 1068 clearly demonstrate that a large mass of highly turbulent molecular gas exists in its inner several kpc. Models for shock heating of molecular clouds imply strong forbidden-line radiation from hyperfine transitions between the groundstates of abundant ions. These predominantly infrared lines will also be the main coolants in relatively cold photo-ionized regions ($T \sim 5000$ K), which may well co-exist with the hotter regions studied by optical forbidden lines. If NGC 1068 is at all typical of Seyfert galaxies, we may expect to detect with ISO many of the lines.

Secondly, the measurement of several high-order recombination lines of neutral hydrogen and helium in a sample of objects having a so-called "broad line region" (eg Seyfert galaxies and quasars) could help unravel the puzzle posed by existing optical and ultraviolet observations. These yield ratios of $Ly\alpha/H\beta$ roughly 10 times smaller than predicted by simple recombination theory, and Balmer decrements (eg $H\alpha/H\beta$, $H\gamma/H\delta$) which cannot be fit by recombination plus reddening. Self-absorption of Lyman and Balmer lines, collisional excitation, internal and external dust, and other more exotic mechanisms have been invoked to explain these data. Existing IR measurements of Paschen α for two quasars are at variance with dust reddening, but more data on higher order recombination lines is clearly needed to evaluate the various possibilities. The strongest lines observable are likely to be redshifted Brackett α ($4.05\mu\text{m}$), Pfund α ($7.46\mu\text{m}$), redshifted Pfund β ($4.65\mu\text{m}$), H6 α ($12.4\mu\text{m}$) and H6 β ($7.5\mu\text{m}$). Redshifted HeI $4.3\mu\text{m}$ ($3^3S - 3^3P$) and $10.9\mu\text{m}$ ($4^3S - 4^3P$) are expected to be greatly enhanced in situations of large optical depth applicable to the broad line region. Many more lines are covered by the bandpass of ISO, but their relative strengths are difficult to estimate given the pathological conditions in the broad line regions.

Thirdly, a study of the line intensities and profiles of redshifted $H\alpha$, [NII] λ 6584 and [SII] λ 6717, λ 6731 for high-redshift quasars and a comparison with optical studies of low redshift quasars would provide information about the possible differences in physical conditions between active nuclei having a large range of intrinsic luminosity.

4.5 Cosmology

Study of the Universe on the largest scales is the natural province of infrared astronomy, for at least two reasons. Firstly, the most luminous objects known in the Universe, active galactic nuclei of various types, radiate much, sometimes most, of their prodigious power in the infrared. Secondly, when any optical object is observed at large distances, the cosmic redshift makes it an infrared object. Thus we may expect that ISO, which can provide the highest sensitivity infrared observations, will enable astronomers to make significant steps towards answering some of the fundamental questions of cosmology.

4.5.1 Classical Cosmology

It is traditional to consider separately the geometrical and astrophysical aspects of cosmology. The geometrical aspects may be summarised by stating that the classes of active extragalactic objects which are all intense far infrared emitters, will be observable at cosmological distances. Figure 4.5.1 shows a selection of such objects, and the redshift/distance out to which they could be observed by ISO using reasonable assumptions for the sensitivity, as covered in Section 2. A systematic survey of the relative numbers of different classes of active galaxy in the far IR is important in determining the energy density of radiation in the Universe at these wavelengths. It is likely that, after the microwave background radiation, the far IR background radiation due to discrete sources is the most important contribution to the extragalactic background radiation. It is always to be hoped that some of those new classes of objective, in these relatively unexplored wavebands, will turn out to possess standard properties which can be used in the classical cosmological tests. The history of cosmology so far indicates that although the objects may not be particularly useful as distance indicators, their systematic observation results in quite different results of great importance for astrophysical cosmology. The examples which can be cited include the counts of radio sources, quasars and X-ray sources which provide evidence on the cosmological evolution of these objects with cosmic epoch. The same types of analysis will be possible for the following classes of object in the far IR - quasars, IR quasars, galaxies with strong far IR excesses and Seyfert galaxies. Because of this strong excess in some of these relatively normal galaxies, they will be observable at much larger redshifts than is possible in the optical waveband. See, for example, figure 1.01.

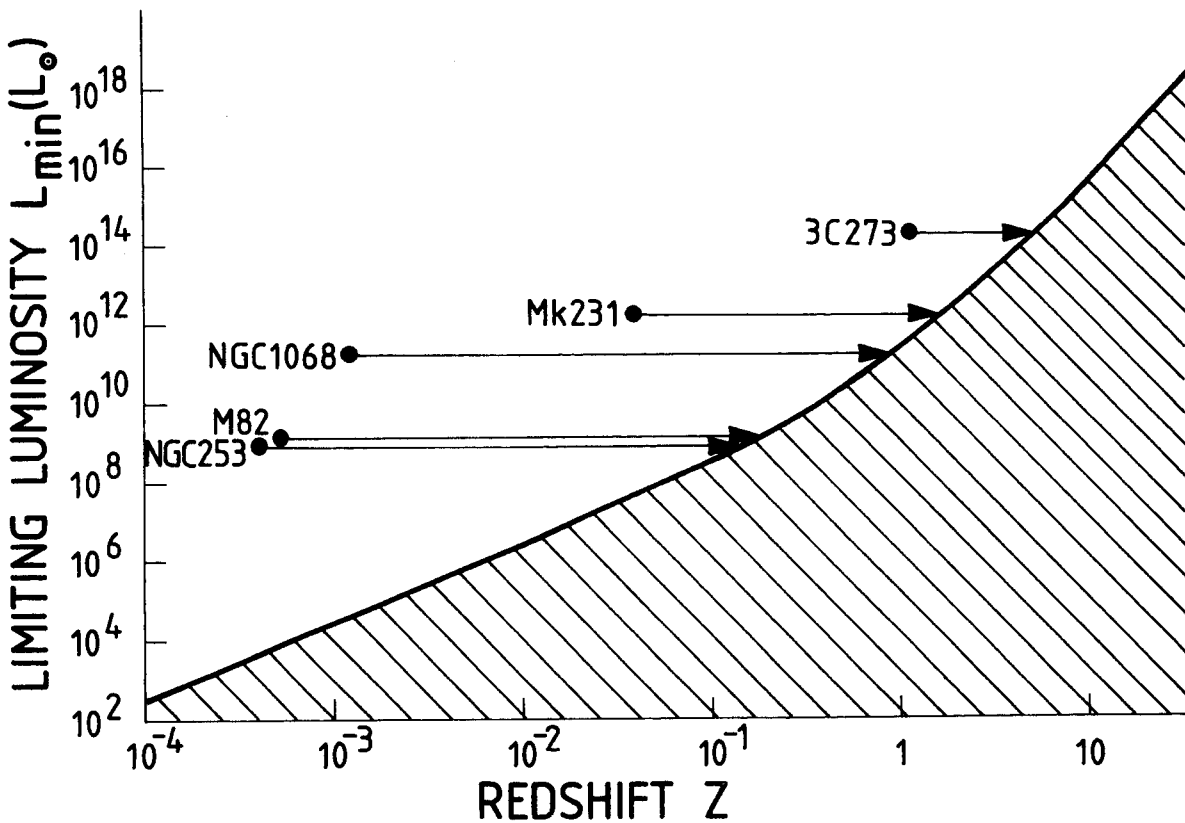


Figure 4.5.1 The luminosity-redshift space available to ISO, taken as the limiting luminosity which would be detectable with a signal/noise of 10 with one hour integration, as a function of redshift. Some well known objects are shown, with an arrow giving the redshift to which they could be persued by ISO.

4.5.2 Astrophysical Cosmology

Perhaps the most exciting studies for ISO are in the field of astrophysical cosmology. Observations of giant elliptical galaxies in the near IR waveband (1-2 μ m), combined with optical studies, have shown that there is definite evidence for significant evolutionary changes in the stellar content of these galaxies with cosmic epoch. This result suggests that the rate of star formation was greater in the recent past than it is at the present epoch. As a consequence, one would expect significant increases in all phenomena associated with star formation to appear in the most distant galaxies, in particular the presence of strong far IR excesses. These phenomena provide direct measures of the total rate of star formation and thus gives constraints upon star formation in massive galaxies as a function of cosmic epoch. These phenomena should be observable at redshifts $z \sim 2$ with the predicted sensitivity of ISO.

The most exciting prospect of all in cosmology is likely to be the search for protogalaxies. The epoch when the first galaxies were formed is not established with any degree of reliability either from theory or from observation. However, one of the more likely proposals, the adiabatic theory, predicts that galaxies formed rather late in the Universe timescale, $z \sim 5-10$, occurring by the fragmentation of large scale systems. Such a late date of formation would be consistent with the observed strong evolution of radio sources and quasars over the redshift interval 0 to 4 and the growing evidence for the evolution of the stellar content of massive galaxies.

These young galaxies should be very bright objects. Whereas in most galaxies, there is very little gas, in the young galaxies most of their mass is in the form of gas and the rate of star formation should be very large. In addition, the first generation of stars may well be responsible for the initial enrichment of the heavy element content in galaxies. In this case, their early luminosities would have to be 10-100 times greater than their present luminosities. In many ways these young galaxies should resemble HII regions of the sizes of galaxies. They have not yet been observed in the optical waveband, and the counts of faint galaxies do not show the type of excess which would be expected if a population of bright galaxies exists which were of this type at early epochs. A plausible solution is that these young systems are so dusty that all the radiation is absorbed by dust and is then reradiated in the thermal and far infrared wavebands. The discovery of such objects in a deep survey by ISO would be one of the most important discoveries in astrophysical cosmology and bring the study of the first generations of galaxies within our observational grasp. Their lack of detection would force us to push back the epoch when galaxies first formed to presently unobservable redshifts.

5. Science Requirements on the Telescope Facility

Following the outline given in Section 2 for the Instrumental Background, the Scientific Objectives covered in Section 4 will be met by a cooled telescope in space accommodating a range of IR photometric and spectroscopic focal plane instruments. These should permit efficient observations at the highest possible sensitivity, covering a wide range of wavelengths, and a lifetime of at least 1.5 years.

5.1 Mission lifetime

An operational lifetime of at least 1.5 years is taken as:

- Compatible with a good overall scientific return.
- Offering the whole sky for observation a number of times.
- Appropriate for observing and categorising a wide range of variable sources.
- Giving a good chance to observe a range of exceptional and periodic phenomena such as novae, comets, etc.
- Leading to operational efficiency from learning during the mission.

5.2 Observational modes

The scientific objectives require the following main operational modes:

- Fixed pointing.
- Offset pointing covering a matrix of sky positions.
- Small raster scan, say 1.5×1.5 arc min. This is applicable, for example, for source location within an IRAS error box or to peak up the pointing of an instrument on a source.
- Large raster scan, say 30×30 arc min, for mapping.

5.3 Optics temperature

To keep the thermal emission of the optics, over a wide range of wavelengths, below that of the zodiacal background radiation and/or that equivalent to a photon background limited NEP of 1×10^{-17} watts $\text{Hz}^{-\frac{1}{2}}$, a temperature of less than 20K is required for the optics. This can be seen from figure 2.1.2, for the conditions noted. As the temperature of the optics is reduced below 20K, operation can be extended to longer wavelengths and very high photometric sensitivity maintained with broad spectral bandwidth. The objective is therefore to obtain the lowest possible temperature for the optics, consistent with efficient cryogenic operation to give a good lifetime. For example a temperature of 10K is consistent with using a detector with a NEP of 1×10^{-17} watts/ $\text{Hz}^{-\frac{1}{2}}$ at wavelengths out to about $200\mu\text{m}$. The photon background noise penalty for operating at even longer wavelengths is quite small.

5.4 Telescope size

For maximising the flux gathering area and the spatial resolution, the largest practical mirror diameter should be considered. The actual limit is established by the mass limit of the payload, of which the telescope and the cryostat/cooling system are the main components. More telescope mass implies less cooling capacity. Pre-phase A studies suggested a clear mirror diameter of 60cm. This value has been substantiated in the present Phase A study, particularly in relation to the trade-off with cryogen lifetime.

5.5 Operating wavelength range

Over the IR wavelength range identified in section 2, no practical limit will come from the reflecting optics, since optical quality mirrors can be produced for operation at cryogenic temperatures using standard techniques with ceramic or silica material. A short wavelength limit out to around $2\mu\text{m}$ is desirable to give some overlap for calibration with wavelengths which are accessible to ground-based telescopes and also perhaps to Space Telescope. The telescope system as a whole is aimed at compatibility with diffraction limited operation down to $5\mu\text{m}$ wavelength. At the long wavelength end of the range, two effects arise. The first is thermal emission from the optics which, as discussed in section 5.3, does not establish any really critical limit for optics temperatures around 10K. The second is the practical question of the size of the diffraction limited field of view produced by the 60cm diameter mirror. At $200\mu\text{m}$ wavelength, for example, the diameter of the first minimum of the Airy pattern is 2.8 arc mins on the sky, which is approaching the whole field of view designed to be available for each instrument.

5.6 Orbit/Integration time

The operational efficiency of ISO as an observatory and its ultimate sensitivity are dependent on the length of time that it can be pointed to selected regions of sky. This should amount to a number of hours, and therefore argues against a low Earth orbit, particularly when the requirement for real-time operation is also included. Observation times for a single field of view of a photometric instrument will normally be of the order of seconds, unless the very highest sensitivity is required. Operational efficiency is derived from being able to observe an object with a range of instruments, or map out a reasonably extended region of the sky or observe a large number of objects, say within a cluster of galaxies, for statistical analysis.

5.7 Telescope pointing accuracy and stability

The concept of an observatory and the operational requirements of a number of infrared instruments appropriate to ISO require a 3-axis stabilised pointing system. The accuracy and stability requirements are largely dictated by the field of view of the measuring instrument. This is selected according to the wavelength and the type of observation. The absolute pointing is required to acquire the selected source within the instrument field of view. If a smaller field is used, this can be refined with a small raster scan to peak-up on the signal.

Pointing stability is required to maintain the source within the instrument field of view during the measurement period. Operationally, these requirements will range from the most stringent, arising from diffraction limited observation with a single detector at 5µm wavelength, to wide field measurements at the longest wavelength. The pointing performance is summarised in Section 9.3.2 and Tables 9.3.1 to 9.3.3.

5.8 Telescope baffling

Very high sensitivity infrared observations require not only low thermal emission from the optics, but also very good rejection of infrared radiation from strong sources outside the telescope field of view - such as from the Sun and Earth. For this, it is necessary to specify the angle to the telescope axis within which the strong source must not be permitted to come. Similar, though less stringent, requirements are also given for the Moon and Jupiter. These are summarised in Table 10.1. In addition to this specification for off-axis rejection performance, thermal emission from the baffle system itself must not compromise the detector sensitivity.

5.9 Sky cover

Combining the orbit requirements from Section 5.6 and the pointing restrictions derived from Section 5.8 allows the time development of the sky available for observation to be calculated. This should be optimised for total sky cover and the periods over which regions of the sky may be observed.

These requirements are summarised in Table 5.1

MEASUREMENT ASPECT	Low temperature for optics	Stray light rejection	Absolute Pointing Accuracy	Pointing Stability	Large Diameter Telescope	Long Orbit Period	Long integration time
Measurement sensitivity	x	x		x	x		x
Measurement efficiency	x	x	x			x	
Long wavelength operation	x	x			x		
High spatial operation			x	x	x		
Wide field operation	x	x					
High spectral resolution							x
Broad spectral bandpass	x	x					
Short wavelength operation			x	x			
Sky availability		x				x	

Table 5.1 - Summary of requirements arising from the science objectives and performance

6. The Instrument Payload

6.1 Selection of a model instrument payload

Since it is proposed that the instruments for the ISO payload should be provided by Institutes, after selection by ESA advisory groups, it was necessary to develop a model instrument payload for this Phase-A study. It was intended that this instrument complement should be scientifically attractive, and capable of defining typical mechanical, thermal and electrical requirements. Table 6.1.1 shows a summary of the main physical processes which are discussed in the Science Objectives, the main wavelength ranges for their observation and the spectral resolving power (R) required (low R = 2 to 20; medium R = 20 to 500; high R = > 500).

Table 6.1.1 - Some Important Astrophysical Processes

Physical Process	Approximate Wavelength Range (Microns)	Spectral Resolution	Special Interest
Thermal emission	5-500	Low	Total infrared luminosity. Re-radiation by dust in obscured regions. Mapping star formation regions.
Molecular transitions	Vib. 1-25 Rot. 15-500	Medium High	Stellar populations. Molecular clouds and dynamics.
Recombination lines Atomic and ionic fine structure lines	1-6 1-300) High)))	Constituents and dynamics of nebulae, etc.
Polarisation	1-500	Low	Non-thermal processes. Dust.
Non-thermal/ thermal emission	2-300 (?)	Low	Infrared "active" galaxies.
Solid state transitions	2-30	Medium	Interstellar dust/ grains.

There is a wide range of IR instrumentation from which the actual ISO instrument payload may be selected. Possible candidates include:

- . Mapping photometric arrays, say 3 or 4 "colours".
- . Photometer/polarimeter system involving a wide choice of filters, apertures, etc.

- . Grating spectrometer, developed into a spectral x spatial scan using a 2D detector array, or pure spectral scan using a 1D array.
- . Fourier transform spectrometer. This can be a rapid scan type or "step and integrate", both with a single detector or an array. This can also be imaging.
- . Camera system using 2D arrays and selectable filters.
- . Fabry-Perot spectrometer.

For each instrument there is considerable freedom for design and optimisation, particularly with regards to wavelength range, and also the possibility to develop a hybrid to combine features of two instruments. With Table 6.1.1 as a guide, the instrument selection shown in Table 6.1.2 was aimed at providing, in total, a broad range of performance consistent with an observatory facility, without very specific observational bias. Operational factors, such as redundancy were also considered. In addition, study of the instruments themselves was intended to explore the design and performance of appropriate mechanisms and sensors, many of which are required by more than one instrument.

Table 6.1.2 - The Model Instrument Payload

Instrument	IR Camera Array	Spectrometers	Photometer/ Polarimeter
Type	InSb 32 x 32 CID Array	Rapid Scan Michelson Interferometer	Si and Ge photo- detectors with band-pass filters
Wavelength Range	2-5 μ m and possibly extended to 6-18 μ m	2-70 μ m covered by two interferometers	8-120 μ m and possibly extended out to 200 μ m
Resolving Power	Set of narrow band filters and continuously variable filter	10 ² - 10 ⁵	4 bands in the range
Telescope Operating Mode	Fixed pointing. Offset to a matrix of points.	Fixed pointing. Offset to a matrix of points.	Fixed pointing and raster scan

The IR camera array is intended for high spatial resolution mapping. Spectroscopy over the wavelength range 2 μ m to 70 μ m is based on the use of two Michelson Interferometers, which have the advantage of variable spectral resolution and high efficiency for exploratory work, or for examining regions with a lot of relevant spectral information. Photometry and polarimetry in the 8 μ m to 120 μ m range is covered by the third instrument. More detailed descriptions of the instruments are given in Sections 6.2, 6.3 and 6.4. It should be emphasised that this instrument complement is a model payload. A variety of instrument

configurations can be considered at this time without unduly affecting the overall instrument accommodation. The payload was deliberately conservative regarding the long wavelength limit, in order not to drive the cryogenic design too hard for a very low temperature for the optics. In the event, a very low temperature was achieved with good overall mission lifetime. The long wavelength limit can therefore be considered in the light of this result, together with the development or qualification effort required for appropriate detectors.

6.2 Michelson Interferometers

Fourier transform spectroscopy, using some type of Michelson interferometer, is well developed for laboratory applications. A study and development programme has been undertaken to extend this work specifically to an instrument which is appropriate for ISO.

Michelson interferometers offer an excellent combination of performance and flexibility for fulfilling the ISO spectroscopic aims. With a relatively compact instrument, it is possible to achieve resolving powers to well over 10^4 at the shorter wavelengths, whilst also exploiting multiplex and throughput advantages. Two Michelsons of the double output type are proposed to cover at least the range 2 μm to 65 μm . At the same time, the double output provides partial redundancy which can be used to eliminate particle radiation effects in the detectors. The general layout is shown in figure 6.2.1.

The interferometer beamsplitter is designed to cover a wide range of wavelengths. Dichroic beamsplitters are used to separate the output into wavelength ranges which match the photoconductive detector characteristics. One of the most critical tasks is the design and construction of the drive and transport mechanism for the moving mirror. This must dissipate very little power (less than 5 mw), when operated at cryogenic temperatures. In addition, the motion must be very smooth and accurately parallel. The model payload design achieves this with a hinged slide system using a number of flexural pivots. This is shown in figure 6.2.2. The slide is actuated by a linear electro-motor. The position and speed of the slide is measured by a laser reference interferometer. The reference signal is used to trigger the interferogram sampling circuitry and to servo-control the drive mechanism.

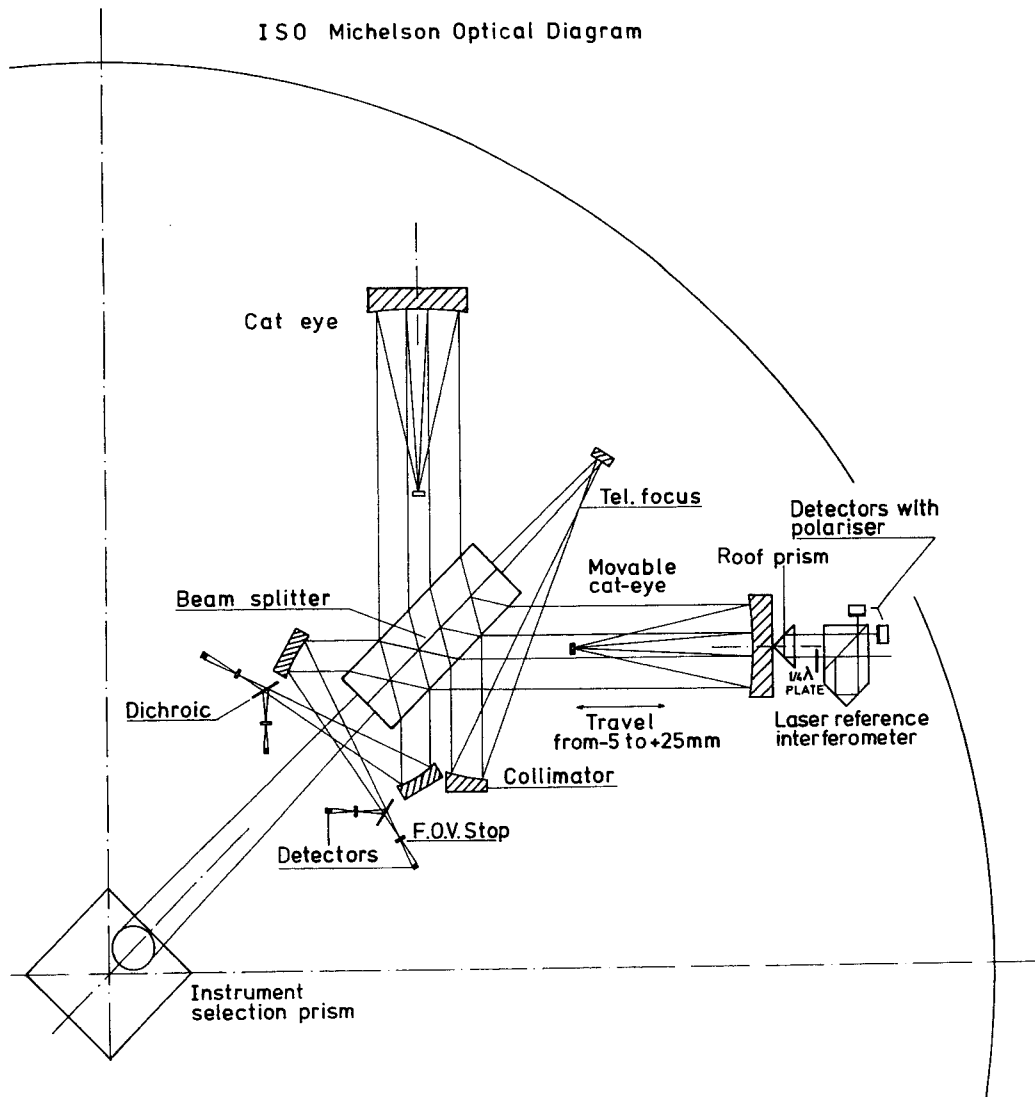


Figure 6.2.1 Optical layout of the Michelson interferometer, fitted within a 1/4 section of the ISO focal plane instrument volume.

An engineering prototype of this system, based on the slide shown in figure 6.2.2, has been built and shown to work reliably at cryogenic temperatures. The power dissipation was measured to be comfortably below the 5 mw objective, with 30 mm travel for the moving mirror. The fixed and moving mirrors of the interferometer were chosen to be "cat eye" reflectors which have greater alignment tolerance than flat mirrors, as well as giving a separation between the input and output beams of the interferometer. The attainable spectral resolving power is dependent on the instrument field of view, the wavelength and the travel distance of the moving mirror. Figure 6.2.3 summarises these aspects.

The main characteristics of the interferometers are summarized as follows:

- Type
Single input, double output with each output being separated into a long and short wavelength band.

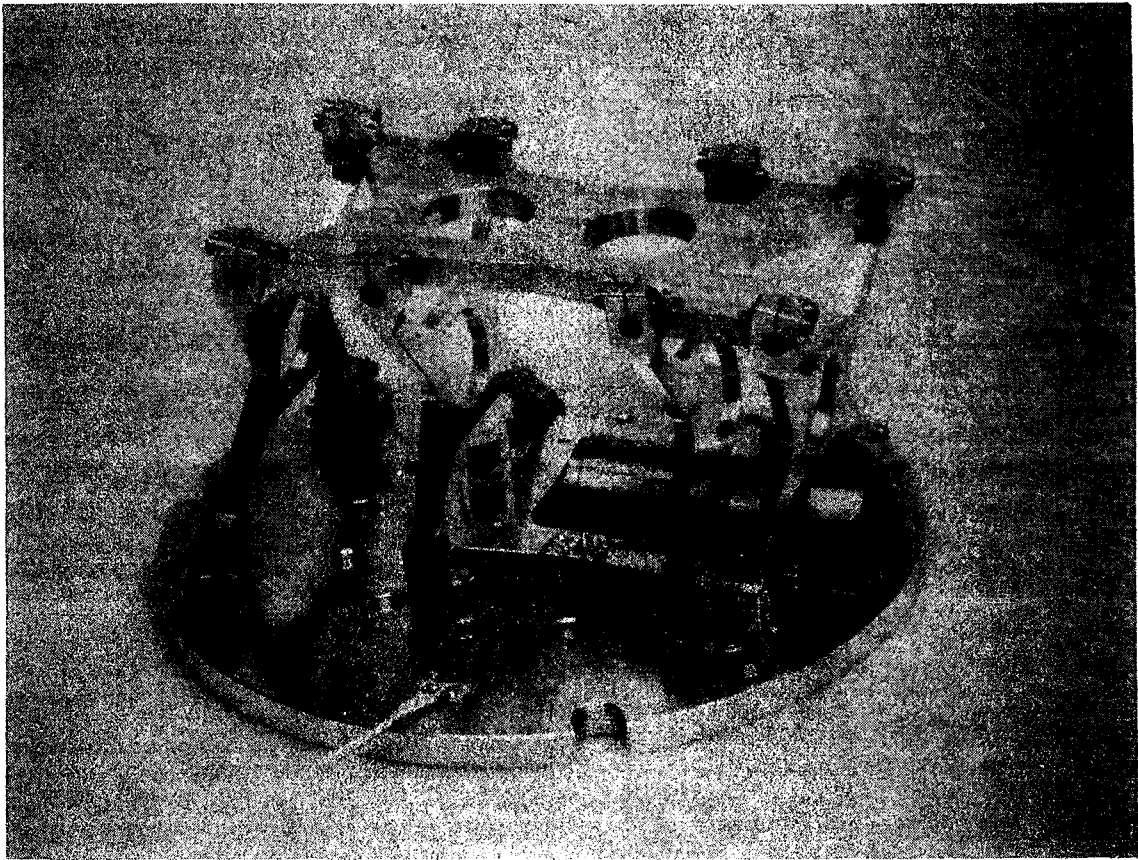


Figure 6.2.2 - Picture of the drive and flex-pivot bridge system for the interferometer moving mirror.

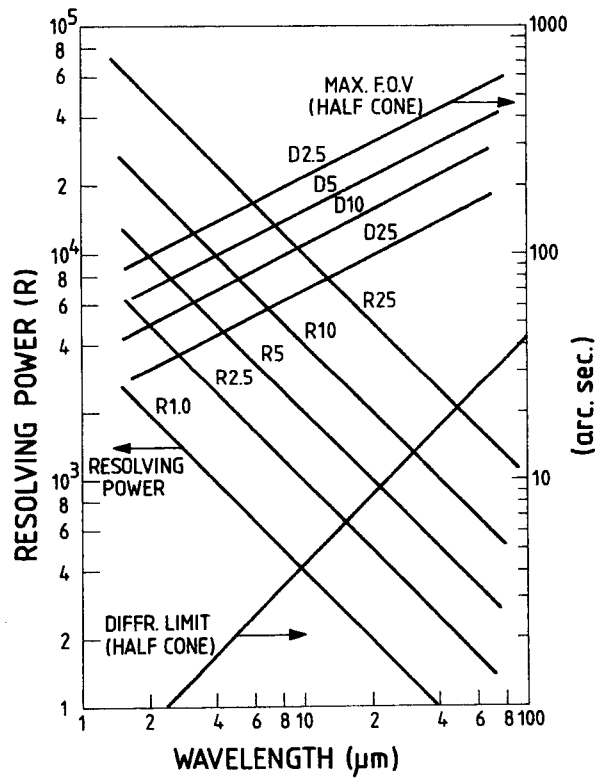


Figure 6.2.3 The spectral resolving power R, the maximum allowable field of view and the diffraction limited field of view is shown as a function of wavelength.

. Wavelength ranges

Interferometer 1 with BaF₂ separator: 2-14 μm (transmission)
30-50 μm (reflection)
Interferometer 2 with KCL separator: 2-31 μm (transmission)
50-65 μm (reflection)

. Beamsplitter

Ge on CsBr with about 0.35 efficiency.

. Filtering

As above with beamsplitter, band separators and additional filters.

. Retro-reflector drive

Linear motor with power dissipation around 5 mw and servo-controlled.

. Velocity sensor

Laser reference interferometer.

. Fields of view

Interferometer 1: 30" for $\lambda < 30 \mu\text{m}$, and 50" for $\lambda > 30 \mu\text{m}$
Interferometer 2: 50"

If an aperture wheel mechanism is provided at the telescope focus position, diffraction limited operation as shown in Figure 6.2.3 is possible.

. Sensitivity

2.10⁻²¹ W/cm² per spectral element using a detector NEP of 1x10⁻¹⁷ W/Hz^{1/2}, 30 minutes integration time and 3 sigma detection level.

. Operation mode

Rapid scan with scan time variable from 10-10³ seconds.

. Detectors

Interferometer 1: 2-14 μm In:Sb and Si:Ga
30-50 μm Ge:Be
Interferometer 2: 2-31 μm Si:P or Si:Sb
50-65 μm Ge:Ga

An alternative configuration has been considered in which the two interferometers are combined into one in order to share the moving mirror system. This gives added complexity, but releases 1/4 of the focal plane instrument volume for another instrument.

6.3 Photometer

6.3.1 Scientific Requirements

The objectives covered in section 4 can be distilled into three types of observational objectives for the ISO photometer:

- . Photometry of faint, extra-galactic sources.
- . Mapping extended regions, both for galactic and for extra-galactic studies.
- . Polarimetry.

In addition, two further features would be desirable to incorporate into the photometer:

- . Absolute photometry for mapping extended sources. This takes good advantage of the low IR background of a cooled telescope and is in contrast to the differential photometry using spatial chopping employed with warm telescopes.
- . Simultaneous photometry in all wavebands. This makes efficient use of the observing time and is achieved using dichroic beamsplitters.

These five requirements have defined the photometer for the ISO model payload.

6.3.2 Design Concept

The photometer optical layout is shown in figure 6.3.1.

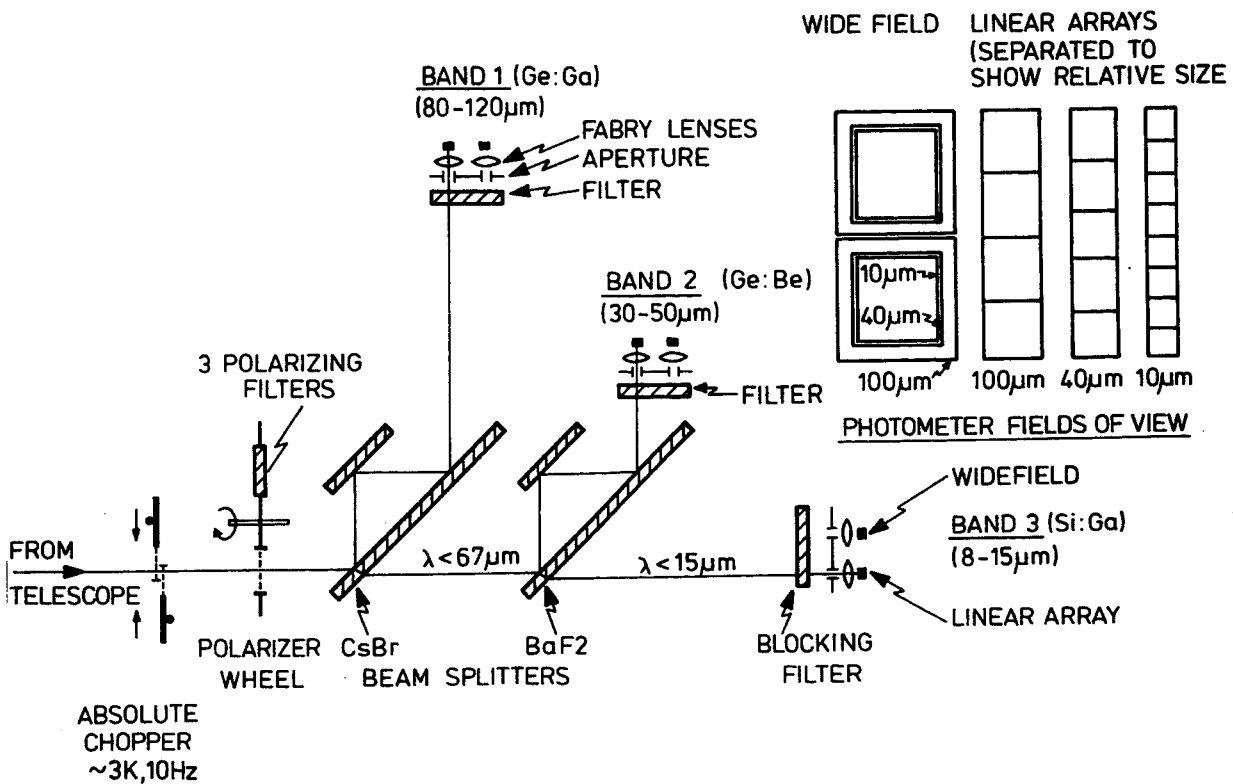


Figure 6.3.1 - Optical layout of the model payload photometer.

The photometer operates simultaneously in three wavelength bands which together span the wavelength range 8 μm to 120 μm . There are two sets of detectors for each waveband, two wide-field detectors for long integrations on faint point-like sources and a linear array of detectors with higher angular resolution for mapping. Using the CsBr and BaF₂ beam splitters, the detectors for the three wavebands view the same field of view on the sky. The detectors, wavebands and pixel sizes for both the wide field and linear arrays are listed in Table 6.3.1.

Waveband μm	Detector	Wide Field		Linear Arrays	
		Pixel Size arcsec.dia.	Number	Pixel Size arcsec.dia.	Number
80 - 120	Ge:Ga	80	2	40	4
30 - 50	Ge:Be	60	2	32	5
8 - 15	Si:Ga	55	2	20	8

Table 6.3.1 - Photometer Detectors

The photometer itself has no moving parts, minimising the heat dissipation and giving the highest reliability. All the detectors have NEP's approaching 10^{-17} W/Hz^{1/2}, transparent contact construction and are available from European manufacturers.

Photometric chopping may be done in two alternative modes. A tuning fork type chopper placed at the photometer entrance aperture permits absolute chopping for measurement and mapping of extended sources. For long integration measurements on extended and point-like sources, a secondary mirror chopper is very desirable. Such a chopper, square wave modulated and with facilities for remotely controlled frequency adjustment up to 50 Hz and amplitude control up to 600 arcsec, has been demonstrated to work reliably for long periods in the laboratory at cryogenic temperature. Operated at low temperature, the heat dissipation was measured to be around 5 mw, which is compatible with the secondary mirror cooling provided for ISO.

The photometer may be used as a polarimeter by inserting analysers in the beam. Three identical wire-grid analysers, set at 30 degree angles to each other, are placed in a switchable wheel at the photometer input. Percentage linear polarization and angle are then measured by observing a source through each of the grids. In this way polarimetry, including polarization maps, can be obtained simultaneously in the three wavelength bands.

The photometric performance obtainable with ISO is discussed in section 2 and set out in figures 2.2.1, 2.2.2 and 2.2.3.

6.4 Near IR Camera

6.4.1 Scientific performance

The infrared camera can provide sensitive measurements of both point-like and extended sources. The spatial resolution obtainable is of the order of arc seconds, enabling detailed studies of extended objects to be performed. The camera constitutes also an efficient means of observing clusters of stars and galaxies. Equipped with a large number of selected spectral band-pass filters, the camera can be used for studying both continuum radiation and spectral features from gas as well as from dust. The addition of polarizers significantly increases the scientific use of the instrument.

6.4.2 Technical aspects

Figure 6.4.1 shows one possible configuration of the IR camera with provision for two array sub-sections: a 2-5 μm array (A) with an existing In:Sb array and a 5-18 μm array (B) with a new development array or a redundant 2-5 μm array.

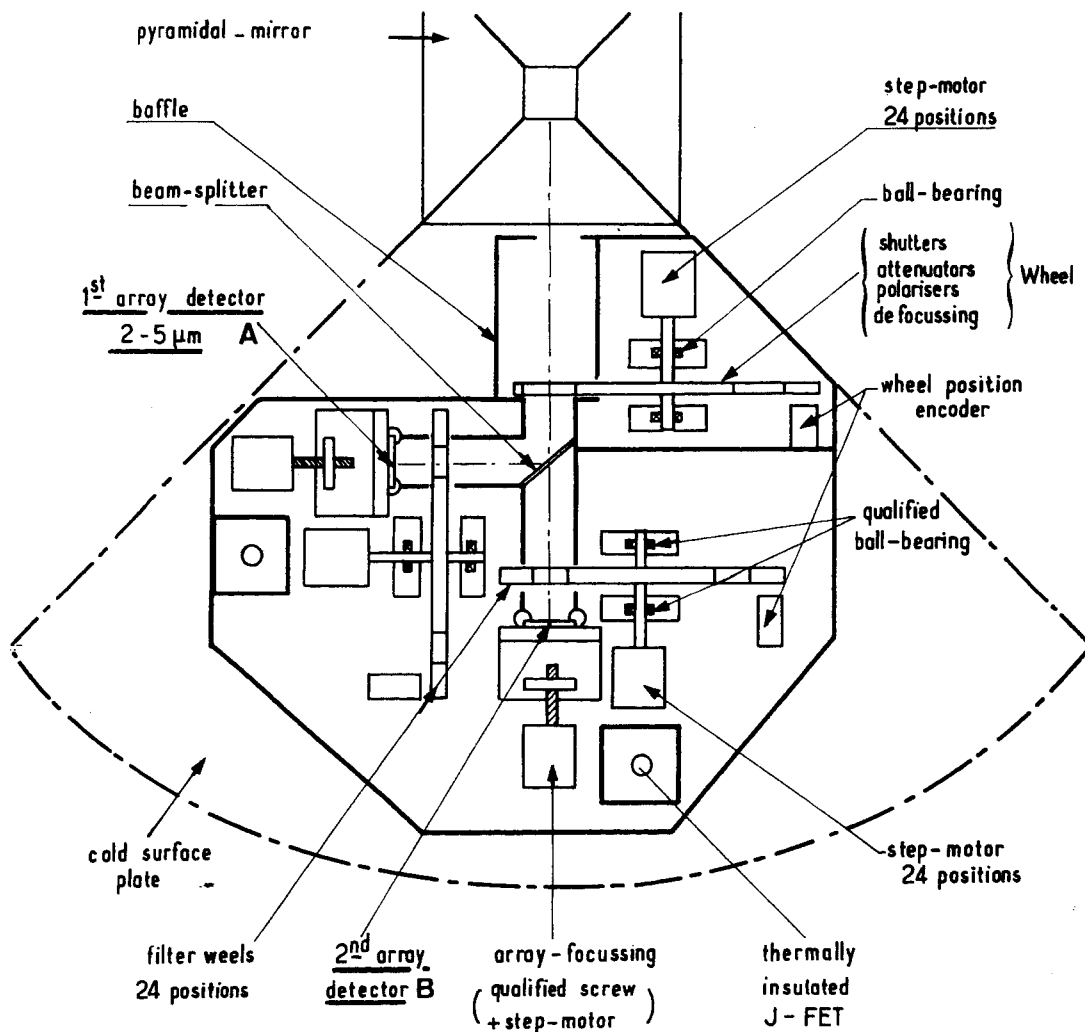


Figure 6.4.1 - Layout of the IR camera in a 1/4 section of the focal plane volume

The pixel sizes and fields of view in Table 6.4.1 represent a trade-off between spatial resolution and surface brightness sensitivity.

	Number of Elements	Pixel F.O.V. arcsec.	Pixel Size μm	Array Size mm	Array F.O.V. arcmin.
Array A	32 x 32	1.9	83	2.6	1
Array B	32 x 32	5.6	244	7.8	3

Table 6.4.1 - Details of IR Camera Arrays

Both arrays share a 24 position wheel placed in the entrance beam, which holds shutters for dark current calibration, attenuators for very bright sources, defocussing optics for photometric calibration and polarizers. A beam splitter separates 2-5 μm (reflected) and 5-18 μm (transmitted) light beams towards the arrays A and B respectively. Each array sub-section contains a 24 position filter wheel with a stepper-motor and a position encoder, an active focussing mechanism and an active temperature control system for the array and appropriate cold pre-amplifiers. All active mechanisms, such as the stepper-motors, the ball bearings and the focussing screws are already space qualified for the FPA environment.

The average overall thermal dissipation can be kept below 10 mW, although certain elements may have higher peak dissipations. Stepper-motors with super-conducting wires with even lower heat dissipation are under development. The photometric calibration and the data acquisition chain can be checked in flight by (a) imaging standard stars on selected pixels, (b) by spreading a defocussed image of a star over a group of pixels and (c) by using an internal calibration source for a reference flat field.

An on-board microprocessor controls all the functions of both arrays under the general RTU and telemetry link control. It also achieves as much on-board data processing as needed to minimize telemetry exchange delay. A simplified scheme is shown in figure 6.4.2.

An array with a quantum efficiency of 30%, 200 electrons RMS read-out noise (equivalent to a detector NEP = 5.10^{-17} W.Hz $^{-1/2}$ at 5 μm), 20% optical efficiency and $\Delta\lambda/\lambda = 0.3$ provides a 10 σ signal in 1 second for a flux of 0.1 Jy, a result which is almost independent of wavelength. The performance is also set out in figures 2.2.2 and 2.2.3.

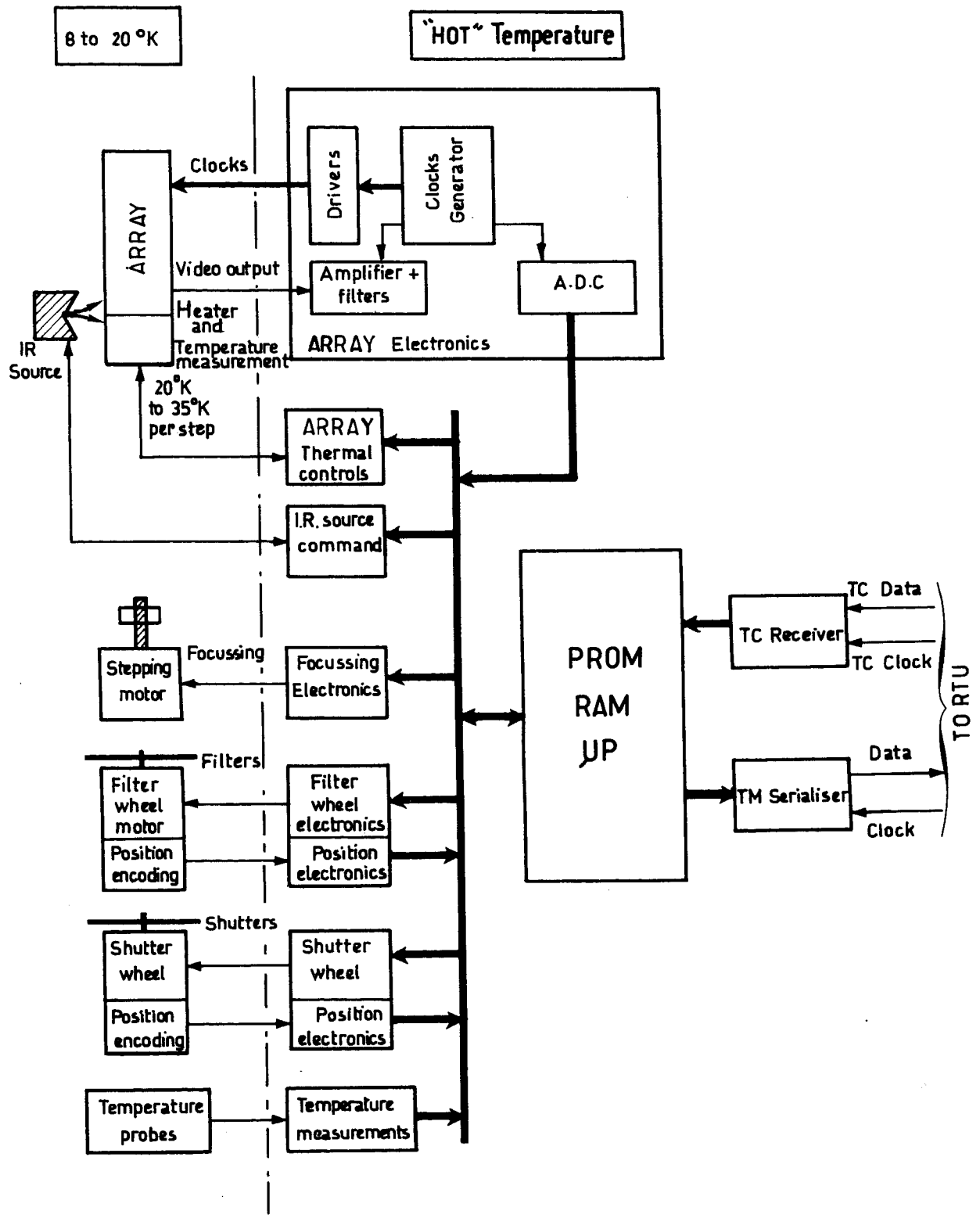


Figure 6.4.2 - Block diagram for one IR camera array electronics and control.

6.5 Detectors

IR detectors and their associated electronics are the key elements in the focal plane instruments. As discussed in section 2, it is the development and availability of low background IR detectors which allows the potential of a cooled telescope in space to be realised. Much of this stems from the support for IRAS. Even though these detectors were integrated into the IRAS focal plane some time ago, this development work has continued both in the USA and Europe. This has involved producing a wider range of photoconductive detectors to give a good selection of peak response from about 3 μ m out to beyond 120 μ m, developments in associated preamps and electronics, and more recently the development of arrays for low background operation.

A summary of this situation is given in the following two sections:

6.5.1 Single Detectors

A wide range of single detectors, fabricated from bulk doped silicon or germanium have been commercially available for some time. Table 6.5.1 shows some details on those which are more commonly used.

Photoconductive Detector	Useful Wavelength Range (μ m)	Reported NEP Watts Hz ^{-1/2}	Available	
			Europe	USA
In: Sb	~2 - 5.6	3 x 10 ⁻¹⁷	*	*
Si: Ga	~5 - 17	7 x 10 ⁻¹⁷	*	*
Si: Bi	~6 - 18	3 x 10 ⁻¹⁷		*
Si: As	~10 - 24	4 x 10 ⁻¹⁷		*
Si: P	~12 - 28	3 x 10 ⁻¹⁷	*	*
Si: Sb	~15 - 29	1 x 10 ⁻¹⁷		*
Ge: Be	~20 - 55	8 x 10 ⁻¹⁷	*	
Ge: Ga	~50 - 120	7 x 10 ⁻¹⁷	*	*
Ge: Ga (stressed)	~100 - 180	6 x 10 ⁻¹⁷	*	*

Table 6.5.1 - Available Photoconductive Detectors

Considerable experience has been gained in using these detectors in medium to low background conditions to build astronomical instruments. This includes work for IRAS (particularly the NL additional experiments), the four main instruments in GIRL, experiments in aircraft, balloons and rockets, and IR equipment for ground based telescopes. Part of this work has been funded by ESA and part with German national funding to support the GIRL project. Further development is aimed at achieving radiation hardened detectors, to minimise the effect of particle impacts when the spacecraft is moving through the Earth's radiation belts, and integrated low-noise electronics to operate cold with the detectors.

6.5.2 Arrays

Apart from making up arrays from single detector elements, advantage can be taken from the industrial effort which has been directed to making integrated arrays for commercial (eg visible CCD arrays for TV) and military applications. Arrays suitable for astronomical applications have normally arisen as spin-off's from these programmes.

For the 2 μm to 5 μm range, S.A.T. (France) has developed InSb CID arrays. The 8x8 format is now available to astronomers and a 32x32 format array which is already developed will be available to French scientific institutes in 83. The performances of the SAT devices, and the results obtained in the USA with similar devices, shows that 10 to 20% quantum efficiency and a read out noise of 200 electrons are very realistic values. This leads to an NEP ranging from 2×10^{-16} to 4×10^{-17} Watt.Hz $^{-1/2}$ for each pixel. Compensation for variations in sensitivity of 20% over the array can be implemented with the data processing. Within the timescale envisaged for selection of proposals from institutes for instruments, hybrid Si:In CCD could also become available with similar performance.

For longer wavelength operation, Si:Bi AM.CID arrays made by Aerojet are becoming available from the USA. These have excellent characteristics for astronomical applications with NEP's at the 10^{-17} Watt.Hz $^{-1/2}$ level.

6.6 Model Payload Accommodation and Interface Requirements

The four instruments of the model instrument payload have each been accommodated within 1/4 of the focal plane volume, as shown in figure 6.6.1.

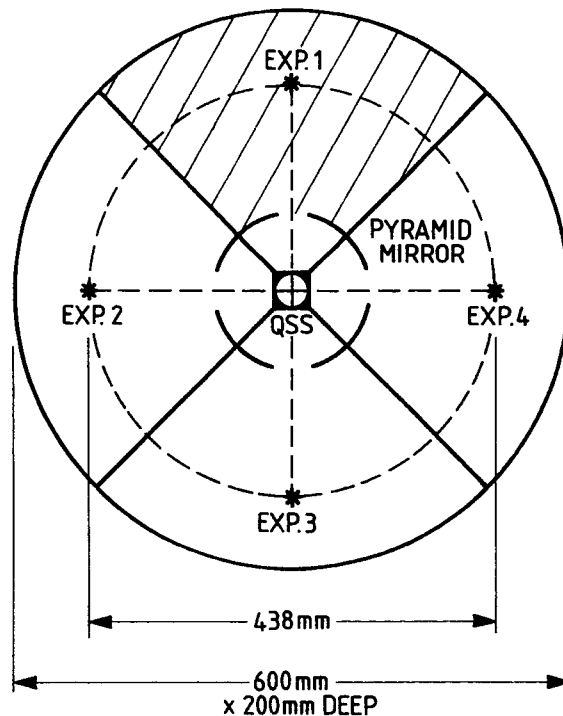


Figure 6.6.1 - Arrangement of the focal plane instruments

The essential parameters for the focal plane instruments are given in Table 6.6.1.

	Within FPA	Outside Cryostat
<u>Mass</u> Spectrometer Photometer IR Camera	Total budget 30 Kg 10 Kg for <u>each</u> 8 Kg 2 Kg	preamp 1.6 Kg main 7 Kg preamp 3 Kg main 7 Kg 7 Kg
<u>Dimensions</u> Spectrometer Photometer IR Camera	Within focal plane volume as shown in figure 6.6.1	preamp .2x.15x.05(m ³) main .2x.15x.2(m ³) preamp .2x.15x.1(m ³) main .2x.15x.15(m ³) .15x.2x.15(m ³)
<u>Temperature</u>	Instrument mounting plate 8 K ± 1 K Ge:x detectors 3 K	+ 20 to + 40°C operating - 20 to + 40°C non-operating and switch on
<u>Dissipation</u> Spectrometer <u>each</u> Photometer IR Camera	2.4 mw at 3 K cont. 21.8 mw at 8 K cont. 10.8 mw operating 3.4 mw operating 10 mw operating QSS 1 mw at 8 K	preamp 1 w main 13 w preamp 1.5 w main 8.5 w 40 w
<u>Cables</u>	254 coax or twisted pairs	
<u>Data Handling</u>	Only 1 expt. active at a time. 30 Kbps for data and instrument house- keeping	

Table 6.6.1 - Model Payload Parameters

7. ISO SYSTEM DESIGN

7.1 Design Philosophy

7.1.1 Technical Objectives

The two major objectives for ISO are:

- . to perform spectroscopic and photometric observations of selected astronomical sources/regions at infrared wavelengths (longer than 2 microns) at a sensitivity which approaches the limit set by the zodiacal background radiation.
- . to provide these facilities to guest astronomers as an observatory facility operating in real-time around-the-clock in a similar way to IUE, for a mission duration of at least 18 months.

The elements contributing directly to the ISO system performance for achieving these objectives are:

The telescope performance which is a function of:

- the optical subsystem design (image quality)
- the straylight rejection
 - . off-axis rejection
 - . diffraction
 - . thermal self emission.
- the telescope pointing accuracy and stability.
- . The detector performance which is a function of:
 - the detector temperature;
 - the background temperature;
 - the particle radiation.
- . The mission lifetime which is related directly to the thermal loads reaching the cryogen tanks by radiation, and by conduction through MLI, structural elements and cables. The cross section of the structural elements is dictated by the mechanical environment of the launch.
- . The ground and sky coverage which are essentially dictated by the orbit, the spacecraft attitude limitations and the number of ground stations.

7.1.2 Computer Aided Design

Computer programmes were used to support the design, guide the trade-offs and selection, and provide an immediate feedback on the system performance. Examples are:

- . The ISO orbit analysis provides basic information on the steady state and transient environment to which the spacecraft would be exposed during the 18 months of lifetime. The on-orbit heat fluxes radiated by the Sun and Earth were essential to the thermal control design. The particle radiation fluxes, resulting from the crossing of the belts, were used to establish the impact on instrument detector performance, and to size the shielding required by the solar cells or other sensitive electronics components to perform adequately until the end of mission.
- . The structural analysis based on NASTRAN computer programme, was used to ensure the integrity of the structural design during the severe launch conditions. This aspect has direct implications on the telescope temperatures and cryogen consumption as discussed in 7.1.1. It was also used to establish the thermal/structural deformation (drift) occurring on orbit between the telescope line of sight and the star tracker. This aspect is important to the establishment of the pointing performance.
- . The thermal analysis was essential to determine the cryogen consumption rate (lifetime) and the temperature levels in critical areas such as telescope optics, baffle, sunshade and Focal Plane Assembly. Both on-orbit and ground (pre-launch) conditions were modelled. The latter was used to simulate a variety of situations such as up to four postponements of the launch, an abort and then launch within the same campaign.
- . Stray light analysis was essential for establishing the overall performance of the ISO facility, particularly at the longer wavelengths.

The analysis was performed with GUERAP to establish the contribution to the straylight by the telescope (self-emission) and by the baffle/sunshade design (off-axis rejection) taking into account the avoidance requirements with respect to Sun, Earth, Moon and Jupiter.

- . Ray tracing analysis was used to define the image quality of the optical system and to define the tolerances on the structural elements supporting the mirrors. This established the tolerable axial and lateral displacements and the tolerable tilt.

These results were essential to assess the need for an active focus control mechanism versus passive compensation materials for the cooled telescope.

- . Extensive simulations were performed to establish the pointing performance both in steady state and in transient conditions and to assess the impact of these performance onto the image quality.

7.1.3 The Low Risk-Low Cost Approach

The ground rule which has guided most of the technical and programmatic decisions of the ISO project has been to minimize the risk in the most cost effective manner.

This principle departs from the pure low cost approach, and results from the following:

- . a protoflight approach, with its initial attractive low cost figure, would not be appropriate to a complex spacecraft such as ISO
- . the cost of a project is essentially driven by:
 - complexity (management, design, testing, operations, etc.)
 - mass (launch-vehicle)
 - manpower involved.

The risks and costs associated with complexity can often be minimized by using experience gained in similar projects. Europe has gained experience in areas such as space cryogenics, large optics and infrared detectors through IRAS, GIRL and other technology programmes (CRHESUS)

Similarly the experience gained through observatories such as IUE, EXOSAT and to a certain extent IRAS provides an excellent basis for defining the ISO Ground Segment concept.

For the Service Module, all subsystems are selected to be conventional.

The mass of a spacecraft is the prime driver for the launch cost. If the spacecraft mass is below a certain threshold (1100 kg for a standard Ariane II Geostationary Transfer Orbit) a dual launch is possible and launch costs are divided by almost 2. Above this threshold and within the Ariane II launch capability there is no need however to constrain mass per se. It is often more rewarding to decrease design or manufacturing complexity at the expense of mass.

Along the same line, it can be advantageous to include generous margins in the design to decrease the level and complexity of the test programme, verification being achieved by worst case analyses. This approach was implemented on ISO once it became obvious that an Ariane II/III dual launch was impossible. An exception to this approach is found in the design of the inner elements of the cryostat where mass results in thick suspension straps and therefore reduces the lifetime of the cryogenics.

Manpower is a major contributor to the cost of a project. Any risk taken in the design or the schedule may result in programme extensions and thereby higher costs.

To this effect the following decisions were taken:

- a) to decouple as much as possible, the conventional Service Module from the more complex Payload Module. This modular approach allows parallel development with minimum management of interfaces,
- b) to phase the development of both modules in such a way that Service Module detailed activities would start at full effort after consolidation of the Payload Module design,
- c) to minimize the manpower in the early phase of the project (phase B) and at that time perform extended theoretical and hardware development work on the Payload Module in conjunction with the overall ISO system definition.

7.2 System Configuration Description

7.2.1 ISO Spacecraft Configuration

The ISO spacecraft configuration, as shown in Figure 7.2.1 and 7.2.2 is modular with a physical separation between a Payload Module (PLM) and a Service Module (SVM). The modularity is required to maintain maximum autonomy in terms of development, integration and testing of both modules. The Ariane II usable volume, shown in dotted line in Figure 7.2.1 restricts the maximum diameter and length of ISO.

The PLM configuration has been centred on the telescope design, covered in paragraph 9.4, and on the cryostat whose dimensions are dictated by the 18 months operational lifetime requirement. The SVM conical configuration is required to interface on one side with the Ariane launch vehicle through an 1.194m diameter adaptor, and on the other side with the PLM which has a diameter of about 2 metres.

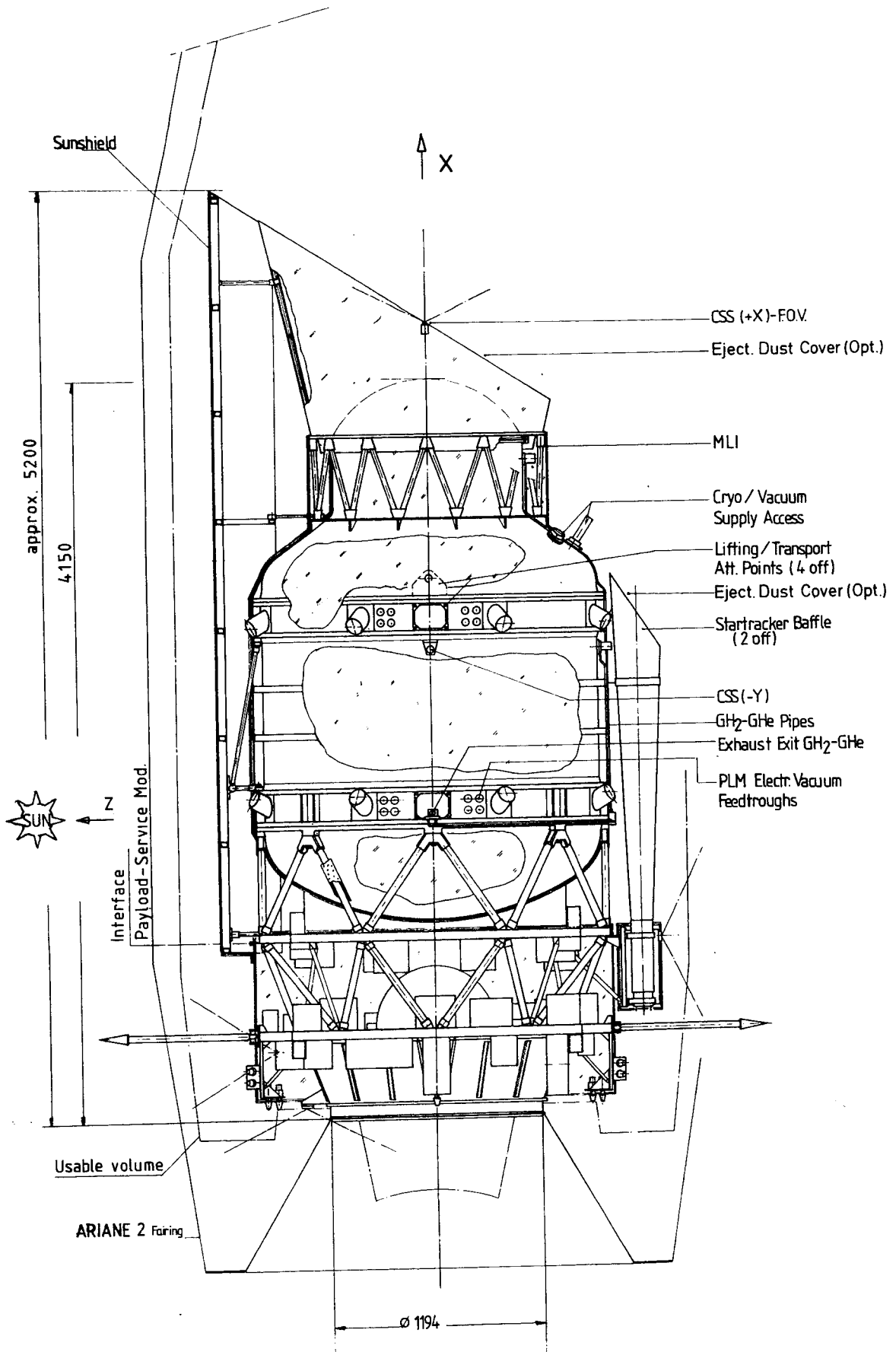
7.2.2 The Payload Module Configuration

The main features of the PLM are shown in Figure 7.2.3 and 7.2.4. It consists of:

- a) The cryostat, with a dual open loop cryogenic system, using 750 litres of liquid hydrogen (LH₂) and 750 litres of superfluid helium (He_{II}). The He_{II} is used to maintain the following temperature levels:

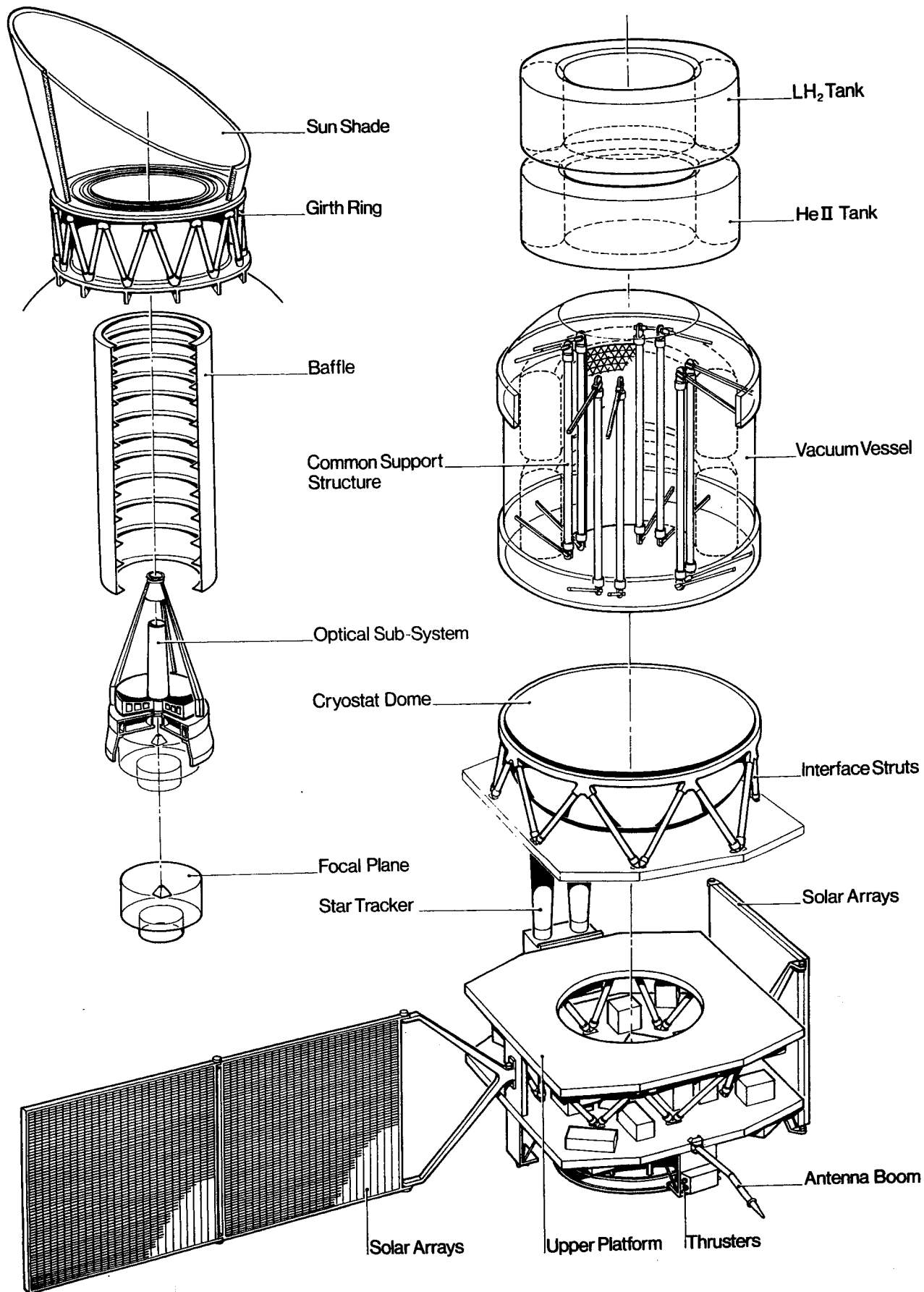
- ge detectors	3K
- Scientific Instruments	7K
- Mirrors	10K
- Baffles	20-40K

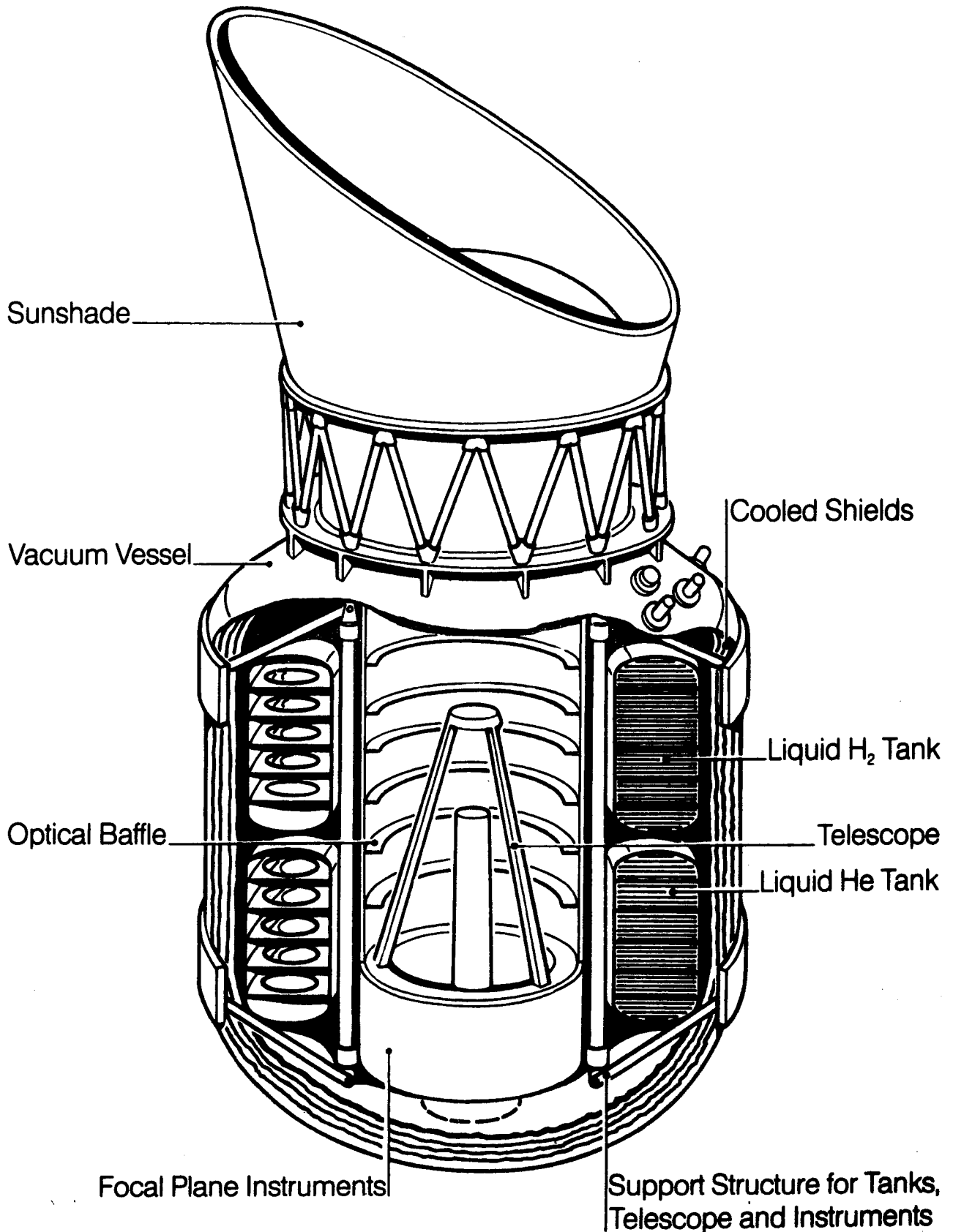
The LH₂ is required to absorb most of the external heat input to the cryostat. It cools the radiation shields surrounding both the He_{II} and LH₂ tanks. Access to the scientific instruments, located in the Focal Plane Assembly of the telescope, is gained through the base of the cryostat.



ISO Configuration

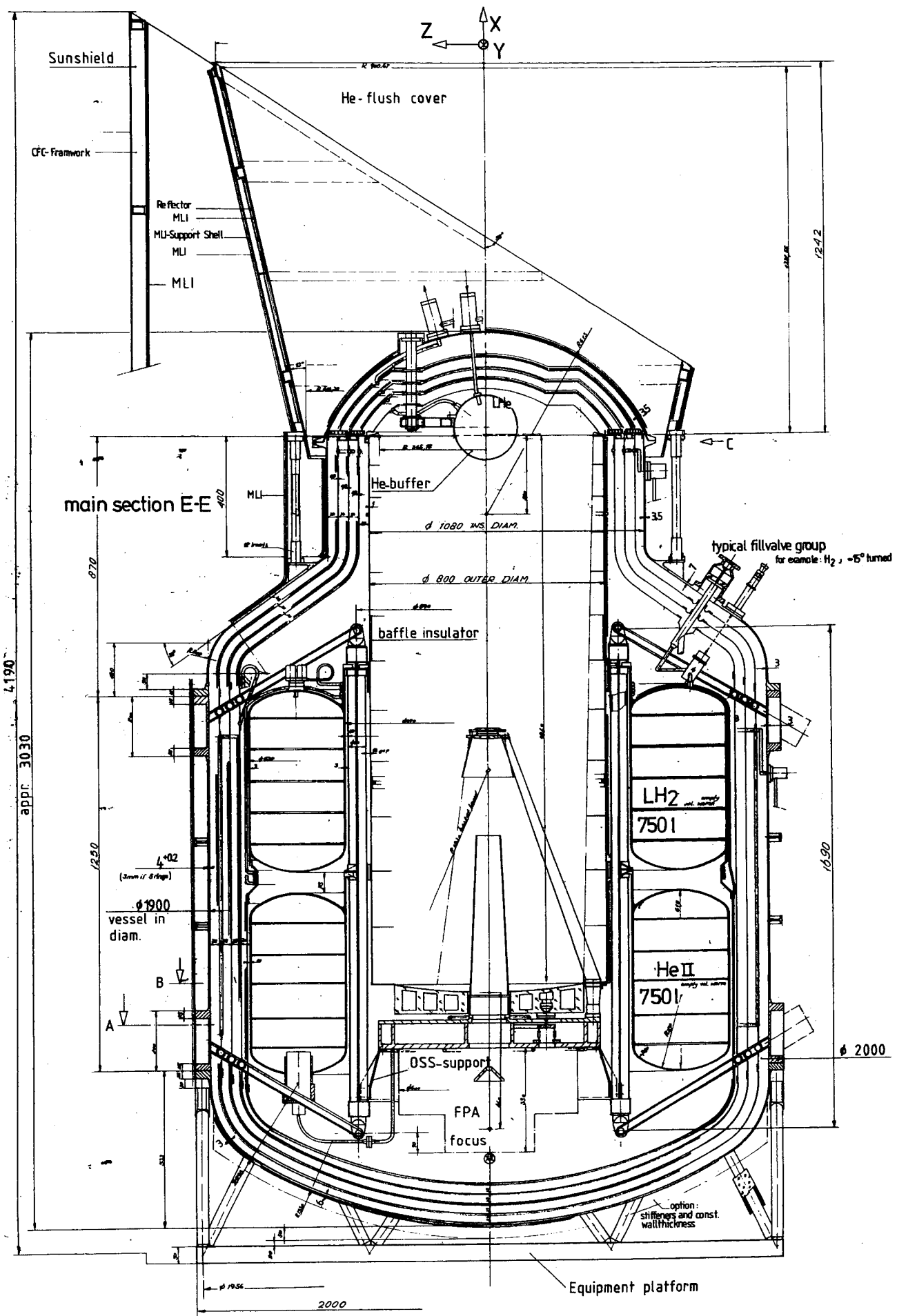
Infrared Space Observatory





ISO Payload Module

ISO Payload Module



b) The Telescope with a Cassegrain optics, a complete baffle system, a sunshade and a Focal Plane Assembly (FPA). The FPA accommodates:

- the four focal plane instruments
- a pyramid mirror to provide each of the four instruments with an unvignetted field of view of 3 arc minutes
- a quadrant star sensor located on a line through the apex of the pyramid mirror to provide the actual line of sight of the telescope.

The FPA is mounted on the lower side of the optical support structure, while the optical system (mirrors and tripod) is mounted on the upper side (Figure 7.2.2).

c) The Sunshield, covered on one side with a reflective and electrically conductive surface (OSR) and on the other side by Multilayer insulation, is mounted with Glass Fibre Compound (GFC) struts to the cryostat vacuum vessel.

d) The Sunshade, designed to fulfil the pointing constraints with respect to Sun, Earth, Moon and Jupiter, is supported by the vacuum vessel through a Carbon Fibre Compound (CFC) structural framework.

e) An ejectable cover, equipped with a LHe flush cooling system to maintain a low temperature at the cover inner side during ground testing or prior to launch. This cover will be ejected once the spacecraft is in its operational orbit, about 11 to 14 days after launch.

The interface with the SVM is formed by a platform connected to the cryostat lower flange with a 16 CFC strut framework. This upper platform belongs to the PLM. It carries all experiment preamps and main electronic units together with the cryostat electronics and the instrumentation box (Figure 7.2.5),

7.2.3 The Service Module Configuration

The SVM has a conical shape and consists of:

- a 16 strut framework made from carbon fibre composite to minimize the heat transfer between the SVM and the PLM. These struts are fixed at eight hard points at the SVM main platform and PLM equipment platform they provide a well defined load path and good accessibility.
- A main octagonal platform (aluminium honeycomb) which carries the SVM equipment (Figure 7.3).
- A main cone which distributes the structural loads evenly to the launcher interface.
- The solar panel wings, each consisting of two panel frames. These are attached to the SVM via hinged yokes.
- Two star trackers are bracket mounted to the SVM/PLM interface platform.
- Two antenna booms and 16 thrusters are mounted on the lower part of the SVM.

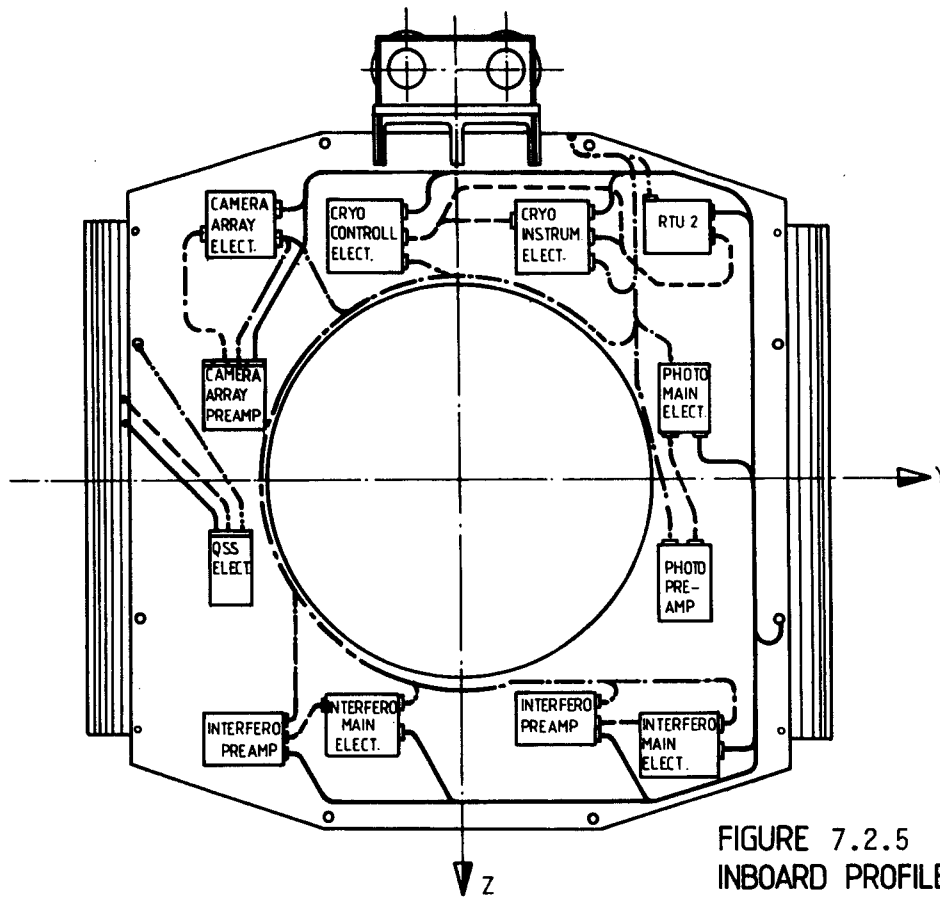


FIGURE 7.2.5
INBOARD PROFILE & HARNESS ROUTING:
BOTTOM VIEW OF EQUIPMENT PLATFORM

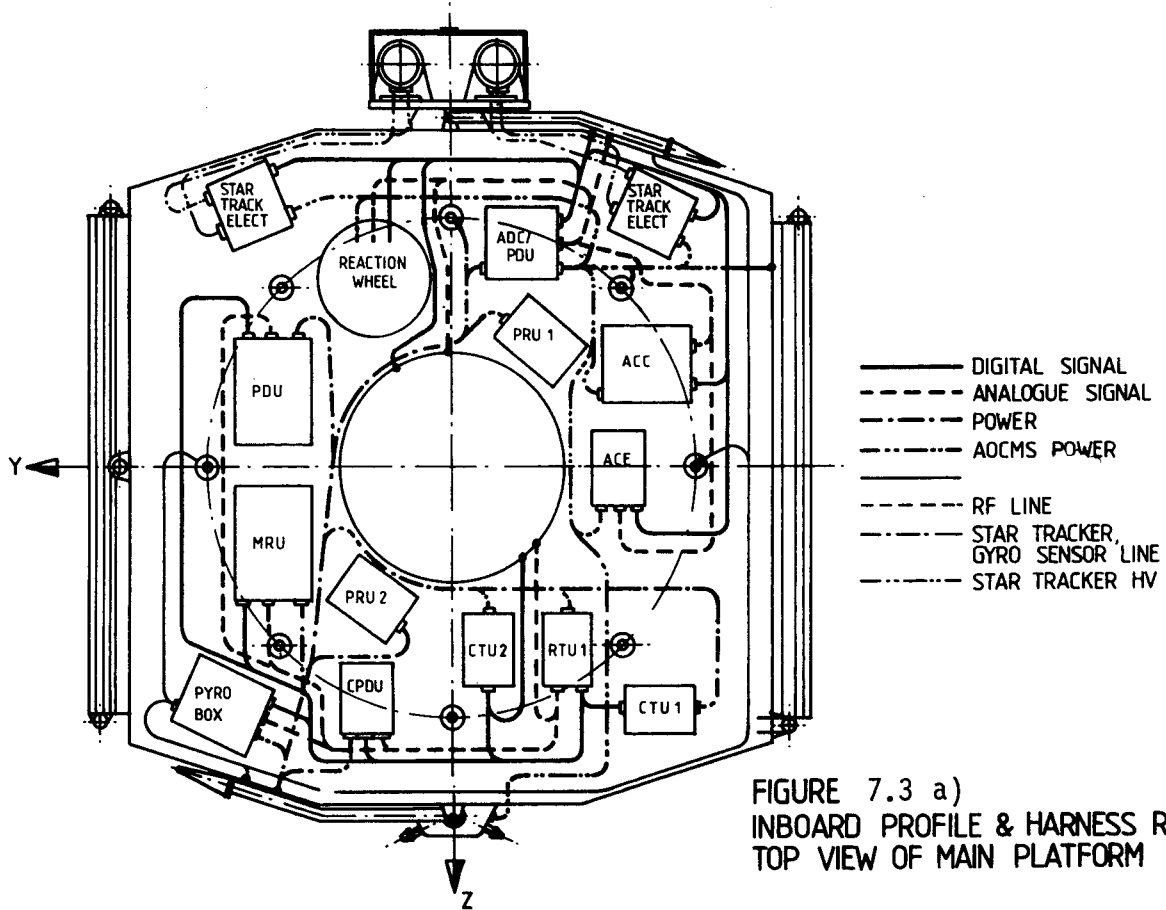


FIGURE 7.3 a)
INBOARD PROFILE & HARNESS ROUTING:
TOP VIEW OF MAIN PLATFORM

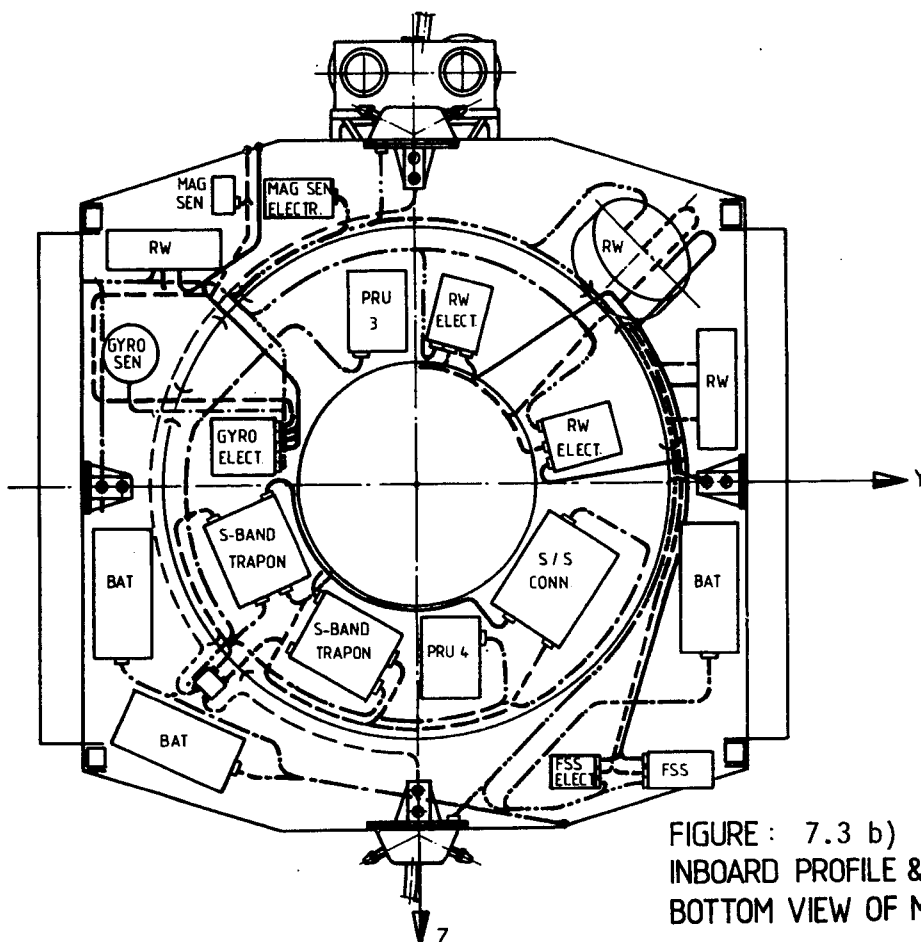


FIGURE : 7.3 b)
INBOARD PROFILE & HARNESS ROUTING:
BOTTOM VIEW OF MAIN PLATFORM

7.2.4 Configurations Trade Off

Several configurations were analysed during the study at system level as shown in the flow diagram of Figure 7.4 and illustrated in Figure 7.5 (a through h). The various options are summarized as follows:

- a) Mounting the telescope external to the cryostat resulted in optics temperatures far above requirements.
- b) A spherical central H₂ tank, attractive in terms of mass saving, is bad for accessibility to the Focal Plane Assembly.
- c) The coaxial tank configuration leads to increased tank mass, which means thicker supporting struts, higher heat leakage in the cryogen tanks and reduced lifetime.
- d) Toroidal tanks with circular cross section require a large vacuum vessel. Tanks with an elongated cross section lead to a lighter vacuum vessel and allow easy adjustment of the relative tank sizes by small changes in the bulkhead dimensions. This provides excellent programme flexibility.
- e) The vacuum vessel and final toroidal tank dimensions were optimized for minimum mass and manufacturing costs.
- f) A Sunshield is required since its use increases the expected mission lifetime by about 200 days.
- g/h) Solar arrays are attached to the SVM for modularity reasons. In addition, thermal analysis showed that the introduction of a yoke hinged mechanism would provide a better thermal radiative decoupling between the warm arrays and the cryostat, leading thus to a longer cryogen lifetime.

7.3 System Functional Description

- . All essential units with their external/internal interfaces are depicted in Figure 7.6.
- . RF up and downlink is accomplished via two deployable hemispherical coverage antennae with two S-Band transponders (Exosat). The antennae are deployed just after separation from the third stage of Ariane.
- . The On-Board Data Handling (OBDH) is designed according to ESA standards and consists of:
 - 1 internally redundant Command and Power Distribution Unit (CPDU) which decodes and verifies telecommands, and distributes serial load commands to the Central Terminal Unit and high level on/off commands directly to users.
 - 2 Central Terminal Units (CTU), one operating and one in cold redundancy, for telemetry format generation and OBDH bus control.
 - 2 OBDH busses (one operating, one in cold redundancy) with interrogation and response lines.
 - 2 Remote Terminal Units (RTU), one dedicated to the PLM, one dedicated to the SVM, for distribution of memory load, low level on/off commands and collection of telemetry data.

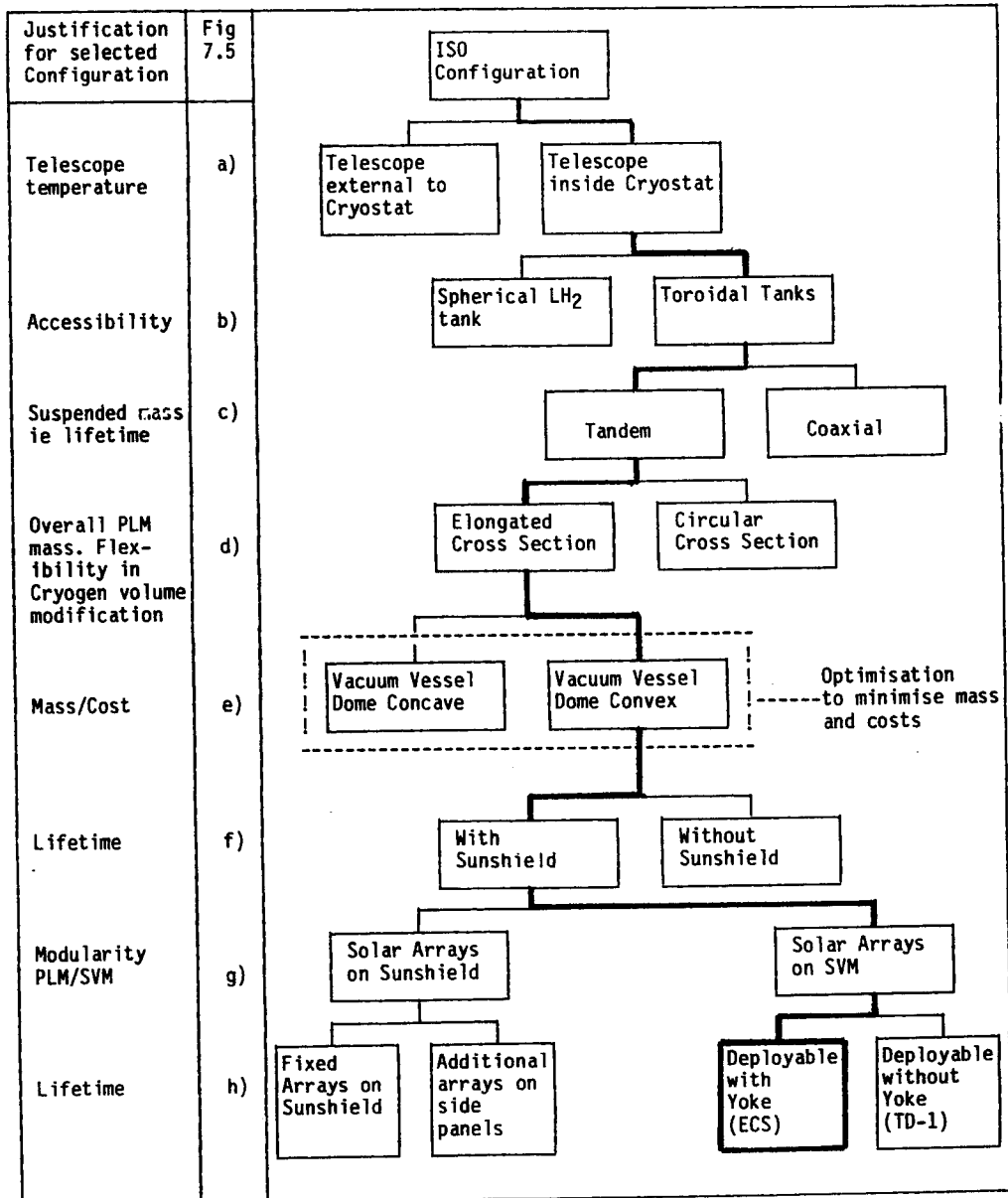
- . The Power Subsystem consists of:
 - The deployable solar arrays consisting of two hinged panels in a Z-shaped configuration which avoids CG shift during deployment. The deployment occurs just after separation from Ariane launch vehicle third stage.
 - The Main Regulator Unit which controls the main bus voltage (+ 28V) by means of three nondissipating shunt regulators and supervises charging/discharging of three battery groups during sunlit/eclipse periods.
 - The convertor providing + 5.5V, \pm 16V to related users.
 - The Power Conditioning and Distribution Unit which distributes the main bus (+ 28V) via switches to users and provides thruster supply and signal conditioning.
 - The Pyro units which provide the ignition current to pyrotechnic users via related safety circuits fed from the batteries.

- . The Attitude and Orbit Control and Measurement (AOCMS) is similar to that of IRAS. It consists of:
 - An internal five line bus to which all subsystems are linked.
 - The Attitude Control Computer (ACC) with the main function of attitude determination from sensor data (Quadrant Star Sensor in FPA for Telescope Line of Sight reference, sun sensors, star trackers, Gyros and magnetometer) and generation of actuator commands (reaction wheels, reaction control thruster). The interface with the OBDH is done via the SVM-RTU.
 - The Analogue Digital Convertor/Power Distribution unit performing A/D conversion of AOCMS analogue signals and AOCMS internal power distribution.
 - The Attitude Control Electronics with interface electronics for Coarse Sun Sensors and Reaction Control Systems accomplishing watchdog function for correct subsystem operations.

- . All experiment preamps and main electronics units are placed on the upper equipment platform close to the PLM/RTU, from which they accept memory load commands and transfer telemetry data to it.

- . The cryostat electronics with the instrumentation box (constant current/power supply and signal conditioning for phase detectors, temperature/pressure flow sensors) and the control box (control of phase separator valves, vent valves, on/off switching of heaters) guarantees correct function of the subsystems.

- . All electrical units within the cryostat vessel (experiment detectors, QSS, cryostat sensor, heaters and valves) will be connected with their associated electronics via vacuum tight connectors located at the lower and upper flange of the vacuum vessel. The vacuum vessel internal harness is composed mainly of stainless steel to minimize heat input to the cold parts.



Major ISO Configurations Trade Off

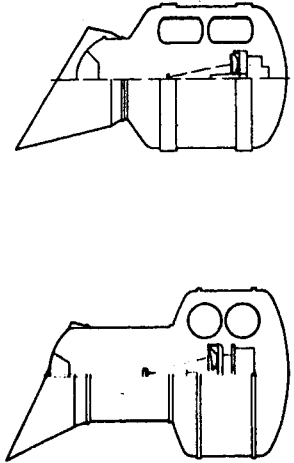
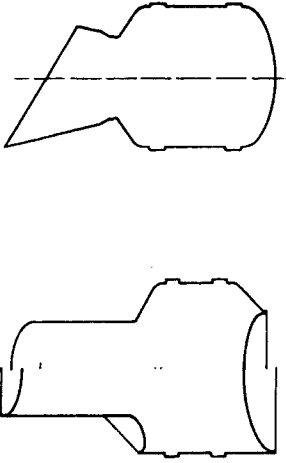
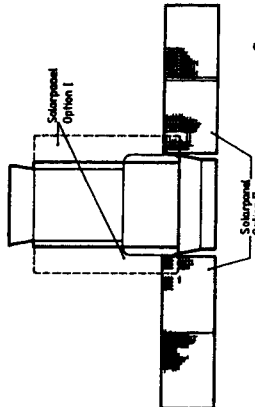
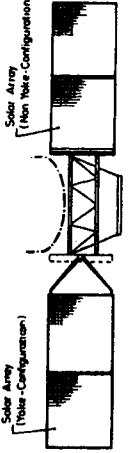
<p>Circular versus elongated tanks</p>		<p>Configuration optimisation</p>	
<p>Solar panels on PLM versus SVM</p>		<p>Solar panels with or without yoke</p>	

Figure 7.5 (continued) Configuration Trade-Off

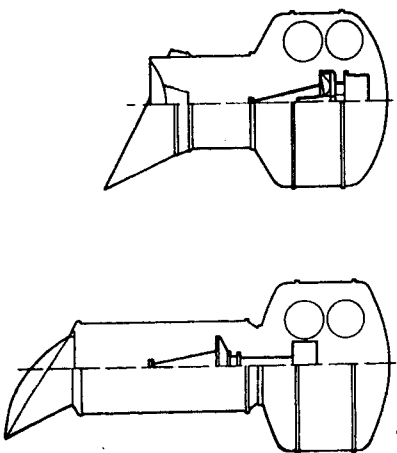
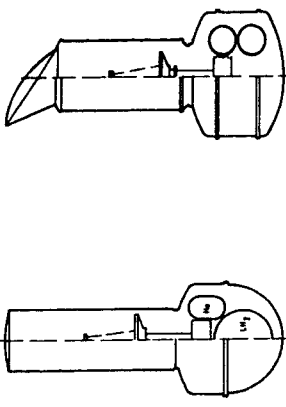
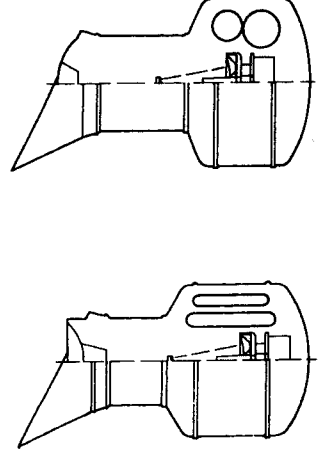
<p>Telescope outside versus inside Cryostat</p>		<p>Spherical LH2 versus toroidal LH2</p>	
<p>Coaxial versus tandem tanks</p>			

Figure 7.5 Configuration Trade-Off

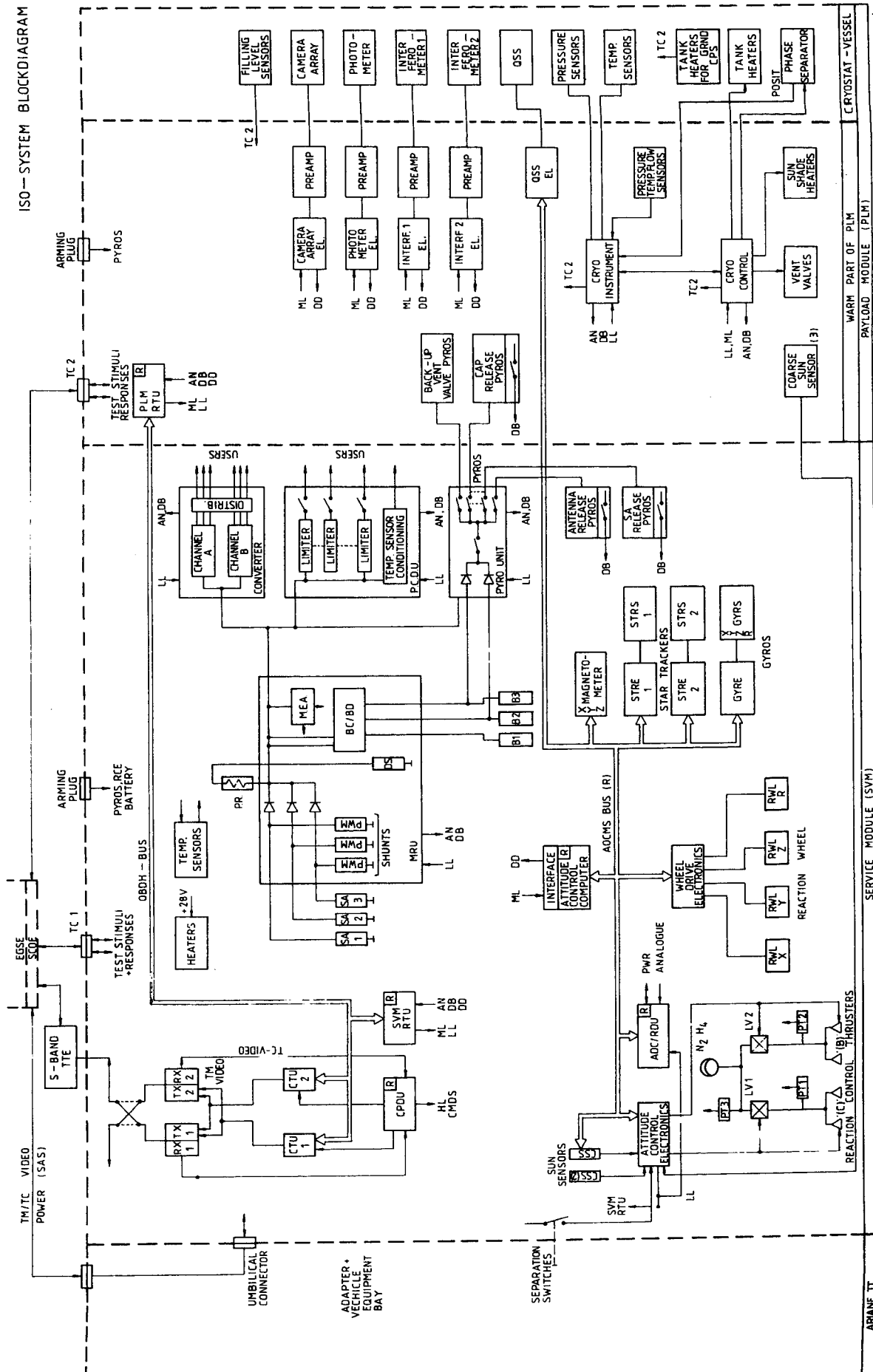


Figure 7.6 ISO Functional Block Diagram

8. LAUNCH and ORBIT ANALYSIS

8.1 Orbit trade-off

The orbits indicated in figure 8.1 were considered:

- . Near Earth Orbits were abandoned since they would neither allow long uninterrupted observation periods on selected sources, nor real-time operations due to the limited ground coverage. Apart from the 12-hour synchronous elliptical orbit, all the orbits require heavy and expensive on-board propulsion system and launch vehicles. The 12-hour synchronous elliptical orbit has the following advantages:
 - It permits long uninterrupted observations (up to ten hours) on selected fields.
 - It requires a very simple and light hydrazine motor to increase the perigee height from 200 km (Standard Ariane Geostationary Transfer Orbit) to the required 1,000 km to minimize atmospheric drag and contamination.
 - It results in a spacecraft mass at launch compatible with the smallest and cheapest version of Ariane (Ariane II or Ariane IV 0 single launch).
- . The 12-hour synchronous elliptical orbit has the following disadvantages:
 - For continuous operation it requires two ground stations Villafranca (Spain) and Carnarvon (Australia). As both stations are not exactly 180° apart in longitude, the downlink is lost for about one hour around perigee. The costs of running an additional station are marginal when compared to those generated by providing a heavy and expensive on-board propulsion system and launch vehicle.
 - Passage through the Earth radiation belts (figure 8.2) disturbs the experiment detectors for approximately two hours centred around perigee. Observations during this time are suspended.

8.2 Launch Vehicle Selection

The estimated spacecraft mass at launch (see paragraph 10.1) of about 1800 kg is compatible with:

- (a) an Ariane II or Ariane IV 0 single launch;
- (b) an Ariane IV 4P/4L dual launch.

On the basis that spacecraft designed for Ariane II are compatible with an Ariane IV single or dual launch (and not vice versa), and that very little technical and cost information was available on Ariane IV at the start of the study, Ariane II is selected as the reference launch vehicle for the ISO technical design.

The actual launch vehicle selection will be done when the detailed cost information is available for the Ariane IV family.

8.3 ISO operational orbit

The selected operational orbit for ISO is a synchronous 12-hour orbit with the following characteristics (osculatory elements at perigee):

Perigee height	1,000 km
Apogee height	39,395 km
Eccentricity	0.722
Inclination (with respect to equator)	5.250°
Orbit period (synodic)	11.977 hours
Argument of perigee at start of operations	142°

Orbit maintenance:

Requirements for an orbit maintenance have been determined taking into account the following perturbations resulting from Sun, Moon, Earth gravity potential (6 zonal and 5 tesseral harmonics). Solar radiation and air drag effects are negligible.

The analysis shows that the maximum delta-V required for all the mission duration is approximately 6 m/s. During the mission lifetime a maximum of 2 manoeuvres is foreseen, to be performed at apogee passes within the following windows:

- . first 50 days of operation
- . between 220 to 300 days, or
- . between 470 to 540 days.

8.4 Launch Window

- . The selection of a launch window is based on the following:
 - minimize eclipse times,
 - satisfy the angular constraints between the telescope line of sight (X-axis) and Sun/Earth, to avoid direct radiation into the telescope baffle and to satisfy the same solar angle constraint at orbit injection.
- . Basically there are four injection periods per year as follows:

Launch Date	Time	Eclipse
2 September - 2 November	Midnight	66 min
11 March - 5 May	Midnight	66 min
13 June - 12 August	Noon	72 min
3 December - 24 January	Noon	77 min

The autumn launch window is taken as the baseline because:

- a) The spring window requires slightly more complex S/C attitude manoeuvres around perigee pass when Sun is on the perigee side of the orbit, to avoid direct Earth radiation into the telescope baffle.
- b) The winter and summer launch windows yield higher eclipse time. In any case, the batteries have been sized for an eclipse duration of 80 minutes.

8.5 Drift Orbit

After separation from the Ariane launch-vehicle, ISO will spend approximately 11 days on a drift orbit during which most of the spacecraft outgassing will take place. Following this the acquisition of the operational orbit is initiated. This involves at least three apogee manoeuvres as follows:

Delta V_1 = 22 m/s (perigee raise to 450 km on third apogee)
Delta V_2 = 49 m/s perigee raise to 1000 km
Delta V_3 = 5 m/s fine correction

8.6 The Sky Coverage

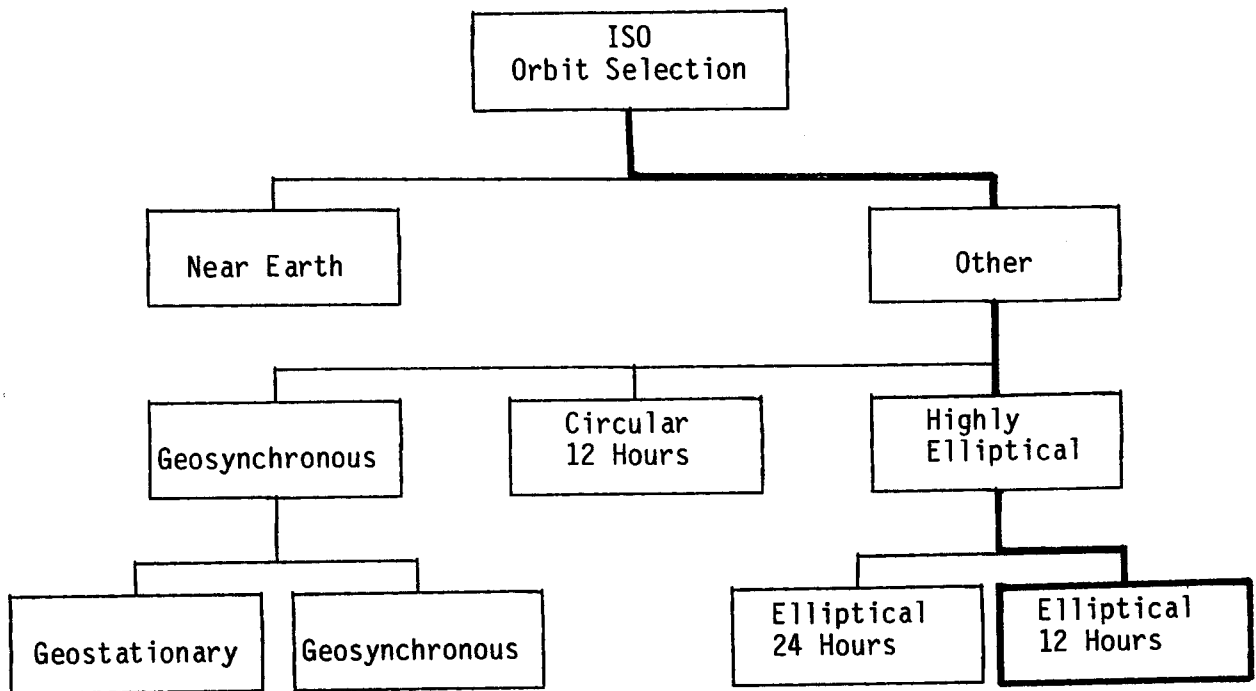
- Figure 8.3 shows the evolution of the spacecraft orbit with respect to Sun during the 18 months lifetime. The rotation of the apsidal line is about 0.7 degree per day.

- Constraints for the celestial sphere coverage are as follows:

- the Sun direction is maintained in the spacecraft (X,Z) plane. The Solar panels are fixed (low cost) along the Y-axis. The spacecraft attitude can rotate by $\pm 30^\circ$ around the Y-axis.
- straylight considerations lead to following constraints:

Earthlimb - X axis	77 degrees
Moon - X axis	24 degrees
Jupiter - X axis	5 degrees

- observations are suspended a couple of hours around perigee.
- Results are displayed in the form of contour lines in terms of
 - total percentage of observation time: a contour line of 10% means that the enclosed area of the sky is available in total for a duration of 54 days
 - longest uninterrupted observation periods: in the area external to a contour line of 6 hours there is at least once during the mission the possibility to observe for 6 hours without interruption
 - Figure 8.4 shows that the minimum observation time is about 3% (16 days) at coordinates 6hr, 30° . The maximum observation time is 80% (14 months) at coordinates 18hr, -85° .
 - Figure 8.5 shows that a minimum of 4 hours of uninterrupted observation is at least once available at coordinates 6hr, 30° . The longest uninterrupted observation period is about 10 hours.
 - Further analyses showed that shifting the launch date influences the sky coverage so that it could be possible if required to select the areas of maximum coverage in function of scientific interest.



Estimated spacecraft operational mass ~1700 kg

Orbits	Near Earth	Geostationary $i = 0$	Geosynchronous $i = 5.25^\circ$	1) Circular 12 Hr	2) Elliptical 24 Hr	1) Elliptical 12 Hr
Criteria						
Observation	≤ 1 hr	> 1 hr continuous	> 1 hr continuous	> 1 hr 5 hr x 2	> 1 hr continuous	> 1 hr 11 hr x 2
Down link	≤ 1 hr					
Propulsion						
- Delta-V		1500 m/s	1500 m/s	1400 m/s	800 m/s	76 m/s
- Type		bi-liquid	bi-liquid	bi-liquid	bi-liquid	hydrazine
- Mass		1500 kg	1500 kg	1300 kg	700 kg	140 kg
- Cost		~ 8 MAU	~ 8 MAU	~ 8 MAU	~ 8 MAU	~ 1.7 MAU
Launcher (single launch)		AR IV 4L	AR IV 4L	AR IV 2L	AR IV 4P	AR II or AR IV 0

Figure 8.1 - ISO Orbit Selection Process

Note

- 1) Require 2 stations eg Villafranca (Spain) and Carnarvon (Australia)
- 2) One ground station. Perigee height: 16000 Km.

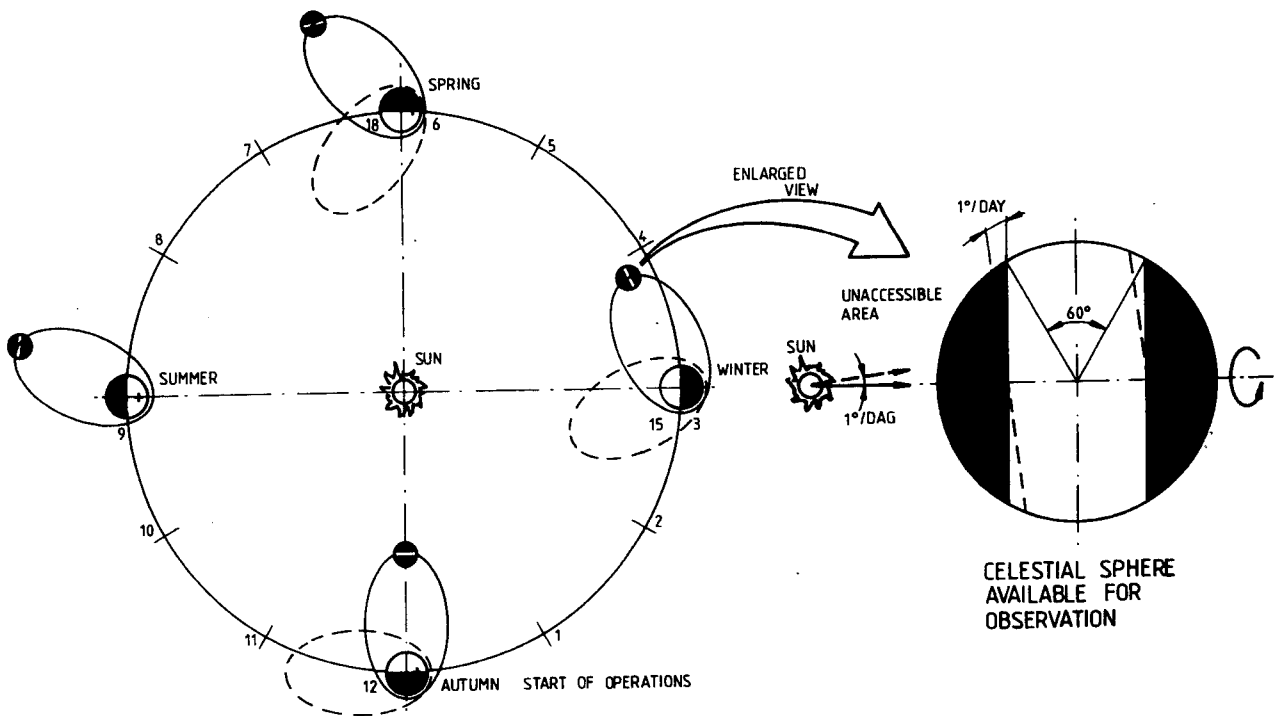
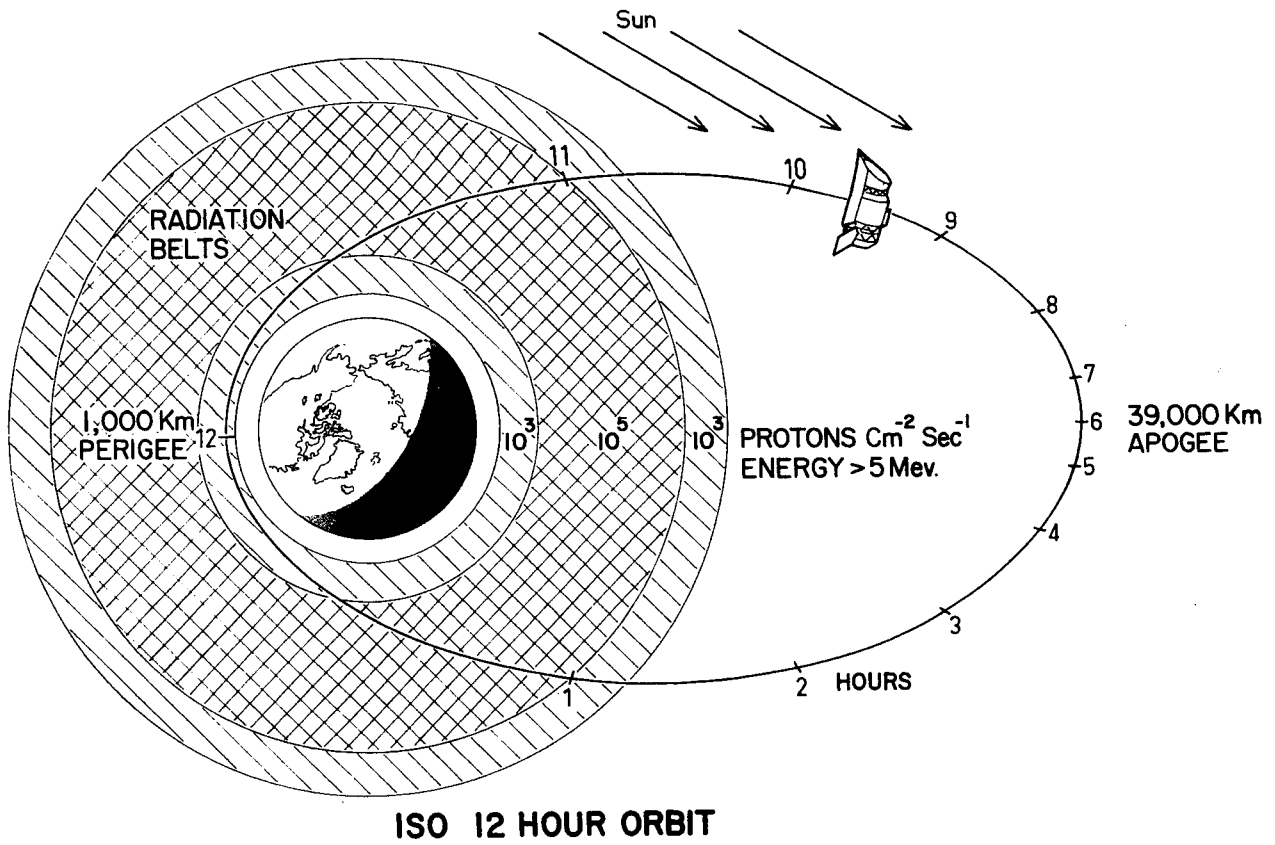


FIG. 8.3

FIG.8.4 % OF OBSERVATION TIME WITH MOON, SUN AND EARTH CONSTRAINT
88/10/2 - 90/3/25

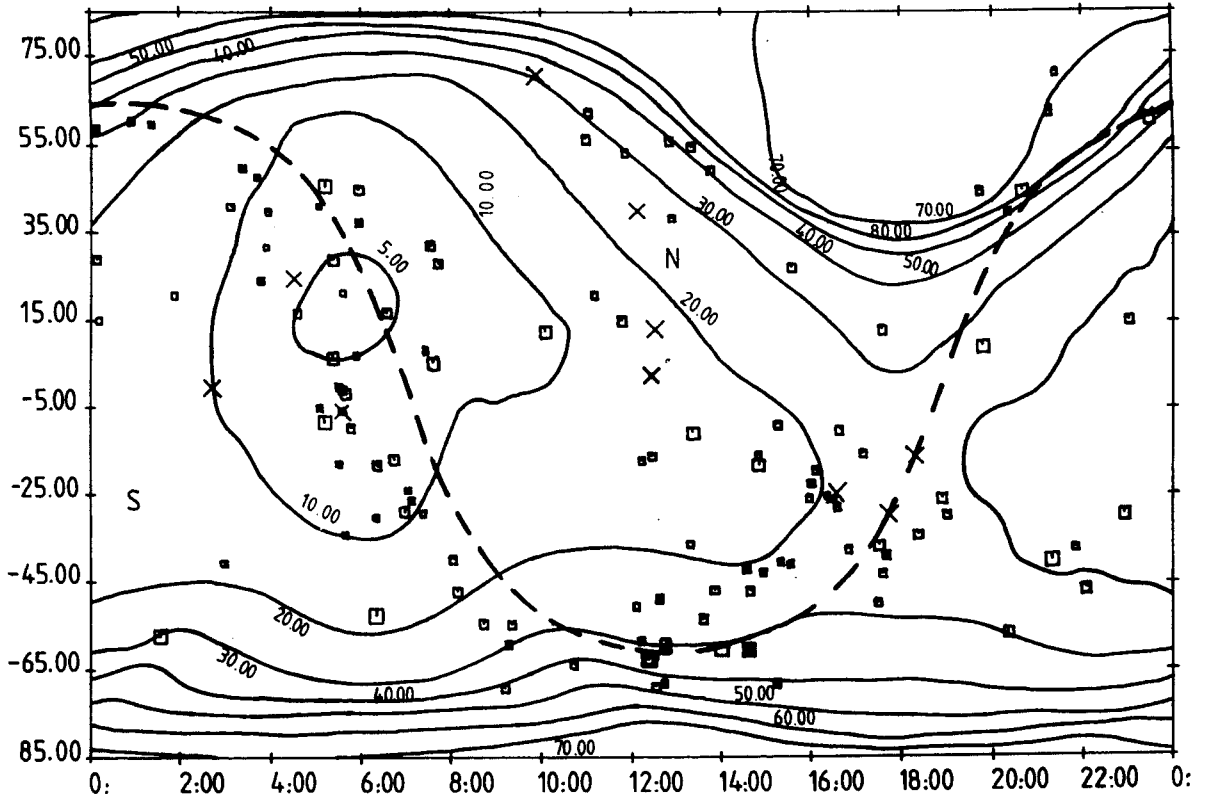
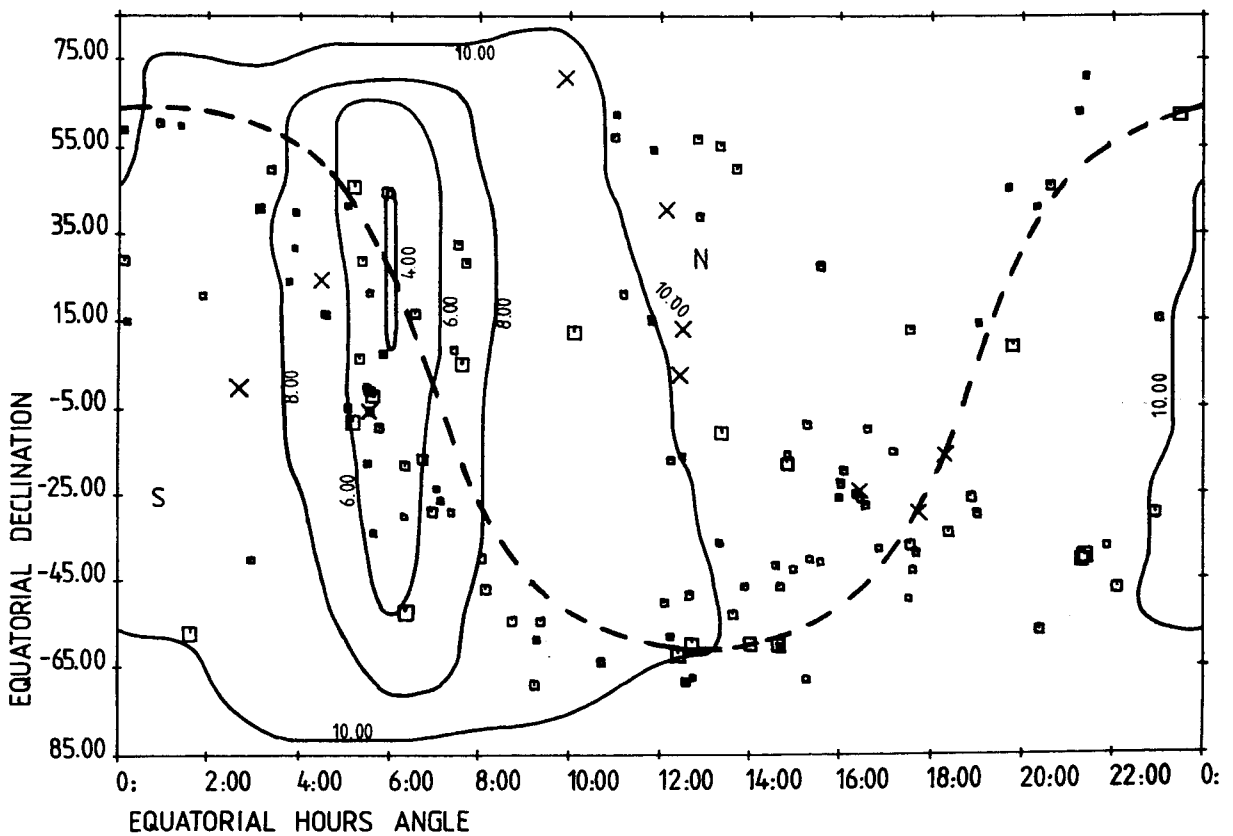


FIG.8.5 LONGEST UNINTERRUPTED OBSERVATION PERIOD (HOUR)
88/10/2 - 90/3/25



9. SUBSYSTEM DESIGN AND PERFORMANCE

9.1 The Structure Subsystem

9.1.1 The Payload Module Structure

The Payload Module Structure consists of two main sub-assemblies:

- a vacuum vessel, whose primary purpose is to provide adequate strength against pressure-induced and flight-induced loads, along with attachment points for the telescope.
- a Common Support Structure, carrying the telescope, the cryogen tanks, the Focal Plane Assembly and all components e.g., tubing, cabling and valves, which are located inside the vacuum vessel.

The vacuum vessel is one of the heaviest components, contributing as much as 25% of the total Payload Module weight. As a consequence, its dimensions (height, diameter) are optimised to have the minimum possible total weight for a given cryogen volume. Since the baffle diameter is fixed, the diameter of the vacuum vessel is dictated only by the shape of the cryogen tanks.

Analysis shows that the minimum overall weight is obtained with two toroidal tanks of elongated cross-section, having a height-width ratio of roughly 2. Reduction of vacuum vessel diameter with respect to a configuration with two tanks of circular cross-section, achieves a weight gain of about 7%, or 20 Kg. The chosen configuration also provides a better protection of the telescope baffle against incoming thermal radiation, as this is almost completely surrounded by cryogen tanks, and leads to better growth flexibility of the tanks. The vacuum vessel was designed to standard German pressure vessel design rules, assuming a safety factor of 3 against buckling, and very conservative empirical design data were used.

Loads from the internally suspended payload are transferred to the vessel through two girth rings, via 16 attachment points for Glass Fibre straps. The lower girth ring also serves as the interface to the Service Module through 16 Carbon Fibre struts.

The internal Common Support Structure provides the most challenging aspects of the structural design, due to the contradictory requirements of low mass, extremely low thermal conductivity and very high strength and stiffness. The chosen configuration consists of 8 Carbon Fibre struts connected by two octagonal rings and an isogrid-type shear web made of filament-wound carbon fibre. Each strut is suspended on the vacuum vessel by means of two Glass Fibre straps, of chain-lug construction. The two tanks are suspended by the 8 struts via bolted brackets, and the Focal Plane Assembly, the mirrors and the baffle are all carried by a conical structure, made of Carbon Fibre and bolted to the lower end of the Common Support Structure.

The main design requirement is a minimum cross-section for both the Glass Fibre struts and the Carbon Fibre struts, to minimise heat leaks into the tanks and to the telescope itself. A conservatively high level of acceleration is specified (15g) both in the axial and in the lateral directions. Since the suspended mass is about 700 Kg, use of composite materials is mandatory in order to meet all thermal, strength and stiffness requirements.

Structural analysis shows that the lateral acceleration plays a major role in the dimensioning of the whole structure, particularly of the 16 Glass Fibre struts, whose required cross-sectional area is approx. 200 mm². Based on experience gained from previous ESA projects, it is very likely that an Ariane/ISO coupled analysis will result in a substantial decrease of the accelerations presently assumed. Such an analysis is foreseen in Phase B. A reduction of the acceleration levels would allow a consequent reduction in cross-sectional area of the whole payload support structure, with beneficial effects on both the weight and lifetime margins (see paragraph 10.3).

The design of the Common Support Structure is based on the following assumptions:

- a safety factor of 1.5 against rupture is used for composite materials provided sufficient test data existed for the actual configuration implemented in the design;
- conservative (ie 3 sigma) values are used for material properties (strength, modulus, etc);
- where test data did not exist or were not directly applicable to the design configuration, the safety factor was doubled;
- room temperature strength data were used while it is known that at low temperatures material properties show a significant improvement.

The resulting configuration fulfils all strength, stiffness and lifetime requirements.

The Payload Module interfaces to the Service Module via 16 High Modulus Carbon Fibre struts, whose function is to provide a direct load path without thermally coupling the warm Service Module to the cold Payload Module.

9.1.2 The Service Module Design

The Service Module consists of a load carrying cone, a row of Carbon Fibre struts and one platform accommodating all Service Module equipment and services. The upper equipment platform, which functionally belongs to the PLM, was considered part of the SVM for structure analysis purposes and proved to be critical with respect to the overall stiffness requirements of the spacecraft, as was shown by dynamic analysis. Stiffening of the upper platform was necessary.

The two platforms are of honeycomb construction, the upper one having Carbon Fibre face sheets to minimise heat conduction radially towards the interface struts. The lower platform and the cone are made of aluminium alloy.

9.1.3 Overall Spacecraft Analysis

Results of finite element analysis showed that stresses were well below allowable values throughout the spacecraft, even assuming a 50% growth margin for the Payload Module mass, and that the first axial and lateral frequencies were also acceptable, as shown below:

Mode	Required	Achieved (hard-mounted)
First axial	35 hz	37.2 hz
First lateral	10 hz	14.5 hz

All components of the spacecraft were designed against a fatigue life of 10^5 cycles at the maximum g-level, which is a very conservative approach, considering the very short duration of the powered flight. Particular care was given to the design of Glass Fibre straps and Common Support Structure struts. For Glass Fibre straps, actual fatigue test data at cryogenic temperatures were used, while for Carbon Fibre struts, room temperature values (very conservative) were used, little data being available at low temperatures.

9.2 The Thermal Control Subsystem

Payload Module

A double cryo system has been selected (Figure 9.2.1 shows the main trade offs carried out on the cryogenic system) in order to provide the necessary cooling capacity and guarantee a lifetime of at least 18 months within the mission constraints. The Superfluid Helium (HeII) loop is used to cool the experiments in the Focal Plane Assembly (FPA) and the optics (mirrors, baffle and baffle shields). The Hydrogen loop is used to cool the cryostat shields which absorb most of the external heat inputs and provide a suitable thermal environment to the He tank. The Hydrogen has been selected for its high cooling capability per unit mass and unit volume.

An additional small tank filled up with normal helium is installed in the Aperture Cover. It is used for contamination trapping and optical tests on ground. It is conceived to work by flushing normal liquid Helium through it.

Cryogenic System Description

The cryo-system and flow schematics are shown in Figure 9.2.2, and the main characteristics of the cryogenic subsystem are summarised below:

HeII Loop

- The temperatures are kept constant under normal operation by use of a passive phase separator in combination with vent gas regulation valve 104. The pressure gradient (in orbit) along the He loop is 16 mbar.

- . Filling operations take place via valve 101. During launch operations the system is closed by valves 104/105.
- . If any hazard produces a slow pressure rise, the venting is via safety release valve SV121. For a fast pressure rise, then, in addition to the ways mentioned above, venting takes place via rupture disc RD 123 to isolation vacuum and via evacuation valve to environment.

H₂ Loop

- . During normal operations the pressure is kept constant by phase separator valves 003 and 004. The pressure gradient (in orbit) along the H₂ loop is 1 bar.
- . Filling operations are via valve 001. During launch operations the system is closed by valve 006.
- . For any hazard producing a slow pressure rise, the venting is via safety release valve SV021 and H₂ vent gas system to torch, stack or something else (balloon). If hazard produces a fast pressure rise, additional venting is via rupture disc RD 023, filling line and external safety device (safety plug 022/RD) to torch or stack.

An electrical heater is installed for tank discharge (on ground) and in order to equalise the lifetime of both cryo-systems (in orbit).

Passive Thermal Control Description

The thermal control has to assist the cryogenic system to keep the temperatures within requirements and to provide a suitable environment to the cryogen tanks. The main characteristics of the passive thermal control are the following (see Figure 9.2.3).

- . Multilayer Insulation (MLI) blankets applied:

- around cryostat and telescope
- around external sunshade surface
- between cryostat shields and between baffle shields
- on the inner face of the first cryostat shield
- around the baffle.

MLI properties are simulated by an effective emissivity of 0.007 and a conductive term: $1.5 \times 10^{-4} \text{ W/m}^2\text{K}$.

- . Optical Properties

The optical properties are shown in Figure 9.2.3. All external coatings are electrically conductive. Degraded (End of Life) values have been used in all the calculations.

- . Additional Thermal Items

A GFC baffle splitter has been introduced between the upper and lower portion of the main baffle to minimise the heat conducted to the tanks.

The Performance

Several thermal mathematical models have been developed in order to:

- Calculate the radiative heat transfer between the different areas in the satellite.
- Calculate the orbital heat inputs in more than 15 orbital points and for several Sun-Earth-spacecraft orbital configurations (considering multireflections).
- Calculate temperature levels in more than 70 isothermal nodes in the PLM
- Calculate the mass flow rates, pressure gradients and lifetime.

More than 150 simulation runs have been done in order to reach a good understanding of the different interactive phenomena involved. This has allowed concentration of efforts in those areas where a design improvement has been found to be possible and feasible.

Figure 9.2.4 shows two examples of parametric simulations: The first considers the impact on lifetime and temperature of the most relevant components when external heat input to the sunshade and baffle are modified. The second shows the sensitivity of the system to variation of heat dissipation by the instruments located in the FPA.

The amount and distribution of heat inputs into the cryosystem are shown in figure 9.2.5.

With the present design and considering a nominal launch, an operational lifetime of approximately 600 days has been found providing a margin of two months. 100 mw of heater dissipation are applied to the LH₂ tank during on-orbit operations with the following rationale:

- cryogens consumption rates are adjusted so that identical tanks are required for both LH₂ and He_{II} reducing development and manufacturing costs
- some margins are required to make up for uncertainties such as final LH₂ phase separator dissipation, need to extend the pre-launch operations where LH₂ carries most of the thermal load, etc..

The resulting on-orbit operational temperatures are as follows:

FPA	7 K
Mirrors	10 K
Baffle (lower part)	17 K
(upper part)	30 K
Sunshade	111 K
Vessel	130 K

- M Motor Actuated
- SV Safety Valve
- △ Valve (△)
- ⊖ Burst Disc
- ⊠ Phase Separator
- ⊞ Heat Exchanger
- F Flow Sensor
- T Temperature Sensor
- L Level Sensor
- P Pressure Sensor
- PC Pressure Control
- ⊞ Adsorber
- H Hand Actuated

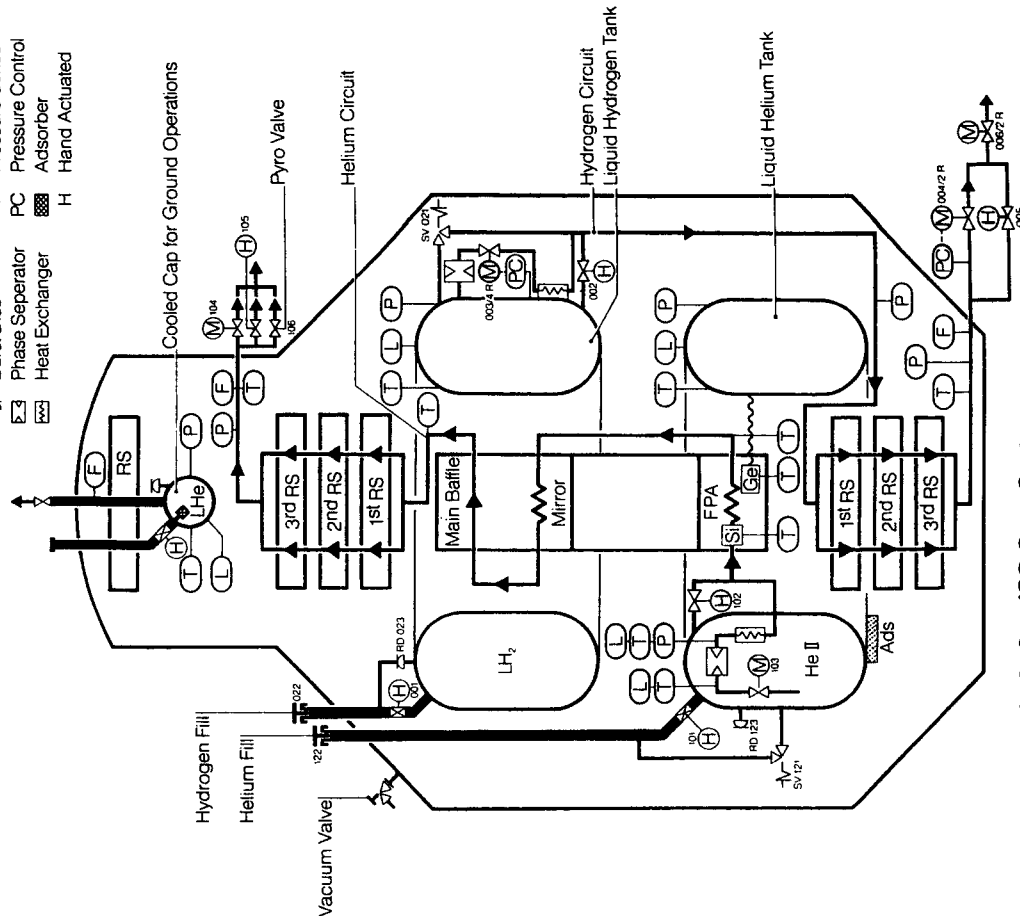


Figure 9.2.2 ISO Cryo-System

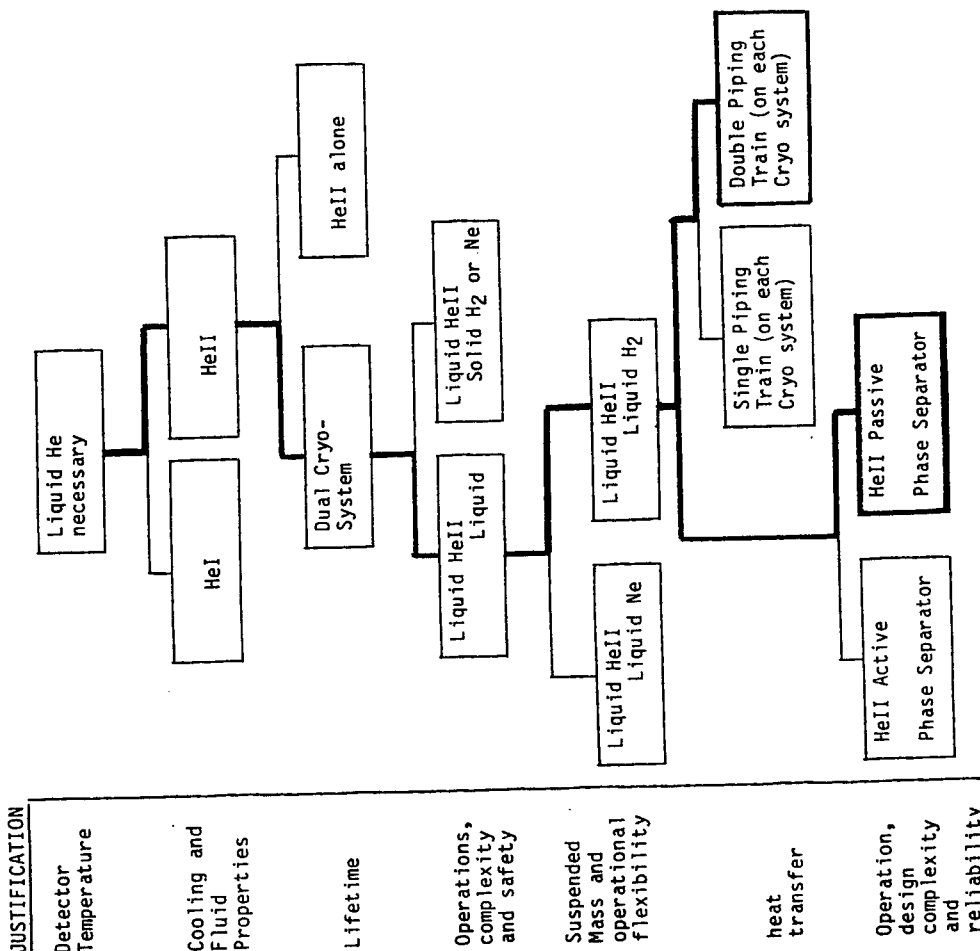


Figure 9.2.1 Cryogenic System Design Trade-offs

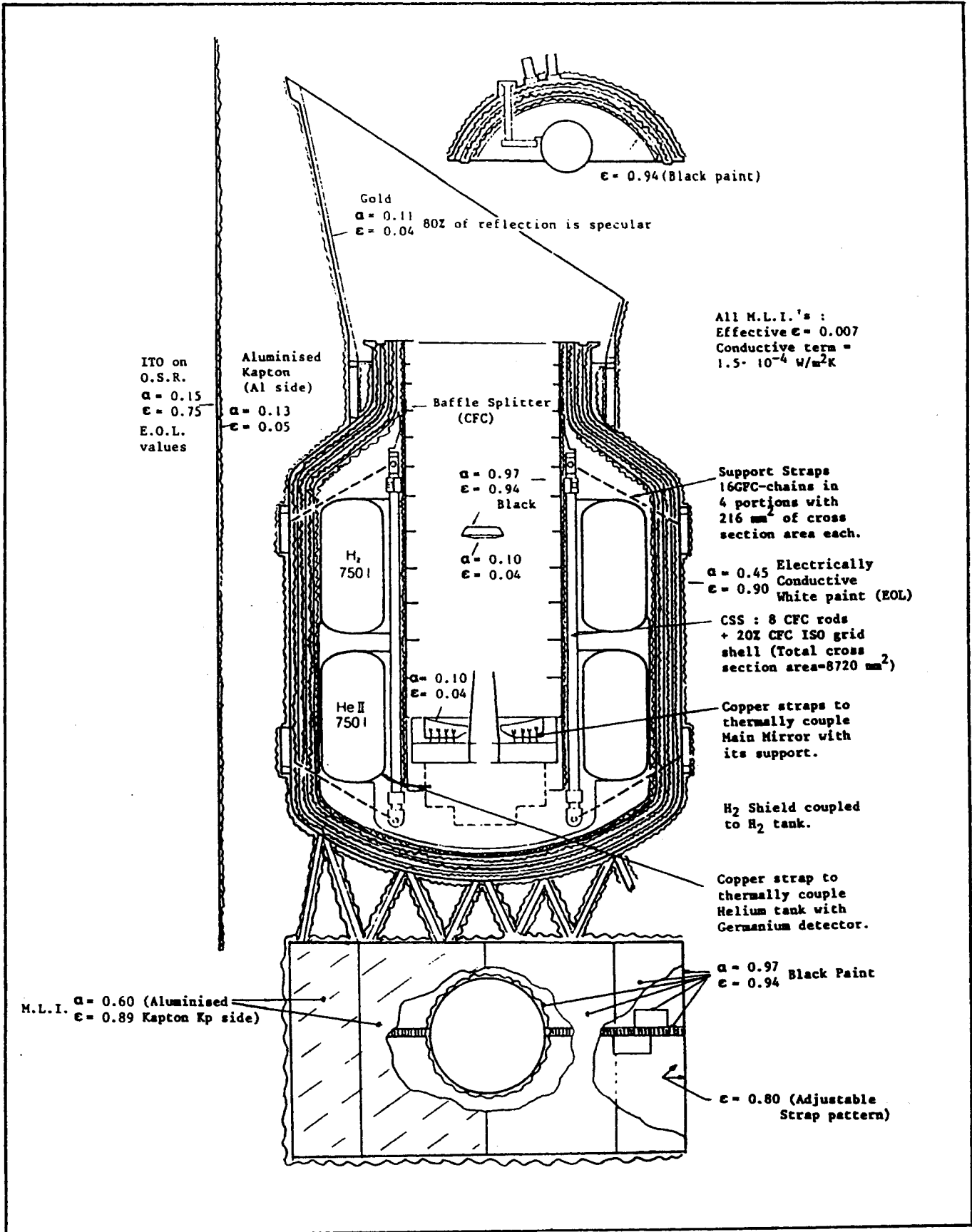
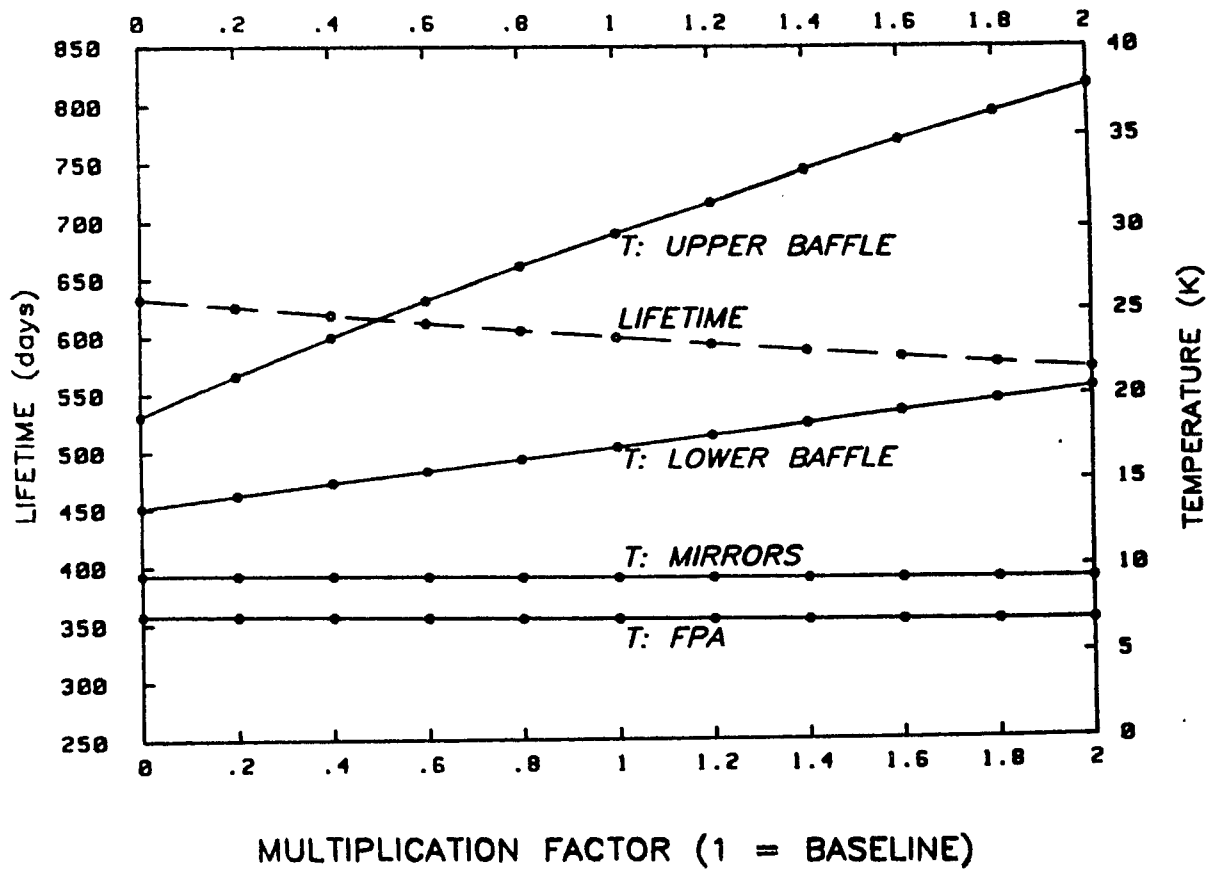


Fig. 9.2.3 ISO Thermal Layout

RESPONSE TO CHANGES IN SUNSHADE AND BAFFLE INPUTS



RESPONSE TO CHANGES IN F.P.A. POWER DISSIPATION

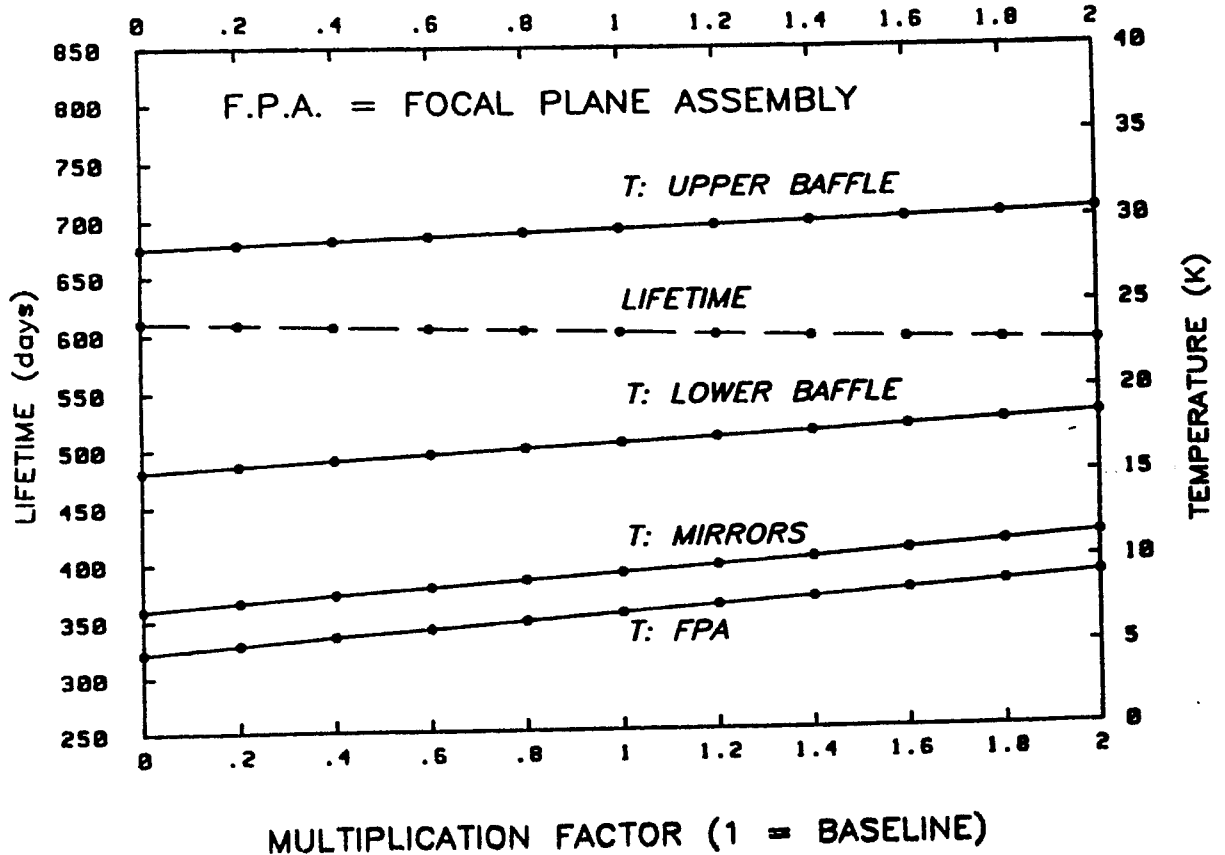


Fig. 9.2.4 Response to parametric changes

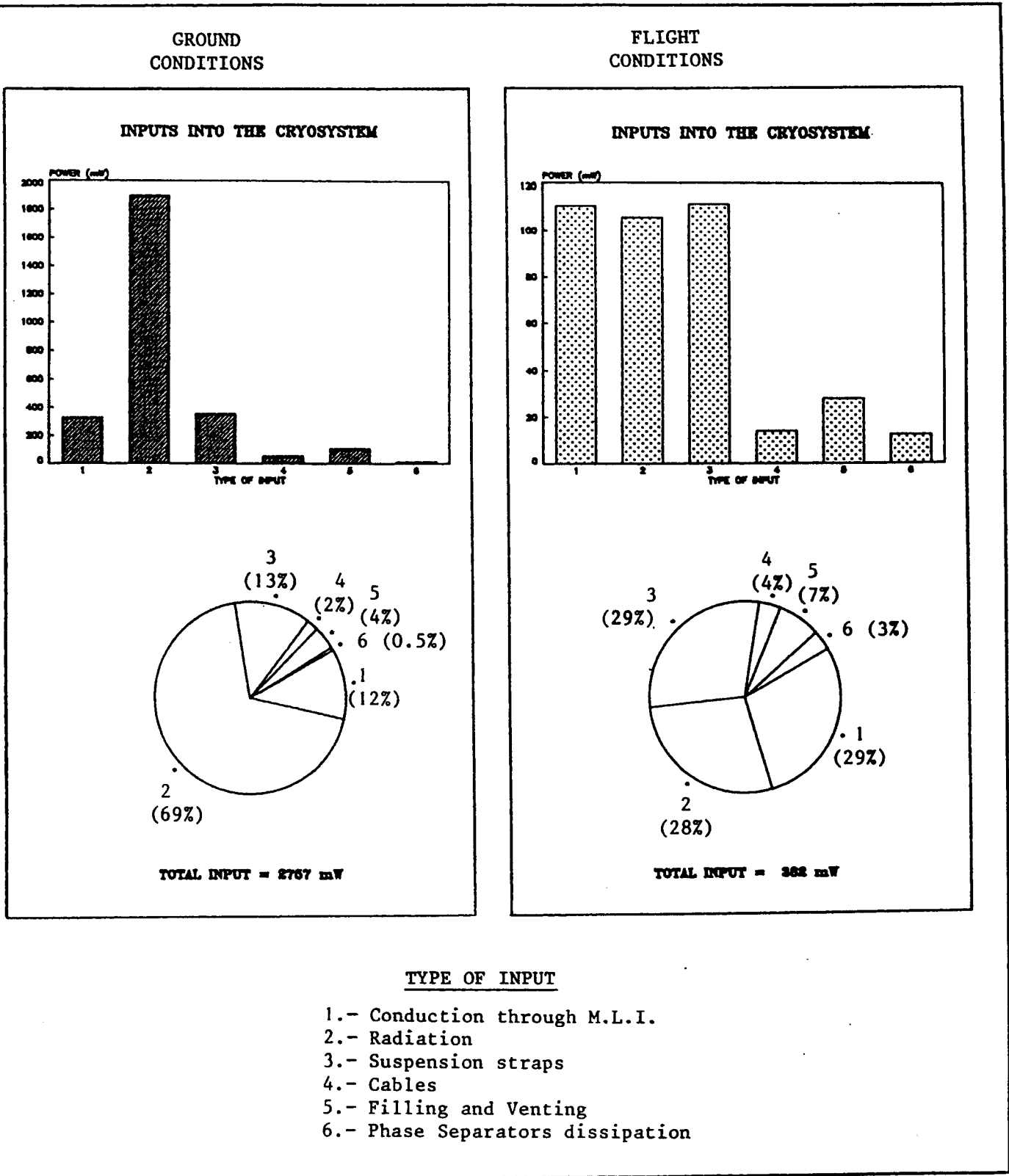


Figure 9.2.5 Heat inputs into the Cryosystem

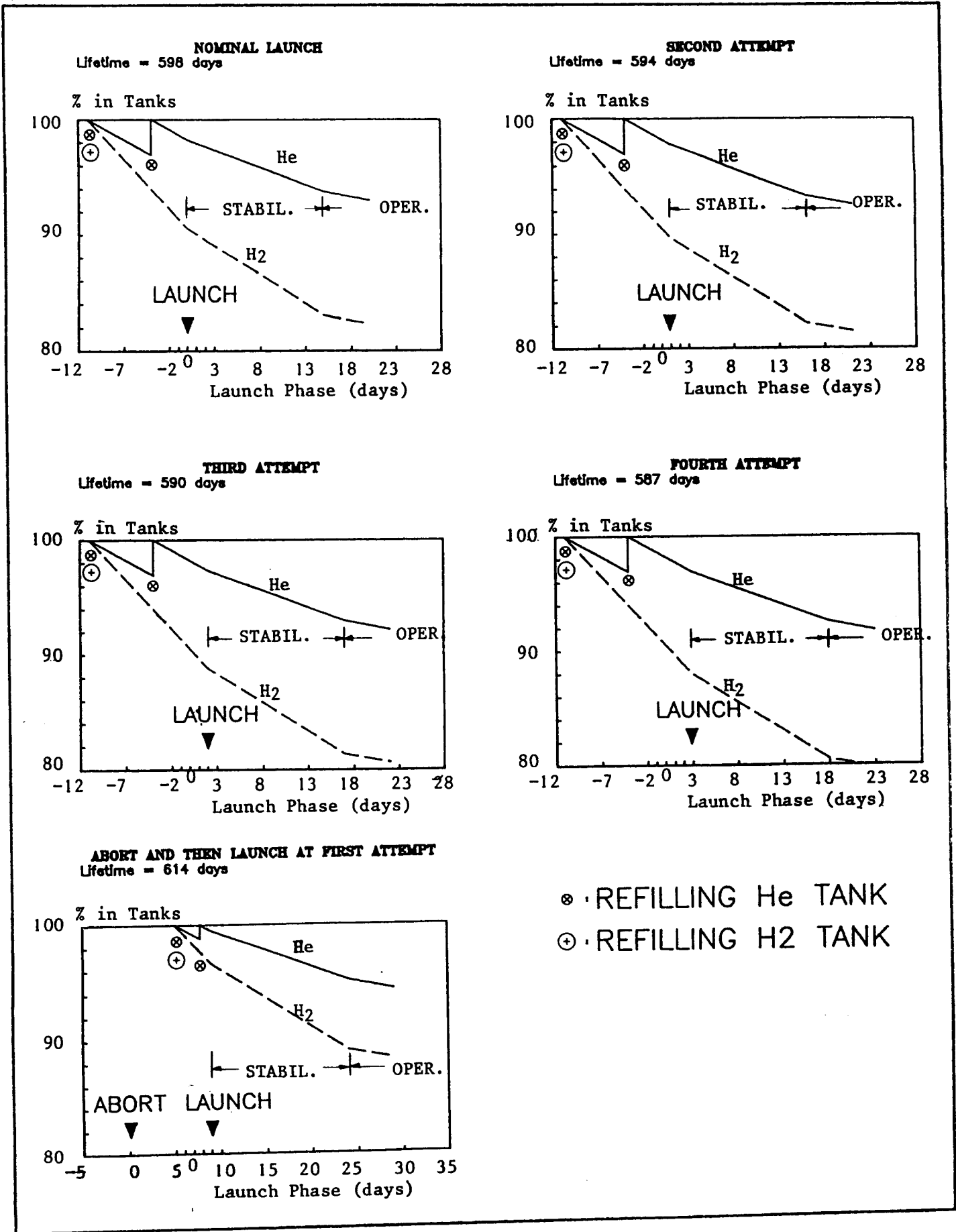


Fig. 9.2.6 Prelaunch Operations impact on coolants consumption

9.2.2 Service Module

The thermal design of the Service Module does not present much complication although a critical area where both thermal and structural subsystems require special attention is the stability of the Star Trackers alignment.

The Star Trackers themselves have their own thermal control, using insulation and electrical heaters.

The Service Module Thermal Layout can be summarised by the following:

- Radiator area (black painted) on opposite face to the Sun. The infrared emissivity of the inner face is used to trim the temperatures inside.
- Insulation blankets in Sun illuminated areas.
- Electrical heaters where necessary.

A Thermal Mathematical Model has also been developed for the Service Module (67 Isothermal nodes). Additional models have been used to calculate the radiative exchange factors and orbital external fluxes.

Several design cases (cold and hot) and parametric runs have been simulated. The results of this analysis have shown the thermal control for this module to be very feasible.

9.2.3 Prelaunch operations and their impacts on operational performance

Figure 9.2.6 shows six different prelaunch cases. All of them correspond to a worst case when the aperture cover tank is empty.

The following assumptions have been considered:

- Refilling of both cryo-tanks at do-11 (except for the abort case).
- Last refilling of the HeII tank at do-4 (except for the abort case).
- Heating power to the H₂ tank is applied only during the on-orbit operational phase.

The scenarios are in line with the preliminary ISO/ARIANE Combined Operations Plan defined with Ariane authorities (figure 12.1.2).

Results show that a postponement of the launch by one day reduces the on-orbit operational lifetime by 3.5 days.

9.3 Attitude/Orbit Control and Measurement Subsystem

9.3.1 The functional performance

The AOCMS fulfils the following functions:

Detumble

The AOCMS reduces the satellite rates to values below

- 2.8 arcmin/sec around X-axis within 3 seconds
- 0.5 arcmin/sec around Y and Z axis within 42 seconds.

Acquisition

The AOCMS brings the satellite in a defined attitude with respect to Sun and Earth:

- it reduces satellite angular rate to zero
- it aligns Z-axis with Sun vector in less than 8 minutes
- it acquires the Earth magnetic field in about 22 minutes
- it performs the transition to coarse mode.

Safe/Coarse Mode

The AOCMS maintains the Z axis along the satellite-sun vector and the X-axis in a fixed position with respect to Earth, both in sunlit and eclipse phase.

This mode serves as a safe mode if a software or hardware failure occurs during fine pointing operations.

Fine Control

During this phase the AOCMS performs:

- initial star acquisition
- operational pointing as described in paragraph 9.3.2.
- alignment calibrations between AOCMS/Telescope line of sight for those experiments requiring better performance than the specified steady state values (paragraph 9.3.2).
- raster scan to perform limited sky survey (30x30 arcmin.)
- raster scan for experiments to peak up on signals (1x1 arcmin.).

Attitude Manoeuvres

Attitude manoeuvres (slews) take place to change the pointing direction of the spacecraft.

- Steady state slew rate is 7 arc degrees/minute.
- Acceleration, deceleration and settling for slews above 30 degrees require about 25 seconds.
- Slews of the order of 1 arcmin require a total time of about 10 secs.

Excess Angular Momentum Dumping

- The AOCMS is capable of unloading with sufficient margins the non-cyclic components of the angular momentum during each of the above mentioned modes.
- Margin in wheel momentum storage capacity for unknown torques is 2nms, taking into account a 6nms slew.
- Margin in propellant budget allows for additional unloading of 19800 nms.

Velocity increment

The velocity increment requirements are:

- | | |
|-------------------------------------|--------|
| - loss due to atmospheric drag | 3 m/s |
| - coarse perigee raising manoeuvres | |
| First delta-V | 22 m/s |
| Second delta-V | 49 m/s |
| - Fine synchronisation delta-V | 5 m/s |
| - Maintenance delta-V | 6 m/s |

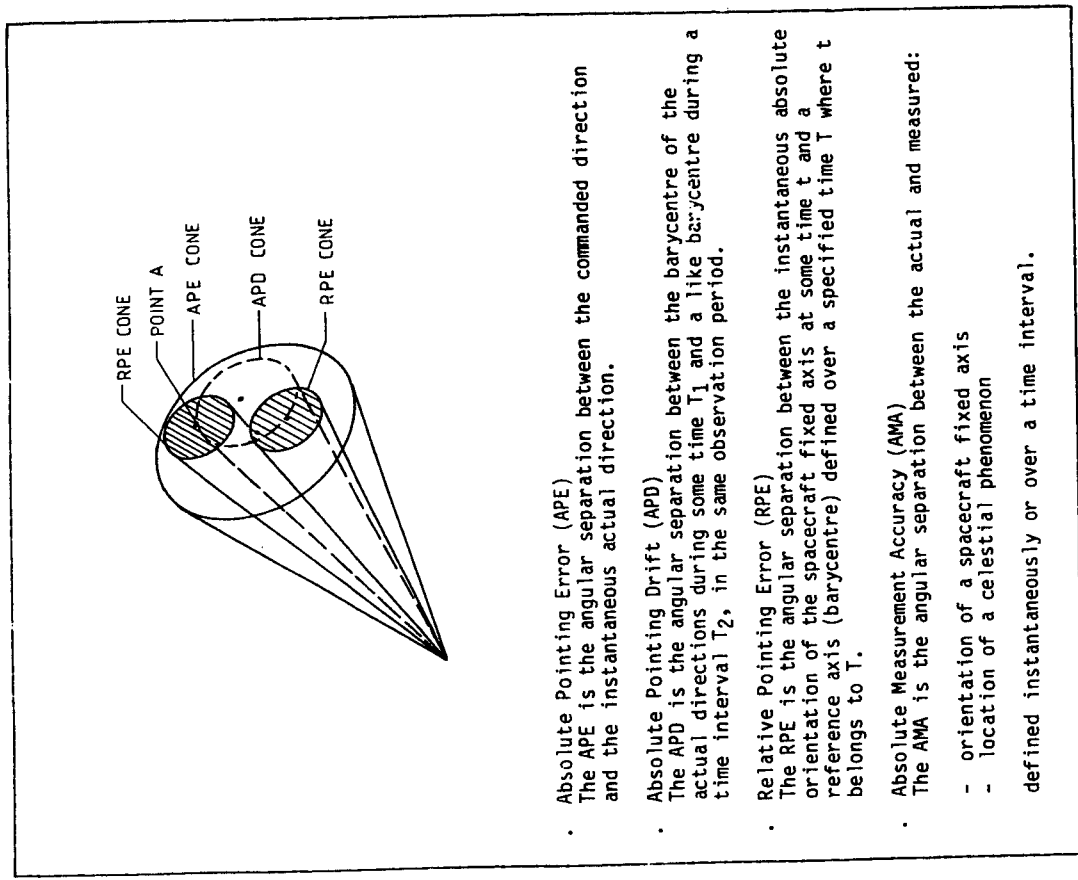
As the total delta-V is relatively small, and since a constant solar aspect angle is preferred from power and thermal point of view, a fixed direction for the thrust vector is implemented.

9.3.2 ISO fine pointing performance summary

- . The pointing terminology and error cone configuration is given in Figure 9.3.1.
- . The elements contributing to the Telescope Pointing Performance are:
 - The Attitude/Orbit Control and Measurement (AOCMS) subsystem performance.
 - The structural/thermal alignment change between the Quadrant Star Sensor (QSS) giving the Telescope line of sight and the star tracker (STR). The alignment errors between the QSS and experiments are estimated to be one order of magnitude lower than alignment changes QSS/STR.
- . The alignment errors between QSS/STR are as follows:
 - Permanent mechanical deformation due to launch loads and gravity sag when going from ground alignment to zero-g conditions. This error is expected to be less than 1 arcmin.
 - Thermal deformations for the transition from ground thermal environment to cold on-orbit condition. This misalignment was analysed with a NASTRAN model and resulted in less than 25 arcsec.
 - On-orbit thermal deformation when passing from an orbit "hot" to "cold" case condition. This absolute peak to peak error was calculated to be less than 18 arcseconds.

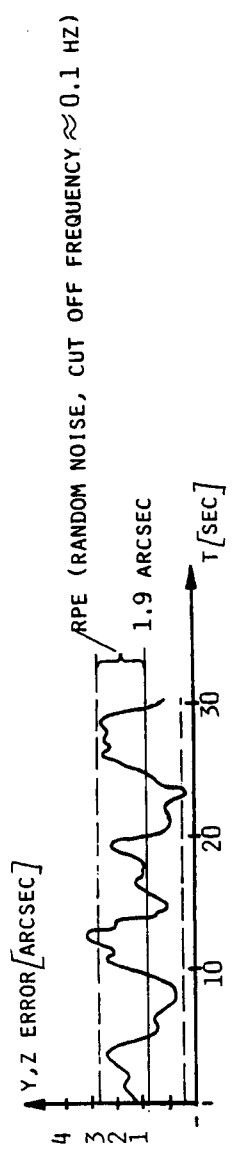
The first two error types play a role for the determination of the QSS field of view (4 arcminutes). These uncertainties are removed after the first on orbit calibration.

The third error is of permanent relevance since the thermal conditions are changing during the mission depending on the spacecraft position and attitude with respect to Earth and Sun.



- **Absolute Pointing Error (APE)**
The APE is the angular separation between the commanded direction and the instantaneous actual direction.
- **Absolute Pointing Drift (APD)**
The APD is the angular separation between the barycentre of the actual directions during some time T_1 and a like barycentre during a time interval T_2 , in the same observation period.
- **Relative Pointing Error (RPE)**
The RPE is the angular separation between the instantaneous absolute orientation of the spacecraft fixed axis at some time t and a reference axis (barycentre) defined over a specified time T where t belongs to T .
- **Absolute Measurement Accuracy (AMA)**
The AMA is the angular separation between the actual and measured:
 - orientation of a spacecraft fixed axis
 - location of a celestial phenomenon
 defined instantaneously or over a time interval.

IMMEDIATELY AFTER CALIBRATION:



OVER ONE ORBIT

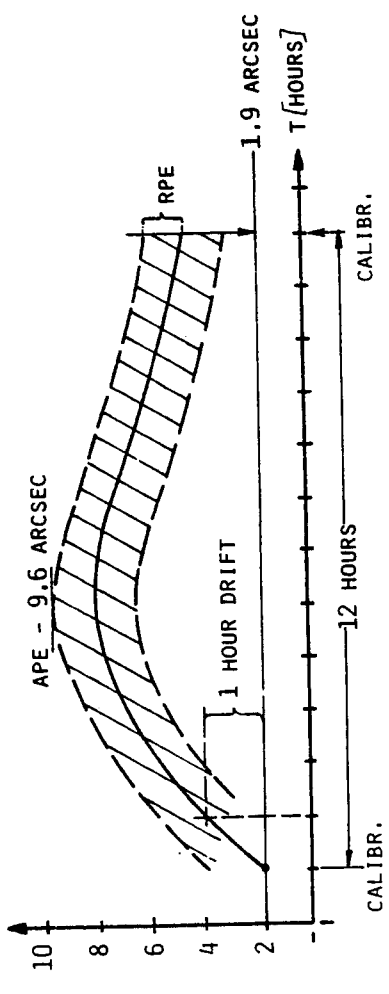
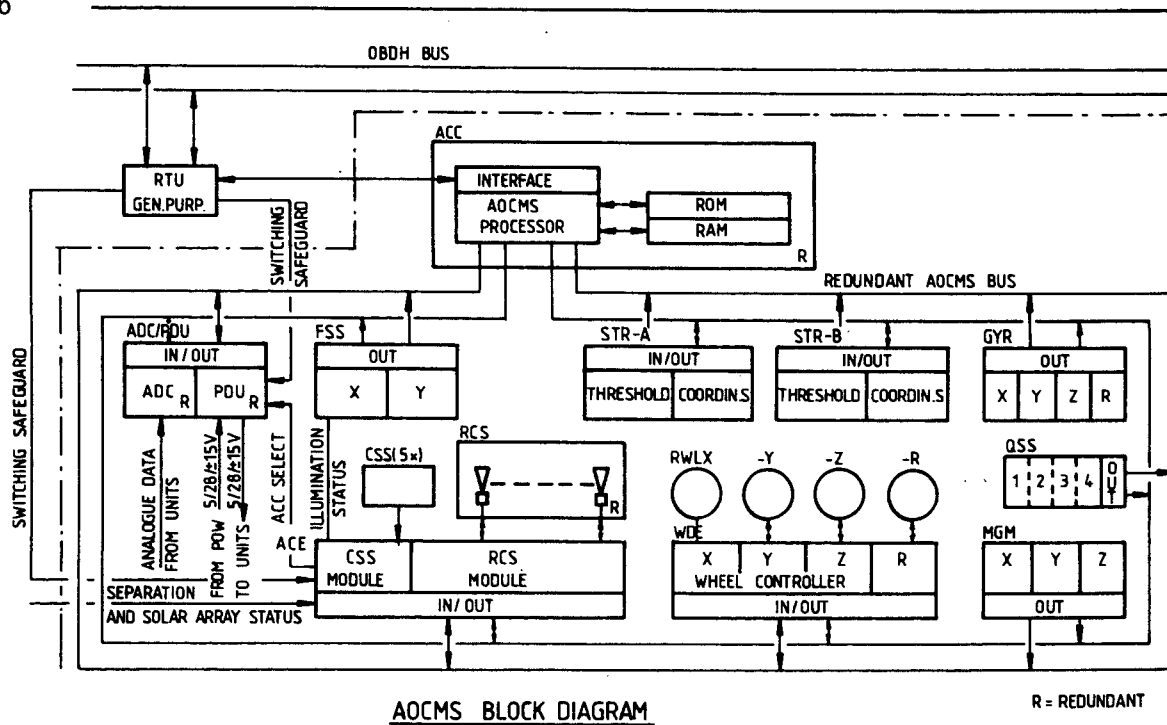


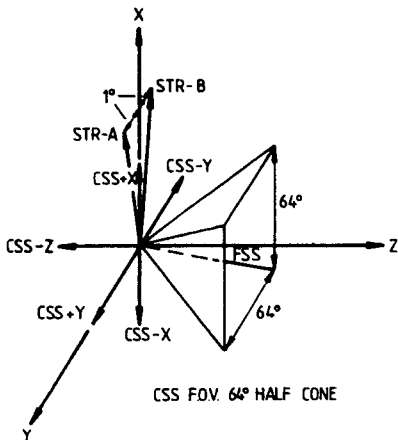
Figure 9.3.2 Typical Error Patterns for APE

Figure 9.3.1 AOCMS Pointing Terminology and Error Cone Configuration



AOCMS BLOCK DIAGRAM

R = REDUNDANT



ORIENTATION OF OPTICAL SENSOR HEADS

AOCMS UNIT	AOCMS FUNCTION												
	LAUNCH 1)	DETUMBLE	SUN ACQUISITION 2)	EARTH ACQUISITION 2)	SAFE / COARSE MODE 2)	INTERMEDIATE MODE	ALIGNMENT CALIBRATION	OPERATIONAL POINTING	ANGULAR MOM. UNLOAD	ATTITUDE MANOEUVRES	V - MANOEUVRES	ATT. SAFEGUARD (ROM) 3)	ATT. SAFEGUARD (RAM)
ACC	X	X	X	X	X	X	X	X	X	X	X	X	X
ADC/PDU	X	X	X	X	X	X	X	X	X	X	X	X	X
RWS			X	X	X	X	X	X	X	X			X
GYR	X	X				X	X	X		X	X		X
MGM				X	X	X ⁴⁾							
STR							X ⁴⁾	X			X	(X)	X
ACE	X	X	X						X		X		X
FSS			X		X	X	X	X		X	X	X	X
CSS			X									X	
RCS	X	X							X		X		
QSS							X						

- 1) STAND BY
- 2) DURING T/O PERIGEE: ACTUATOR RCS
- 3) HARDWIRED (COMPUTER SWITCH) SAFEGUARD IN ACE
- 4) NOT IN CONTROL-LOOP

CORRELATION DIAGRAM AOCMS SENSORS ACTUATORS AND FUNCTIONS.

AOCMS DESCRIPTION

THE ABBREVIATIONS USED ARE :

- | | | | |
|---------|--|------|-------------------------|
| ACC | ATTITUDE CONTROL COMPUTER | RTU | REMOTE TERMINAL UNIT |
| ACE | ATTITUDE CONTROL ELECTRONICS | RWL | REACTION WHEEL |
| CSS | COARSE SUN SENSOR | RWS | REACTION WHEEL SYSTEM |
| -E | ELECTRONICS | (-R) | REDUNDANT |
| FSS | FINE SUN SENSOR | STR | STARTRACKER |
| GYR | GYRO PACKAGE | -S | SENSOR HEAD |
| MGM | MAGNETOMETER | WDE | WHEEL DRIVE ELECTRONICS |
| ADC/PDU | ANALOGUE DIGITAL CONVERTOR / POWER DISTRIBUTION UNIT | (-X) | X-AXIS |
| QSS | QUADRANT STAR SENSOR | (-Y) | Y-AXIS |
| RCS | REACTION CONTROL SYSTEM | (-Z) | Z-AXIS |

FIGURE 9.3-3.

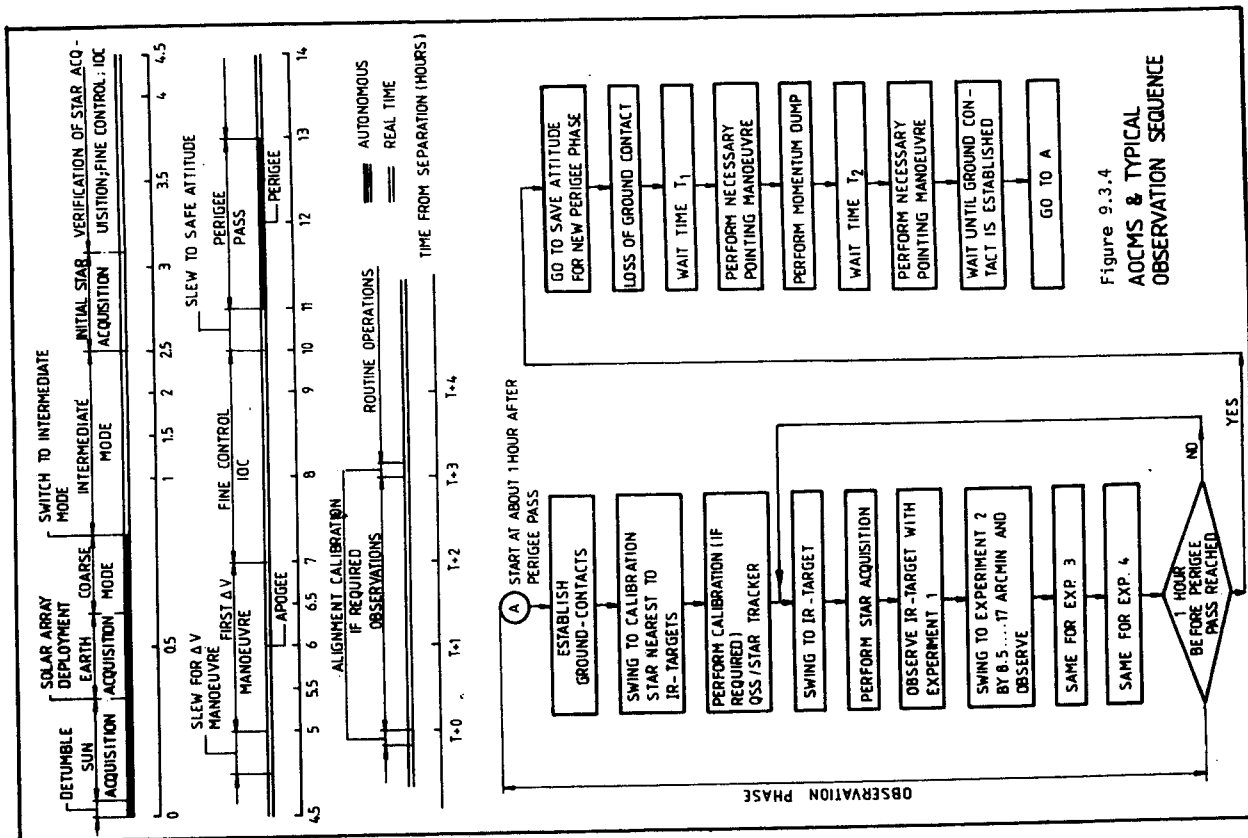


Figure 9.3.4
AOCMS & TYPICAL
OBSERVATION SEQUENCE

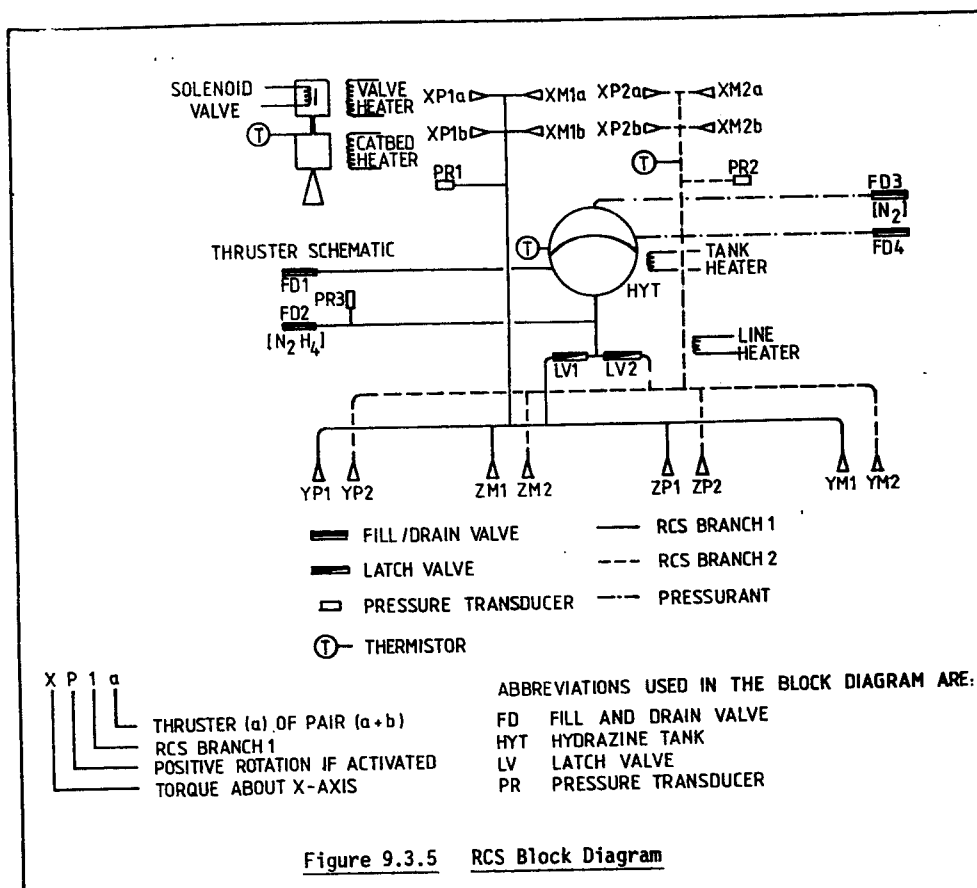


Figure 9.3.5 RCS Block Diagram

- . The Pointing Performance is summarized in table 9.3.1 for three QSS/STR calibration frequencies:
 - once at start of mission
 - once per orbit
 - once per hour
- APE and APD are mainly produced by thermal deflection in the structural chain QSS/STR.
- RPE is not influenced by thermal deformation and is well within the specified limits.
- AMA performance requirement is referred to as "a posteriori knowledge" and by evaluation of all QSS, STR calibration data a considerable reduction of error is possible thus lessening APE, APD and AMA.
- . The development of the pointing errors in time is important as it gives information on the actual pointing performance just after calibration between QSS and STR, and on the rate of degradation with respect to time. Typical transient performance are shown in Figure 9.3.2.
- . Any pointing direction which does not violate the Sun, Earth, Moon and Jupiter avoidance requirement may be maintained over the period of at least one orbit. Details on pointing direction capability are found in paragraph 8.6 related to sky coverage.
- . Performance for an offset pointing angle of two degrees between the infrared target and a reference star are shown in Table 9.3.2. The specified error limits are not exceeded.
- . Raster scan capabilities for two different fields (30x30 and 1x1 arcmin) are shown in Table 9.3.3.

9.3.3 The AOCMS Description

The AOCMS block diagram, the AOCMS functions with a correlation diagram between sensors and actuators, and the configuration of the optical sensors are shown in Figure 9.3.3.

9.3.4 The AOCMS Sequence Event

The AOCMS events from launch up to routine observations are shown schematically in Figure 9.3.4.

9.3.5 The Reaction Control System (RCS)

The RCS block diagram is given in Figure 9.3.5. The major components are:

- a spherical diaphragm tank of 0.7m diameter;
- 16 thrust chamber assemblies providing a thrust of 0.6 to 2N with an accuracy of $\pm 5\%$.

The total propellant mass is 116.1 Kg.

ERROR TYPE	REQUIREMENTS (half cone angle)			PERFORMANCE			
				Calibration once at start of mission	Calibration once per orbit	Calibration once per hour	Error in X-axis in all cases
	Optical Axis (Arcsec)	Y/Z Axis (Arcsec)	X-Axis (Arcmin)	Y/Z Axis (Arcsec)	Y/Z Axis (Arcsec)	Y/Z Axis (Arcsec)	X-Axis (Arcmin)
Absolute Pointing Error (APE)	17	13.9	6.6	12.6	9.6	5.7	2.2
Absolute Pointing Drift (APD) 1 hour	10	8.2	3.9	3.2	2.3	2.3	0.5
Relative Pointing Error (RPE) 30 sec.	4	3.3	1.6	1.7	1.7	1.7	0.1
Absolute measurement accuracy (AMA)	9	7.2	3.5	10.8	5.8	3.8	2.1

Table 9.3.1 ISO Pointing Accuracy (95% Values)

ERROR TYPE (Offset 2 deg)	E _{Y,z} (arcsec.)	E _x (arcmin)	E (arcsec.)
APE	10.2	2.2	12.4
APD(1 hour)	2.5	0.5	3.0
RPE(30 sec.)	1.7	0.1	2.1
AMA	6.6	2.1	8.1

Table 9.3.2 Offset Pointing Performance
(95% values, half cone)

Raster Scan Characteristics	30 x 30 Arcmin.	1 x 1 Arcmin.
Non-Orthogonality	30 Arcsec.	6 Arcsec.
Tracks separation	1 Arcmin.	5 Arcsec.
Scan Rate	2 Arcmin/Sec.	5 Arcsec/Sec.
Duration	40 Minutes	10 Minutes

Table 9.3.3 Raster Scan Performance

9.4 Optical Subsystem

The optical Subsystem includes the telescope and the straylight baffles. The main components are indicated in figure 9.4.1.

9.4.1 Telescope

First order telescope parameters are shown in Table 9.4.1. A Ritchey-Chretien configuration has been selected, based on simplicity and adequate performance for the ISO field of view and image quality requirements. In the baseline design the secondary mirror is used as the entrance pupil so that the primary mirror mount is not visible from the focal plane. For an effective telescope aperture of 600 mm, this results in a free primary mirror diameter of 634 mm.

Table 9.4.1: Telescope Parameters

Effective Primary Dia. (mm)	600
Free Primary Dia. (mm)	634
Primary Focal Length (mm)	1000
Secondary Focal Length (mm)	- 164.25
Mirror Separation (mm)	854
Back Focal Length (mm)	460
Telescope Focal Length (mm)	9000
Linear Obscuration Ratio	
Unbaffled	0.15
Baffled	0.29
Image Field Radius of Curvature (mm)	- 153
Fields of View (arc min)	
Telescope : Unvignetted	20
Total	40
Experiment : Unvignetted	3
Total	14
QSS : Unvignetted	0 (Opt.Axis)
35% Vignetting	2

9.4.1.1 Optical Performance

Since the Ritchey-Chretien telescope has a spherical image field, the optical quality has been assessed in a tilted plane which contains the optimised image at field angles of 8.5 arc min (centre of the experiment unvignetted field) and 10.0 arc min (outer edge of the telescope unvignetted field). Spot diagrams show that the blur circle diameter is less than 0.5 arc sec over the experiment field, and increases to 4 arc sec at a field angle of 20 arc min.

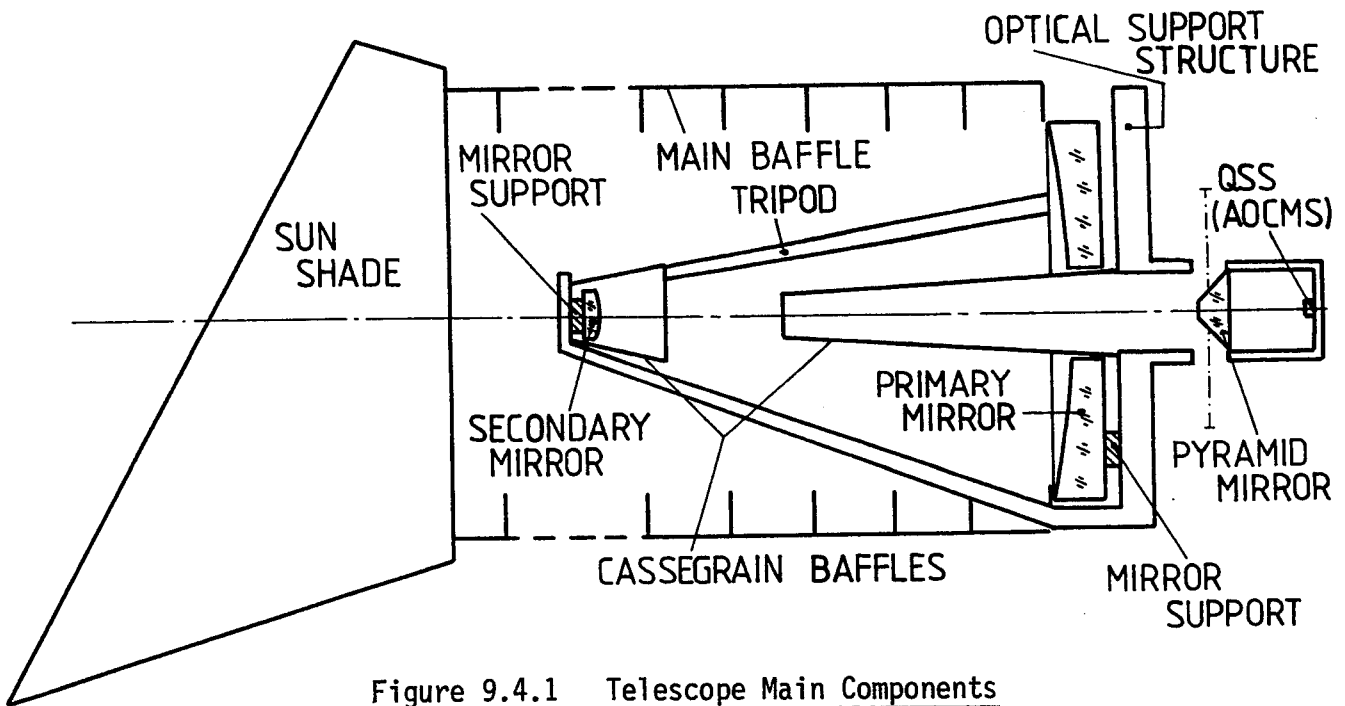


Figure 9.4.1 Telescope Main Components

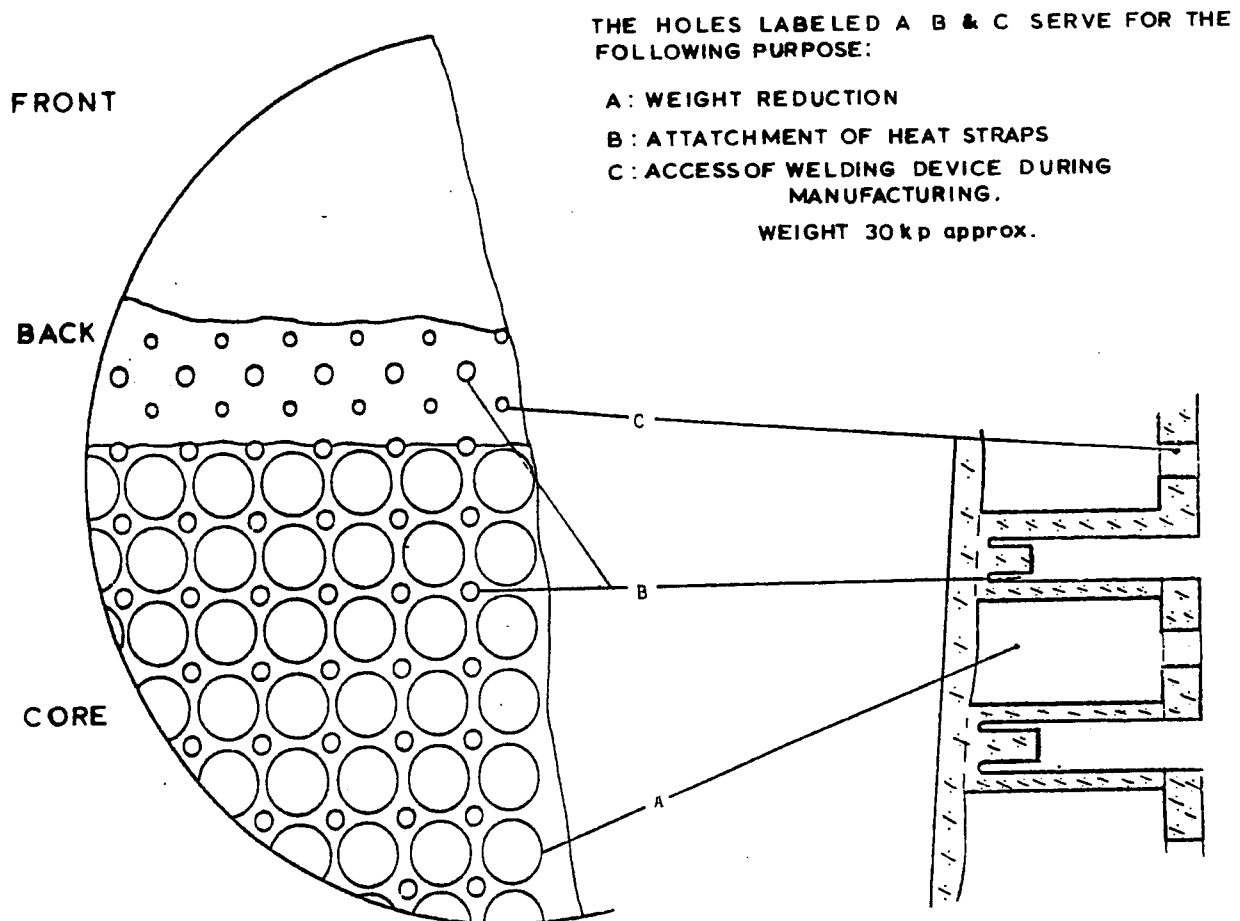
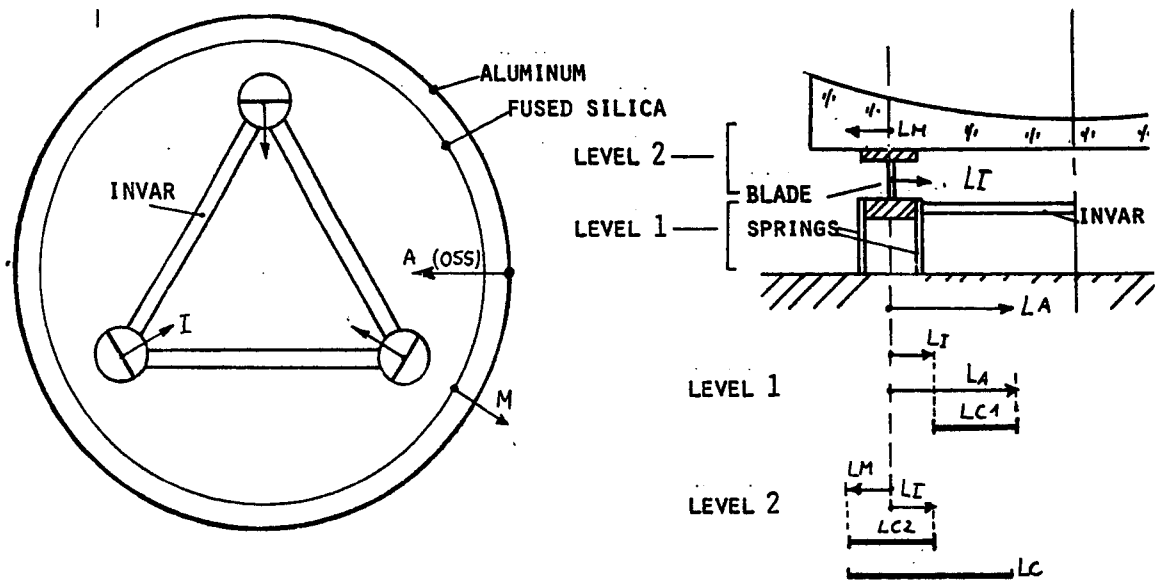


Figure 9.4.2 Heraeus Reduced Weight Mirror



PRINCIPLE OF THERMAL EXPANSION COMPENSATION OF THE ISO PRIMARY SUPPORT

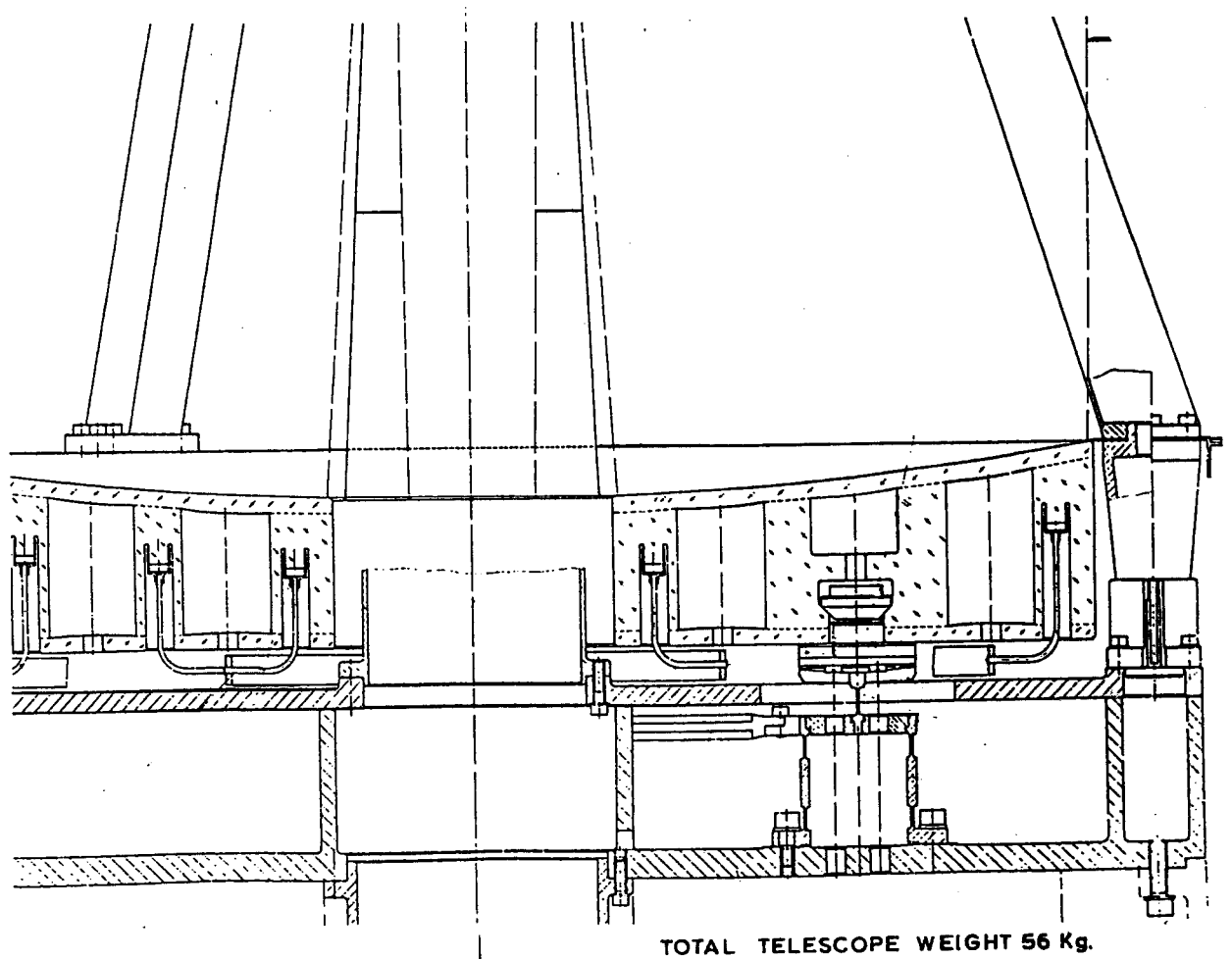


FIG. 9.4.3 DESIGN OF PRIMARY MIRROR GROUP

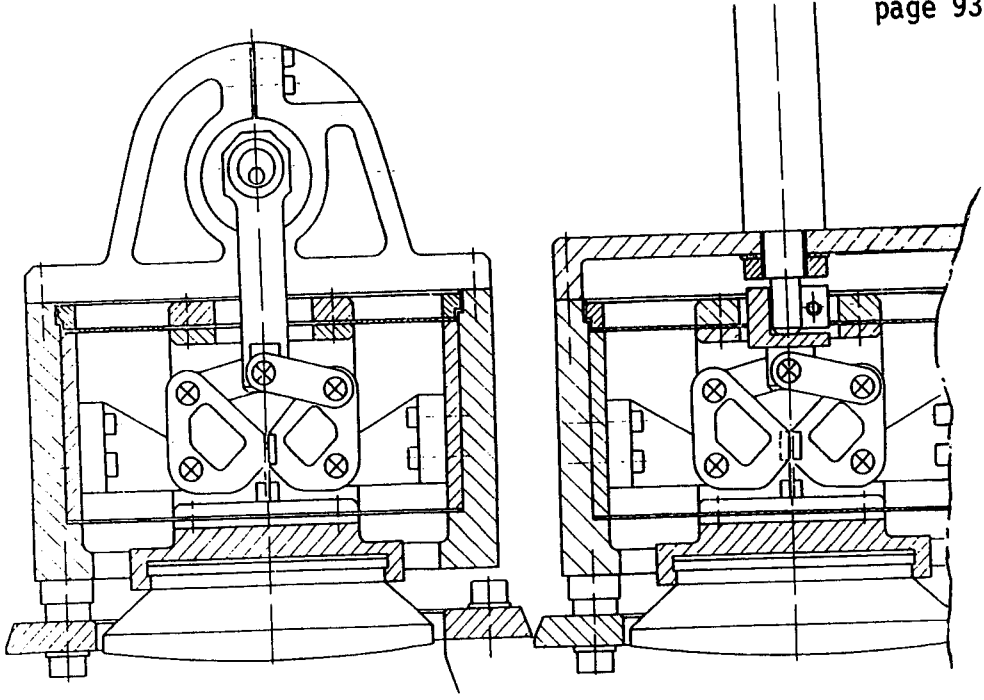
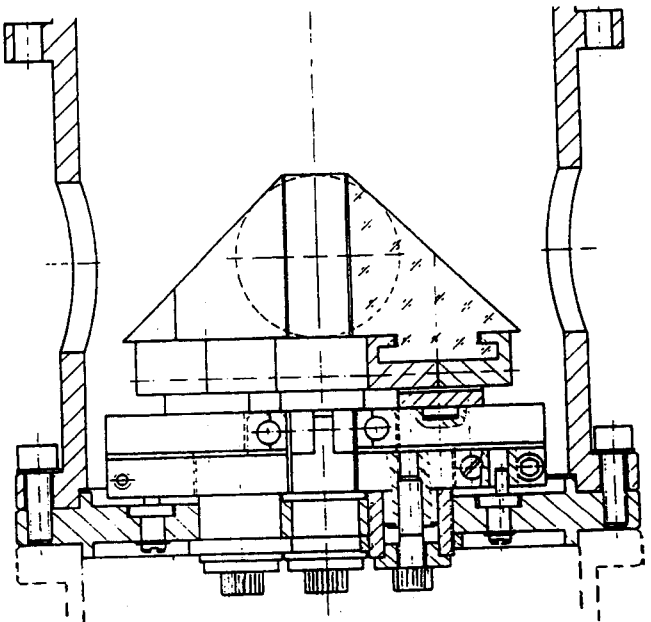
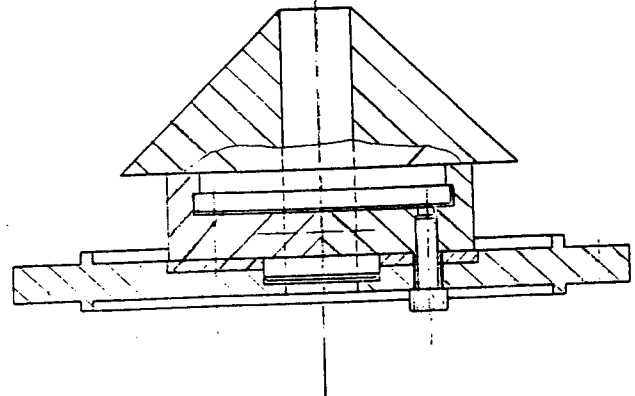


FIG. 9.4.4 ACTIVE FOCUSING DEVICE: Activation by stepper motor or INCHWORM



4. INDEPENDENTLY
ADJUSTABLE MIRROR
ELEMENTS



SIMPLIFIED PYRAMID
BLOCK

FIG. 9.4.5 PYRAMID MIRROR DESIGN

Defocus tolerances, derived from a Strehl ratio of 0.9 at 5 μm , are ± 2.25 mm for the focus and ± 27 μm for the mirror separation. This is achievable by thermal expansion compensation in the design. However, other considerations such as simplicity of the test programme lead to the adoption of an active focus control. Placing a limit of 1 arcsec. on the coma produced by the mirror centering tolerances leads to values of 72 microns for the lateral displacement and 103 arcsec for mirror tilt. These can be easily accommodated by the telescope design and are well within the requirement for diffraction limited performance at 5 micron.

9.4.1.2 Primary Mirror

A weight-reduced fused silica mirror design has been selected for the primary (Figure 9.4.2). The blank consists of a core with a series of weight-reduction bores and a curved front plate welded on it. The rear side is a plate with small holes concentric with the weight-reduction holes. Since a welding technique is used, the mirror consists of a pure one-component material. The weight reduction permits the use of a three point mirror support rather than the complex and heavy six-point support which would be required for a solid Zerodur mirror. The mirror figuring accuracy has been estimated at 60 nm rms, and the wave front aberration of the mounted mirror at 80 nm rms. The mirror is gold coated. The thermally compensated three-point support, which provides the attachment between the fused silica mirror and the Al-alloy Optical Support Structure (OSS), consists of an equilateral triangle of Invar rods, which is connected to the mirror and to the OSS by separate plane blade springs normal to the radial direction (Figure 9.4.3). The thermal connection between the mirror and the heat sink is by 65 heat conducting straps. The cool down time is estimated at less than 50 hours.

9.4.1.3 Secondary Mirror

Due to its small size, the secondary mirror is of solid fused silica. The tripod supporting the secondary consists of Invar tubes of rectangular cross-section. During telescope cool-down the contraction of the OSS causes a reduction in the tripod angle which slightly increases the mirror separation so that focus is maintained. This passive focusing concept has been retained as a first order control, with final adjustment being available with an active method. Preliminary designs have been developed in which the secondary mirror mount is suspended by blade springs and an axial motion of ± 0.25 mm is produced by a stepper motor/cam or a piezoelectric "inch worm" acting through a lever with a reduction of 10:1 (Figure 9.4.4).

9.4.1.4 Pyramid Mirror

The pyramid mirror (Figure 9.4.5) includes four mirror elements which can be adjusted independently in three degrees of freedom; rotation around two axes (azimuth and elevation) and translation parallel to the telescope optical axis. A central hole is provided for the quadrant star sensor.

Simplification of the design may be possible once the instrument payload options have been selected.

9.4.2 Straylight Baffles

9.4.2.1 Straylight Requirements

The design of the straylight baffles is based on the requirement that the straylight intensity at the focal plane should not exceed 10% of the zodiacal emission at the ecliptic poles, for internal thermal emission and for diffracted and scattered radiation from off-axis sources. Table 9.4.2 shows the required levels of thermal emission and baffle attenuation for bright off-axis sources for the most stringent case. The attenuation factors are related to the effective telescope area of 0.26 m².

Table 9.4.2

(a) Zodiacal Background - Thermal Emission Requirement

Channel	Wavelength (μm)	Zodiacal Background (W)	Internal Thermal Emission (W)
D	80-120	2.5E-15	3E-16

(b) Off-Axis Attenuation Requirement (off-axis rejection factor)

Channel	Jupiter 5°	Moon 24°	Sun 60°	Earth 77° Perigee	Earth 77° Apogee
A	1.2E9	1.4E13	7.7E18	4.8E17	5.3E16

9.4.2.2 Baffle Design

The baffle system consists of the following components: sunshade, main baffle, Cassegrain baffles (secondary and primary bore), pyramid stop and detector housing.

The conical sunshade is truncated so that direct sunlight at an incidence angle of 60 deg off axis cannot strike its inner surface, and earth radiation at 77 deg cannot directly enter the main baffle aperture. On its sun-facing side, the outside rim of the sunshade is fitted with a double knife-edge so that sunlight can only enter the main baffle aperture after two diffractions. The inside surface of the sunshade has a specular reflecting gold coating.

The Cassegrain baffles and main baffle are sized to give a fully baffled system; there is no direct path for stray light to the focal plane. In addition, the length of the main baffle ensures that moonlight at 24 deg cannot strike the secondary baffle or primary mirror.

9.4.2.3 Straylight Calculations

Calculations have been made of the straylight performance using the GUERAP III computer program. Internal thermal emission has been calculated for channel D with "clean" mirror coatings (0% diffuse reflection) and with "dirty" mirrors (1% diffuse reflection). The requirement of Table 9.4.2(a) is met with both mirror coatings. Attenuation calculations were made for channel A, for off-axis angles of 5, 24, 60 and 77 deg (in the 60 deg case a combined diffraction/attenuation calculation was made). The results show that channel A is critical for the moon at 24 deg and the Earth at perigee.

Examination of the ray histories shows that the critical surface is the inner surface of the primary bore baffle. In Phase B parametric studies will be required as improved surface coating data becomes available.

9.4.2.4 The Pointing Stability Impact on Image Quality

Figure 9.3.2 shows the degradation of the pointing performance with time. The result of this is to establish a short wavelength limit for diffraction limited operation depending on the type of instrument and on the integration time required. Figure 9.4.6. shows the effect of this for the most critical situation when the smallest detector field of view is required. It gives the fraction of the energy of a point source imaged at the focal plane when a diffraction limited aperture (defined as $2.44 \lambda / D$) is used with the detector. The energy fraction varies with wavelength and is shown for two integration times, 60 seconds and 1 hour. The curves show that diffraction limited operation is generally available at wavelengths down to about 10 microns but extension down to 5 microns could be achieved with special facilities within the instrument itself. As an example drift compensation can be achieved using detector arrays and it is at the shortest wavelength that detector arrays are presently being developed and used. The compensation could involve re-centring, consecutive scans of the array using a bright reference source within the field of view or the information given directly by the star tracker. This would leave the RPE over the sample period of the array, as the only remaining drift.

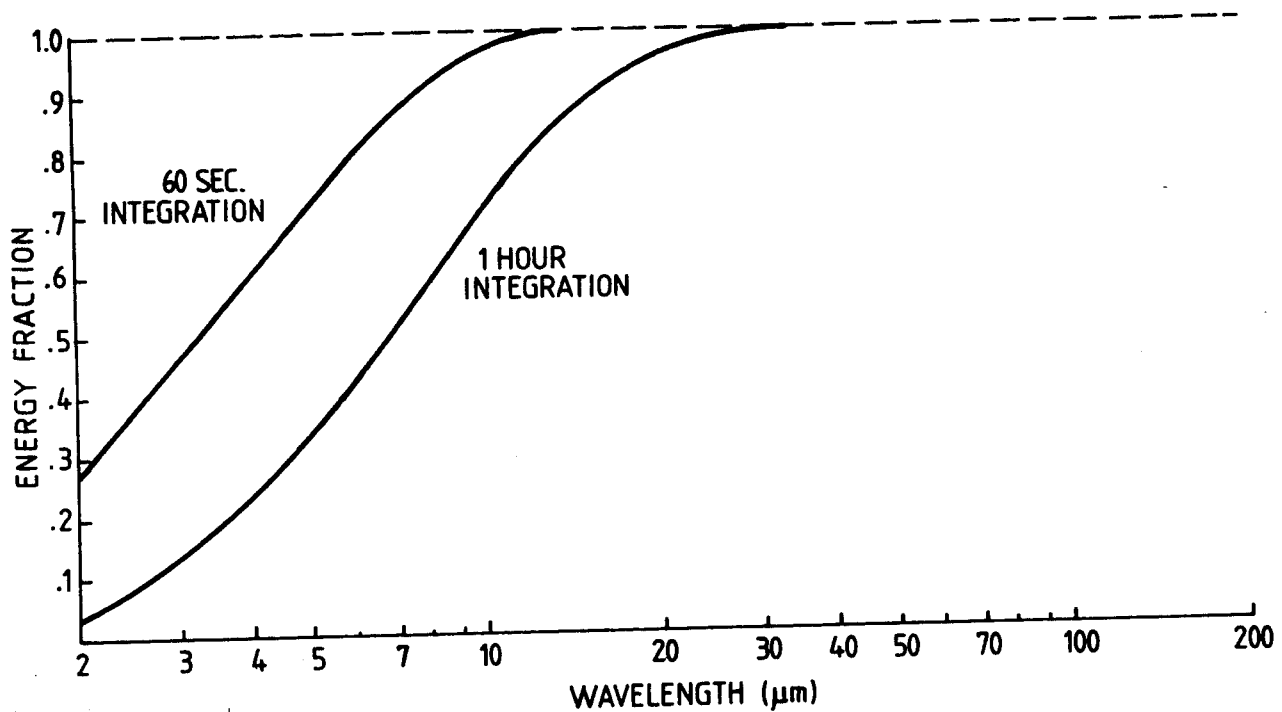


Figure 9.4.6 FRACTION OF THE ENERGY AT THE FOCAL PLANE DUE TO A POINT SOURCE PASSING THROUGH A DIFFRACTION LIMITED APERTURE (ANGULAR F.O.V. DIAMETER = $2.44 \lambda/D$) SHOWN AS A FUNCTION OF THE WAVELENGTH, FOR TWO INTEGRATION TIMES

9.5 The Electrical Subsystem

9.5.1 The Payload Module

The PLM electrical subsystem comprises the following items:

- the scientific instruments whose characteristics are given in Section 6.6.
- the cryosystem instrumentation and associated electronics;
- the control electronics;
- the "cold" harness inside the cryo vessel;
- the "warm" harness interconnecting warm electronics to cold harness.

9.5.2 The Service Module

9.5.2.1 The Solar Array

. The Configuration

The Solar Array consists of two wings, each wing comprised of two panels. In their stowed configuration, each wing is connected to the Service Module structure by four hold-down bracket assemblies. In the deployed configuration each wing is connected to the SVM structure by means of a simple non-rotating yoke assembly. The yoke is required to minimise thermal coupling between the sunlit array and the cooled payload.

Deployment of the array is initiated by independent pyro release mechanisms for each wing and accomplished by built-in deployment springs. Synchronous deployment is ensured by an appropriate mechanism.

. The Electrical Performance

At satellite End Of Life (EOL) the solar array provides 589 watts at 50 volts providing a margin slightly above 15%. This figure is applicable for:

- solar radiation perpendicular to solar array
- solar cell degradation due to the severe particle radiation environment of the ISO orbit.

For a 500 microns coverslide shielding on both front and rearside, the estimated 1 MeV equivalent fluxes are:

trapped protons	3.48 E15 e/cm ² at 1 MeV
solar flare protons	4.08 E13 e/cm ² at 1 MeV
trapped electrons	1.64 E14 e/cm ² at 1 MeV
Total	3.68 E15 e/cm ² at 1 MeV

In stowed condition there is no power generation by the solar array.

9.5.2.2 Power Distribution and Storage

As shown in the block diagram (Figure 7.6) the power subsystem consists of:

- . Main Regulator Unit including the battery charger and discharge regulators.
- . Power Resistor Unit (for power emergency).
- . 3 Batteries.
- . Power Distribution Unit.
- . Pyro Unit.
- . Convertor Unit.

- Three electrically separate solar array sections supply three sections of a sequential switchable shunt regulator being located in the Main Regulator Unit (MRU).
- The MRU also contains the regulators for charging and discharging the three batteries. The MRU generates the 28V main bus which is distributed to the Power Distribution Unit (PDU), the Converter and the Pyro Unit.
- The PDU distributes all 28V lines through limiters and switches. It also contains the circuits for temperature measurements.
- The Converter supplies those data handling subsystem units and AOCMS units which require supply lines other than the 28V main bus.
- The Pyro Unit contains all necessary circuitry to ignite the pyros by using battery power with the constraints of safety and reliability. The Pyro Unit distributes battery power for the ignition of six Pyro Units. Each circuit consists of two redundant parts. Circuits are supplied to release antenna 1, antenna 2, solar panel 1, solar panel 2, cryostat cap, HEI and H₂ vent valves.
- The energy storage consists of three Ni-Cd batteries with 18 A hr each. Number of cells per battery is 16. The Depth of Discharge in nominal mode is 45%. The DOD in case of failure of one battery or 1 BCR or 1 BDR is 67%.

9.6 The On-Board Data Handling Subsystem

The OBDH has been designed in compliance with the ESA OBDH standard.

9.6.1 The Function

The main functions of the ISO mission data handling subsystem are:

- acquire data from experiments and subsystems for transmission to ground.
- distribute data sent from the ground or generated by the on-board processor.
- provide a time base.
- issue telecommand compatible with the PCM telecommand standard.
- be able to acquire telemetry data compatible with the PCM telemetry standard.
- access all S/C subsystems through housekeeping telemetry interface.
- generate time and data tagged command using the CTU processing capabilities.
- provide, during observational periods, a downlink bit rate of about 43.7 kbps.
- provide during Launch and Early Orbit Phase (LEOP) a housekeeping format with a lower bit rate 4.1 kbps.
- identify unambiguously each downlink format.
- generate one re-programmable format, for experiments, and at least one fixed format for housekeeping data at a low bit rate.

9.6.2 The Design

Reference is made to the simplified block diagram of Figure 7.6. Uplink command signal is linked via a receiver equipment to the Command and Power Distribution Unit (CPDU). This unit decodes the command word, extracts the user address, distributes high priority commands directly to appropriate user (CTU on/off switching) and distributes low level and memory load commands via Remote Terminal Units (RTU's).

High speed scientific data coming from experiments are formatted, multiplexed with low speed housekeeping data, and transmitted to ground. A Central Terminal Unit (CTU) smart controller, is necessary on board to have a re-programmable scientific format and for generation of time/data tagged commands. It is also available for on board data processing (thermal control of star trackers and experiment pre-amplifiers).

Acquisition of telemetry information is performed through two RTU's: one devoted to data from several spacecraft subsystems (SVM-RTU), while the other RTU is used experiment data and cryostat signals (PLM-RTU). In order to ensure good reliability, there are two redundant CTU's and each RTU is internally redundant.

9.6.3 The Formats

The OBDH supplies the following telemetry formats:

Experiment Format

Four identical operational formats, one for each experiment. The format consists of 64 frames of 128 words each, a word having 8 bits.

Frequency:	43.7 Kbps
Transmission time:	1.5 seconds

Housekeeping Format

Two Launch and Early Orbit Phase housekeeping formats, one for each AOCMS dedicated to orbit debugging activities. The format consists of 16 frames of 64 words.

Frequency:	4.1 Kbps
Transmission time:	2.0 seconds

One nominal housekeeping format to be used during integration and test for both AOCMS I and II. The format consists of 64 frames of 16 words.

Frequency:	8.2 Kbps
Transmission time:	1.0 second

9.7 Telecommunication Subsystem

9.7.1 Function

The telecommunication subsystem fulfils the following functions:

- reception of an S-Band RF carrier modulated with the telecommand video.
- delivery of the demodulated telecommand video to the CPDU's.
- modulation of the TLM video as an RF carrier.
- multiplication of the modulated RF carrier into S-Band, amplification up to the required output power and transmission to the ground station.
- reception of a ranging signal modulated on an RF carrier.
- demodulation of the ranging signal and modulation of the ranging signal on the downlink carrier.
- transmission of the RF carrier simultaneously modulated with the ranging signal and the TLM video to the ground station.
- coherent operation with a fixed ratio of the downlink to the uplink frequency of 240/221, in order to allow range rate measurements.
- provision of a full spherical antenna coverage to perform the above functions under all possible orientations of the spacecraft with respect to the ground station.

9.7.2 Design

The design is essentially derived from the Exosat Programme. The block diagram of the telecommunication subsystem is shown in Figure 7.6.

The subsystem consists of:

- 2 fully redundant transponders (S-Band).
- 2 antennae each one having an hemispherical coverage.
- 1 transfer switch in order to have the possibility to connect each antenna.
- the RF cabling.

9.7.3 Essential performance versus requirements

<u>Requirement</u>	<u>Performance</u>
- Full Spherical Coverage	- 2 Antennae with Semispherical Coverage, overlapping for 100°
- Receiver and Transmitter Frequency Range	- Compliant with ESA standard PSS 44 in the range of 2020 to 2125 MHZ and 2200 to 2300 MHZ
- Absence of Single Point Failure except RF Cables and Antennae	- Receiver and Transmitter are duplicated for redundancy
- Capability to handle up to 2,000 BPS in the uplink	- The receiver section can handle bitstream data up to 4,000 BPS
- Capability to handle in the down - link-bit rate greater than 40 KBPS	- A bit rate of 43.7 KBPS with a link budget margin of more than 3 DB is obtained with a transmitter output of 6W.

10 SYSTEM BUDGETS AND PERFORMANCE

10.1 ISO System Budgets

10.1.1 System Mass Budget

<u>Payload Module</u>	
<u>Cryostat</u>	Mass (kg)
Aperture Cover	35.00
Cover He-Filling	5.00
Struts and Bolts/Knots for Sunshade	9.00
16 Straps and Coupling Bolts	12.00
All Vapour Cooled Shields	113.40
All Multilayer Insulation	20.80
He and H ₂ Piping	6.00
He and H ₂ Tanks, Dry	168.60
LH ₂ (95% filling of 750L)	50.40
HEII (95% filling of 750L)	105.40
Common Support Structure	46.00
Cryo Harness	8.00
Outer Vessel	339.20
Outer Valves and Piping	15.00
Screws	4.00
16 Strap Tension Devices	10.00
Total Cryostat	947.80
<u>Optical Subsystem</u>	
Sunshade	50.00
Baffle	50.00
Telescope	55.90
Optical Support Structure	21.00
Total Optical Subsystem	176.90
<u>Scientific Experiments</u>	30.00
<u>Sunshield</u>	15.00
<u>PLM/SVM Connection Struts and Equipment Platform</u>	95.90
TOTAL PAYLOAD MODULE	1,265.60

<u>Service Module</u>	Mass (Kg)
Telecommunication S/S	12.00
OBDH (without RTU 2)	13.50
Thermal Control	28.00
AOCMS (without QSSE)	215.40
Power S/S (including SA)	102.40
Structure	98.80
Harness	25.00
Total Service Module	495.10
PLM	1,265.60
SVM	495.10
Adapter	43.00
Total Spacecraft	1,803.70
<u>Margins</u>	
Allowed mass for Ariane 2	2,065.00
Mass Margin	261.30
Hidden Design Margin (see paragraph 10.3)	

10.1.2 ISO Power Budget

Mean power consumption at bus level in watts:

	+ 28V (watts)	Convertor Load (watts)	Total (watts)
Experiments	79.5	-	79.5
Cryostat	12.0	-	12.0
Thermal Control (SVM)	55.0	-	55.0
AOCMS	39.8	35.8	75.6
OBDH	-	48.0	48.0
RF	44.0	-	44.0
Power	48.0	3.0	51.0*
Harness			6.0
TOTAL BUS POWER	278.3	86.8	371.1

* Without MRU

Power Margin For selected design case: 80 min eclipse duration		
Unit/Level	Power (watts)	
	Begin of Life	End of Life
Loads	371	371
MRU*	32	24
Battery Charge	90	90
Required power at SA	493	485
Available power (30° tilting of SA)	686	510
Margin	193 W = 28%	25 W = 5%

For actual eclipse durations: 66 min at about 350 days, 30 min at EOL		
Unit/Level	Power (watts)	
	350 days	EOL
Loads	371	371
MRU	27	24
Battery Charge	75	34
Required power at SA	473	429
Available power 30° tilting of SA	572	510
Margin	99 = 17%	81 = 16%

10.1.3 Telemetry

	Acquisition Channels				
	Analogue		Digital		
	AS	AD	DB	DS	DD
Thermal and Power	50	-	7 x 8	-	-
RF	10	-	1 x 8	-	-
DH	8	-	-	8*Int	4*
AOCMS	-	-	-	-	2
Subtotal SVM	68	-	64	8*	6*(2)
Experiments	-	-	-	-	4
Cryostat	100	-	2 x 8	-	-
Subtotal PLM	100	-	16	-	4
TOTAL	168	-	80	8*	10*(6)

* not to be accounted for n° of RTU channels.

10.1.4 Telecommands

Telecommand Budget	LL	ML	SL
Thermal and Power	80		
RF	16		
DH	8		4
AOCMS	6	8	
Sub-Total SVM	110	8	4
Experiments	-	4	
Cryostat	40	2	
Sub-Total PLM	40	6	
TOTAL	150	14	4*

* Not to be accounted for number of RTU channels.

10.1.5 ISO Link Margins

MOP Station (Carnarvon)

Link Budget		Nominal dB	RSS Worst Case dB	Mean-3 Sigma dB
Telecommand	Carrier:	10.7	9.2	9.0
	Data:	4.2	2.7	2.3
Telemetry Only	Carrier:	25.1	23.7	23.3
	Data:	7.1	5.4	4.7
Telemetry	Carrier:	23.2	21.7	21.3
	Data:	5.2	3.5	2.8
	Ranging	23.7	20.6	19.9
Specified			1.0	0.0

<u>Down Link Parameters</u>		<u>Up Link Parameters</u>	
Bit rate:	43.7 Kbps	Bitrate:	1050 bps
Mod Index TLM:	M=1.2 RADS Pk	Mod Index TC:	1.2 RADS Pk
Mod Index Range:	M=0.7 RADS Pk	Mod Index Range 1:	0.7 RADS Pk
Frequency:	2100 MHz	Mod Index Range 2:	0.3 RADS Pk
Polarisation RHC		Ranging Bandwidth:	300 KHz
G/S Elevation Angle:	10 Degrees	Frequency:	2300 MHz

10.2 ISO Facility Performance Summary

The system budgets shown above combined with the subsystem performance described in section 9 give an appraisal of the ISO system capability. This paragraph is dedicated to the ISO facility performance, specifically to those essential aspects discussed in para 7.1.1. Results are presented in table 10.1.

10.3 System Margins and Confidence in the Design

Following the low risk, low cost philosophy outlined in para 7.1.3, the ISO design includes a substantial amount of conservatism built-up through subsystem design worst case assumptions and system level margins. The detailed monitoring and reporting of the overall margin is in general a complex task. This can be best summarised by comparison with a similar project. ISO can be compared in some aspects to IRAS. Two runs were therefore performed to simulate the IRAS conditions.

- a) The acceleration levels of the IRAS design were adopted for ISO Payload Module design (ref. para 9.1.1). As a result the cross sections of the structural elements (GFC straps) supporting the tanks and telescope were reduced by a factor of 2 yielding an estimated ISO lifetime of more than 2 years.
- b) Secondly, the ISO acceleration levels were reinstated but the hydrogen loop was suppressed. Only superfluid helium was used in a loop configuration similar to IRAS. The resulting predicted on-orbit operational lifetime is then about 300 days using 1500 l of He, which shows that the ISO design has a considerable margin as the same analysis using the IRAS tank volume (5401) results in a predicted life of 150 days.

The meaning of those results should not be carried beyond their intended purpose, which is to justify the confidence existing in the present design and to emphasize the conservatism of the predictions.

REQUIREMENT	PERFORMANCE	REF.								
<p><u>ORBIT</u> 12 hour elliptical (1000 km, 39000 km)</p> <ul style="list-style-type: none"> . Availability of whole sky a number of times . Long uninterrupted observations on selected sources/regions . Extended periods of accessibility to selected regions . Not too restrictive launch window . Continuous downlink (real-time observatory) . Minimum disturbance from particle radiation 	<ul style="list-style-type: none"> . Full sky coverage within 6 months - 3 times access to whole sky in 18 months mission duration . Within 18 months mission, any point in the sky can be observed uninterrupted at least once for a minimum of 4 hours. The longest uninterrupted observation period is 10 hours . Out of 18 months mission duration some regions in the sky can be observed for a total duration of 16 days (shortest) some for a total duration of 14 months (longest). Shifting the launch date provides a means to select coverage of interesting areas for long periods of time. . 4 periods of 2 months each . 2x11 hours per day with 2 ground stations (Spain-Australia) . Observations suspended for 2 hours around each perigee pass, overlapping with loss of downlink 	<p>para 8.6</p> <p>para 8.6</p> <p>para 8.6</p> <p>para 8.4</p>								
<p><u>ATTITUDE</u></p> <ul style="list-style-type: none"> . Fixed pointing . Optimize aspect angles wrt bright sources to maximise sky coverage (allow telescope l.o.s. to come close to bright source) and to remain compatible with acceptable straylight levels. 	<ul style="list-style-type: none"> . 3-axis stabilised . Aspect angles: <table style="margin-left: 20px;"> <tr><td>Sun</td><td>60°</td></tr> <tr><td>Earth</td><td>77°</td></tr> <tr><td>Moon</td><td>24°</td></tr> <tr><td>Jupiter</td><td>5°</td></tr> </table> <p>Result of an iterative process involving orbit analysis, design of sunshade and baffles, straylight analysis.</p>	Sun	60°	Earth	77°	Moon	24°	Jupiter	5°	<p>para 9.3.1</p> <p>para 7.1.2</p>
Sun	60°									
Earth	77°									
Moon	24°									
Jupiter	5°									

REQUIREMENT	PERFORMANCE	REF.
<ul style="list-style-type: none"> . Steady state and transient . Off-set pointing . Small raster scan for source location or for experiment to peak-up on signal . Large raster scan for mapping . Slewrate: 6 arc degree/minute 	<ul style="list-style-type: none"> . Performance available in Tables 9.3.1 to 9.3.3. & Fig. 9.3.2 . Swing from experiment 1 to experiment 2 and stabilize within 10 seconds and within 2" of required object. . 1.x 1. arc min with accuracy levels consistent with those associated to fine pointing Duration: 10 minutes . 30x30 arc min - as above Duration: 40 minutes . 7 arc degree/minute. Time for acceleration, deceleration and settling for slews above 30 degrees require 25 seconds. Slews of the order of 1 arcmin require 10 seconds. 	<p>para 9.3.2</p> <p>para 9.3.2</p> <p>para 9.3.2</p> <p>para 9.3.2</p> <p>para 9.3.1</p>
<p><u>TELESCOPE TEMPERATURES</u></p> <ul style="list-style-type: none"> . Optics Less than 20 K . Baffles Less than 40 K . Sunshade T B D . Focal Plane Assembly 8 K . Doped Germanium Detectors 3 K <p>The lower the thermal emission of the telescope, the better the facility performance, operations being extended to longer wavelengths. (up to 115 microns as a goal)</p>	<ul style="list-style-type: none"> 10 K 18 K lower part 30 K upper part 111 K 7 K 3 K <p>Temperatures achieved are consistent with using a detector with a NEP of 1×10^{-17} watts Hz^{-1/2} at wavelengths out to about 200 microns.</p>	

Table 10.1

REQUIREMENT	PERFORMANCE	REF.
<p><u>LIFETIME</u></p> <ul style="list-style-type: none"> . On-orbit operational: 18 months . On-ground T.B.D. . Launch Early Orbit Phase: less than 30 days <p><u>OPTICAL SUBSYSTEM</u></p> <ul style="list-style-type: none"> . Plate scale 2.6 mm/arcmin. . Primary mirror diameter 600 mm . System focal length 9000 mm . Field of view (full cone) 15 arcmin. <p><u>STRAY-LIGHT</u></p> <ul style="list-style-type: none"> . Admissible background by thermal self emission at 115 microns wavelengths (worst case) 3×10^{-16} watt . Stray-light rejection factors at 5 micron (worst case) at defined aspect angles Sunlight: 7.7×10^{18} Earth: 5.3×10^{16} Moon: 1.4×10^{13} Jupiter: 1.2×10^9 	<ul style="list-style-type: none"> . 20 months consistent with: <ul style="list-style-type: none"> 11 days of ground autonomy of LH₂ 4 days of ground autonomy of He^I 4 launch postponements (4 days) 11 to 14 days to allow on-orbit outgassing prior to start of operation 2.6 mm/arcmin. effective diameter 600mm. (Free diameter 634 mm.) 9000 mm 20 arcmin unvignetted (3 arcmin per experiment) 40 arcmin total . clean mirror: $1.2 \cdot 10^{-23}$ W (uncertainty factor ± 100) . dirty mirror: $3 \cdot 10^{-20}$ W (uncertainty factor ± 57) 1.7 10^{22} uncertainty factor 5 5.6 10^{17} uncertainty factor 13. Critical at perigee pass (when instrument non operational) 5.2 10^{13} uncertainty factor 17. Critical at 24° aspect angle 3.6 10^{11} uncertainty factor 2.6 	<p>para 9.2.1 and para 10.3</p> <p>para 9.4.1</p> <p>para 9.4.2</p>

Table 10.1 (continued) ISO Facility Performance Summary

11. SPECIAL ASPECTS

11.1 Contamination

Degraded straylight performance and false detection could impact the ISO scientific mission's reliability.

The industrial phase A was limited to identify potential contamination sources and transport mechanisms and to propose a contamination control approach.

11.1.1 Hazard

The major sources of contamination of the ISO optical subsystem are divided into gaseous and particulate contributors

. gaseous:

- outgassing from non-metallic materials like thermal paints, thermal blankets, adhesives, epoxy, solar panels etc.. used in the ISO design will be a principal source of gaseous contaminants.
- the hydrazine RCS used for attitude control (desaturation of reaction wheels during perigee pass) and orbit control manoeuvres (one or twice at apogee during the operational phase) will be another potential source of contamination (NH_3 , N_2H_4 and also N_2) for the optics.
- outgassing of absorbed molecules of the ambient atmosphere like H_2O , O_2 , N_2 and CO_2 will be of major contribution in the early orbit phase when telescope cover is still on and will decay significantly after some days of vacuum exposure. The telescope cover is ejected around 14 days after launch.
- ambient atmospheric constituents on the ISO orbit are not a critical contribution, since during perigee pass the telescope line of sight is controlled such that no scooping of the atmosphere occurs.

. particulate

- potential sources are ice crystals, dust, particles abraded from paints and thermal blankets.
- potential hazardous transport mechanisms of gaseous and particulate contaminants are assessed to be
 - . return fluxes from outgassed contaminant to contaminant molecular collisions (self-scattering)
 - . return flux of contaminants by back-scatter with natural atmosphere in the perigee pass. The relative contribution of this process appears to be minor.

11.1.2 Contamination Control Methodology

Preparation of contamination control plans shall be initiated during the detailed design phase requiring to perform the following work:

- assess analytically the admissible induced background noise due to contaminated sensitive surfaces (mirrors, baffles, sunshade..) and particles passing the telescope - f.o.v. with respect to detector sensitivities of the selected scientific instruments.

- assess analytically the expected contamination
- perform sensitivity analyses of critical surfaces acting as potential straylight sources with the Guerap-computer model.
- perform tests to assess the impact of contamination on IR-measurement, e.g. inject controlled contaminants in a vacuum cryochamber, measure the deposit on a small mirror and measure the degradation of the IR performance.
- derive strict requirements on materials fabrication techniques, cleaning procedure, cleanliness of facilities, etc..

11.2 Safety Considerations

The potential hazards identified during the study are:

- . propellants
- . pressure system
- . pyrotechnics
- . r.f. radiation sources
- . cryogenics
- . electrical systems

All of these would be controlled in the phase B-C/D by implementation of safety control measures in compliance with standard ESA specifications, Ariane Users Manual/Safety specifications and National safety standards.

The most specific of the above mentioned hazards to the ISO project is the one related to cryogenics. In particular the handling of hydrogen is now a well developed technique within aerospace companies, (e.g. Ariane II 3rd stage). Experience is available in Europe and facilities have been designed (hydrogen proof) to host payloads containing liquid hydrogen. This aspect has been covered in the study during the survey of facilities required by the test programme.

The only problem identified during the study is the handling of liquid hydrogen at KOUROU CSG, building S3, where the spacecraft is assembled and tested prior to its transport and lifting on platform 8 of the launch tower (para 12.1). Building S3 is presently not expected to handle hydrogen. Modifications are possible, discussions have taken place with CNES and ESA Ariane authorities and the cost of those modifications has been included in the ISO cost at completion estimate, even though work around solutions such as filling the hydrogen outside S3 in a clean tent are being contemplated.

11.3 Particle Radiation

The ISO spacecraft is subject to a flux of charged particles which will accumulate on dielectric surfaces and possibly discharge into the spacecraft body. Comparison with radiation loads of the EXOSAT program show them to be considerably higher (10 to 30 times).

Particle fluxes for trapped protons, electrons and induced solar protons were calculated at ESTEC for worst case conditions (high solar activities and solar flares) and used to calculate the degradation of the solar cells (para 9.5.2.1) and assessing the impact on the scientific detectors performance. Care was taken in selecting external surfaces electrically conductive such that proper controlled discharges would occur.

Similarly radiation loads of electronics parts were considered so far to identify radiation sensitive technology and foresee alternatives. For instance in the On-Board Data Handling subsystem, CMOS technology could be replaced by low-power Schottky. In anticipation of such a need, to be verified in phase B an allocation of 40W in addition has been included in the power budget.

The ISO grounding concept is compliant with the ESA standard.

11.4 New Developments

In line with the design philosophy of para 7.1.3 new developments have been kept to a minimum. All subsystems are based on space qualified or already flown hardware. The exceptions are:

- a) the Quadrant Star Sensor located in the telescope FPA. The QSS provides the line of sight of the telescope and is used to perform calibration with the star tracker. A suitable QSS is currently under development by TPD-TNO.
- b) the hydrogen phase separator, which is presently developed under ESA Technology Research Programme. A laboratory model has been manufactured and tested. It confirmed the feasibility and good performance of the selected concept. The space qualification is planned for 1983-1984.
- c) The cryostat instrumentation e.g. flowmeters, pressure sensors, etc, to be adapted to ISO specific needs is presently covered by the ESA Technology Research Programme.

12. ISO OPERATIONS

12.1 Pre-launch activities

Pre-launched activities are described in the preliminary ISO/Ariane Combined Operation Plan given in figure 12.1.1. The activities specific to the cryogenic system are shown in figure 12.1.2.

12.2 Launch and Early Orbit Phase

12.2.1 LEOP Support Ground Network

The Launch and Early Orbit Phase will be supported by the standard ESA GTO S-Band Network consisting of ground stations at:

- Kourou (French Guiana)
- Malindi (Kenya)
- Carnarvon (Australia)

For satellite control during the LEOP the baseline solution is the use of the Operations Control Centre (OCC) at ESOC, Darmstadt, supported by the Multi-Satellite Support System (MSSS) for data processing.

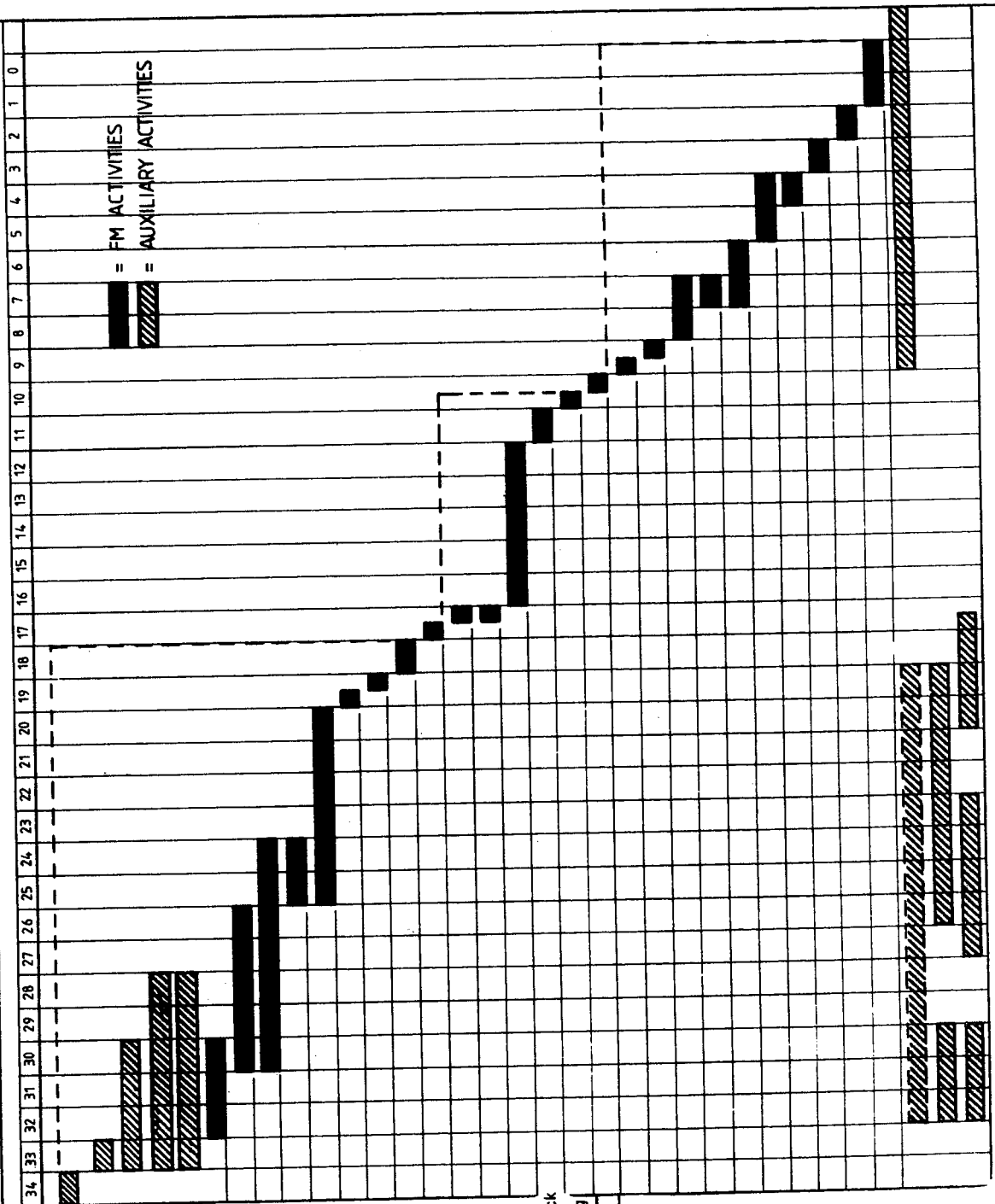
12.2.2 LEOP Operations

Time	Event	Location	Remarks
0	- Lift-off (LO)	Launcher sequencing system	
About mid off second stage flight	- Fairing Jettison		
LO + 12 min	- 3rd stage propulsion cut off	Launcher sequencing system	- Begin of ISO transfer orbit
LO + 12 min	- separation 3rd stage/ISO	Launcher sequencing system	- 3rd stage remains attitude controlled after propulsion cut off. ISO is forced apart by spring action. Separation signal provided to ISO by means of micro switches.
	- Switch to fine attitude control	Ground CMD	- After star recognition on ground using star tracker, FSS, Gyro, RW

12.2.2 LEOP Operations (continued)

Time	Event	Location	Remarks
LO + 4 hrs	<u>Drift Phase</u>		
	- Swing + X-axis to desired direction	Ground CMD	- Star acquisition near delta V-direction and subsequent fine control
	- Switch off RWS, switch on RCS	Ground CMD	- Sensors used: FSS, GYR, STR
LO + (depends on V)	- Enable first delta V burn	Ground CMD	- Planned during first or third apogee pass under ground supervision, max. expected duration: 3...4 hours
LO + 8 hrs	- Return to fine control	End signal	- Switch of RCS, switch on RWS
	- Start experiment check out	Ground CMD	- Start in orbit AOCMS calibrations - Detector and preamplifier switch on status up to this point TBD
	<u>Operational Phase</u>		
LO + 8 days	- Switch on experiments and QSS	Ground CMD	
LO + 8 days	- Perform multiple alignment measurements and necessary calibrations	Ground CMD	- to compensate for misalignment star tracker/telescope under various conditions
LO + 11 to 15 days	- Perform second and third delta-V manoeuvre	Ground CMD	- At apogee pass, as per first, third manoeuvre could become necessary for injection accuracy reasons
LO + 15 days	- Release telescope cover	Ground CMD	- Time selected to allow for outgassing of ISO.
	- Start of operational observations		- Perigee pass: before ground contact loss point + X-axis into safe direction.

EUROPEAN SPACE AGENCY - ISO - LAUNCH OPERATIONS SCHEDULE



0-DAYS

OPERATIONS

Flight to CSG - Satellite and GSE

Unload aircraft - Transport to CSG

Unload - Unpack - Install in Bldg S1

I/F Verification - Handling activities

GSE installation and commissioning

FM sat. - Install & post transport inspection

Preparation for Leak Detect. & Leak Meas.

Evacuation Isolation Vacuum System

Alignment Measurement

Preparations for Integrated System Test

Short Countdown Rehearsal

Pyros Installation and Functional Check

Part Multi Layer Insulation (MLI) Install.

Batt. Install. - Inspect. - Prep. for Transp.

Transport Bldg. S1 Bldg. S3

Reconfigure and inspection

Solar Array Installation

F111 Cryostat LHE/JH2

F111 Hydrazine RCE & Init. Press. + Funct. Check

Final Sat. Prep. - MLI Completion - Weighing

Transport S3 - PFB

Mating with Launch Vehicle

Cryostat Activities (HE II)

Fairing Installation

Satellite Activities + Umbilical Checks

Satellite ISC

Final Filling LHE (with HE II)

Final Pressurisation Hydrazine RCE

Countdown Rehearsal

Sat. Monitoring - Final Electr. Checks - Preparations for Countdown

Terminal Countdown

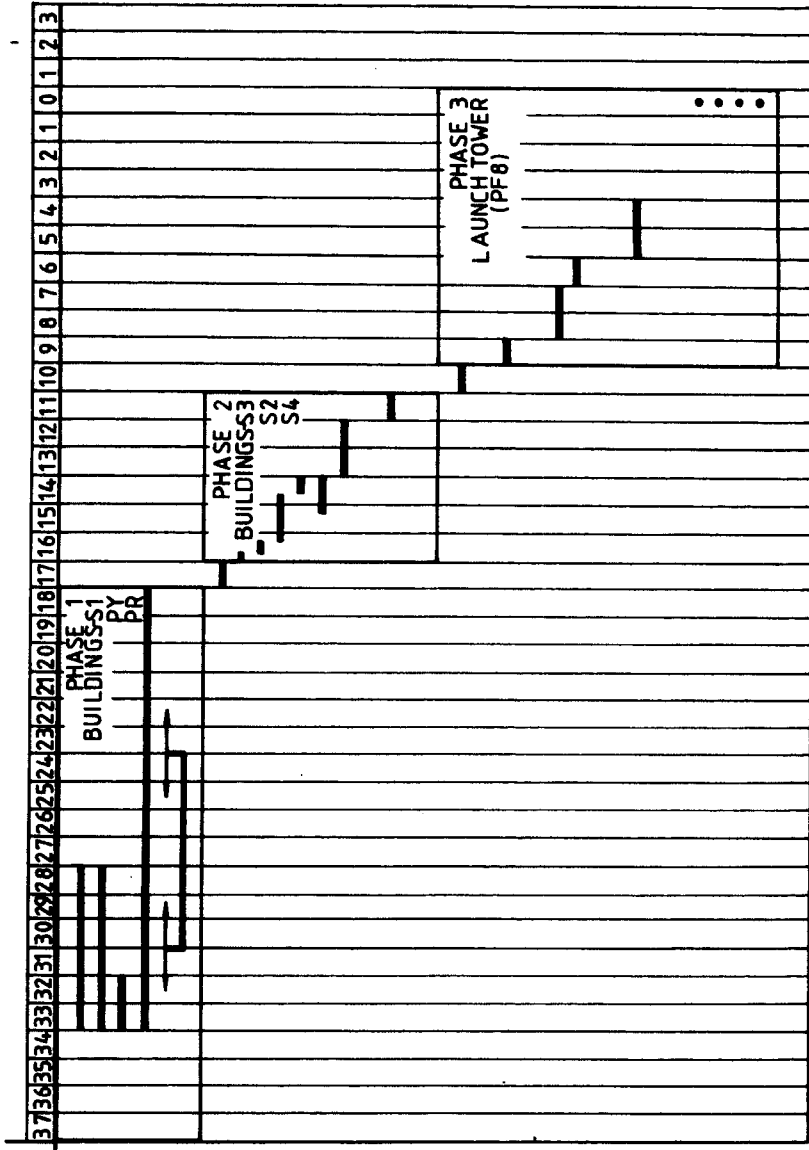
Battery Conditioning and Selection

Filling/Pressur. Equipment for hydrazine

CTU Compatibility Test Unit

RF/Video links tests

3 / 2257 / 4



INTERFACES VERIFICATION & HANDLING ACTIVITIES.
GSE INSTALLATION AND TEST.
S/C INSTALLATION INSPECTION.
S/C PREPARATION.
EVACUATION OF THE ISOLATION VACUUM SYSTEM.
(NO DATE REQUIRED).

TRANSPORT S/C S1 - S3
EVACUATION OF HE/H₂ SYSTEMS.
FLUSHING BOTH SYSTEMS WITH HE, H₂ RESPECTIVELY.
CONTROLLED COOL DOWN.
FILLING OF BOTH SYSTEMS UP TO MAX. LEVEL.
EVACUATION, FLUSHING, FILLING CAP-CRYOSTAT.
THERMAL STABILIZATION OF THE CRYOSYSTEM.
REFILLING HE AND H₂ UP TO MAX. LEVEL (1.1 BAR)
DISCONNECTION OF ISOL. VACUUM PUMP AND
LH₂ FILLING DEVICES: FILLING LINE AND EVACUATION
LOCK SEALED.

TRANSPORT OF S/C FROM S3 TO PF 8.
FINAL FILLING OF CAP-CRYOSTAT.
LOWERING HE TANK PRESSURE TO ACHIEVE 1.8 K
DISCONNECTION OF CAP-CRYOST. FILL DEVICES. FILLING
LINE SEALED.

INSTALLATION OF FAIRING.
S/C ACTIVITIES (REF. BATTERY).
REFILLING HE SYSTEM, REPEATED PRESSURE
LOWERING AND REFILLING, FINAL FILLING (17 m BAR)
DISCONNECTION OF THE FILLING DEVICES. FILLING LINE
SEALED. DISCONNECTION INDICATOR, OPERATOR CONTROL
PANEL.

HE VENT-GAS REGULATION VALVE CLOSED.
UMBILICAL LINES FOR HE AND H₂ VENT-GAS
DISCONNECTED (AUTOMATICALLY).
H₂ VENT-GAS OUTLET CLOSING LIFT-OFF.

FIG. 12.1.2 CRYOGENICS ACTIVITIES IN LAUNCH RANGE

12.3 On-orbit operations

The functional diagram of the ground segment during on-orbit operations is given in figure 12.3.

12.3.1 Ground Network

Due to its eccentric 12-hour orbit, ISO requires two ground stations in opposite hemispheres of the earth, in order to achieve maximum ground station coverage.

ESA stations suitable for this task are located in Carnarvon (Australia), and at Odenwald (Germany) or Villafranca (Spain). With ground station at Carnarvon and one of the European sites, an average ground coverage of 95% is achieved. The choice between the two sites in Europe does not influence this result significantly and can be made at a later stage, in co-ordination with other ESA programmes.

12.3.2 The Observatory concept

General

The ground observatory or "guest observer facility" proposal for ISO follows the concept implemented for the IUE, Exosat and Space Telescope missions. It will allow observations to be conducted by scientists in a manner similar to those at ground-based telescopes with a possibility to control in real time target acquisition, instrument parameter settings and integration time.

The observatory will be co-located with the satellite control facility in order to ensure optimal interaction between spacecraft and payload control. For the location of the combined facility the choice between the two options, ESOC or VILLAFRANCA, is still open and is largely a function of facility usage optimisation.

With respect to the observatory concept outlined below, this choice will have no consequences.

Mission Planning

Following the peer review of observation proposals with respect to their scientific merits, a mission planning software package will be used to compute possible observation time compatible with the sky coverage constraints imposed by the orbit and by the Sun, Earth and Moon viewing limits (Sect. 8.6). It is also anticipated that all accepted proposals will be globally scrutinized in advance of the start of mission operations, in order to achieve a baseline observation programme with well-defined back-up targets. Flexibility will exist and is essential to introduce changes at short notice to accommodate targets of opportunity.

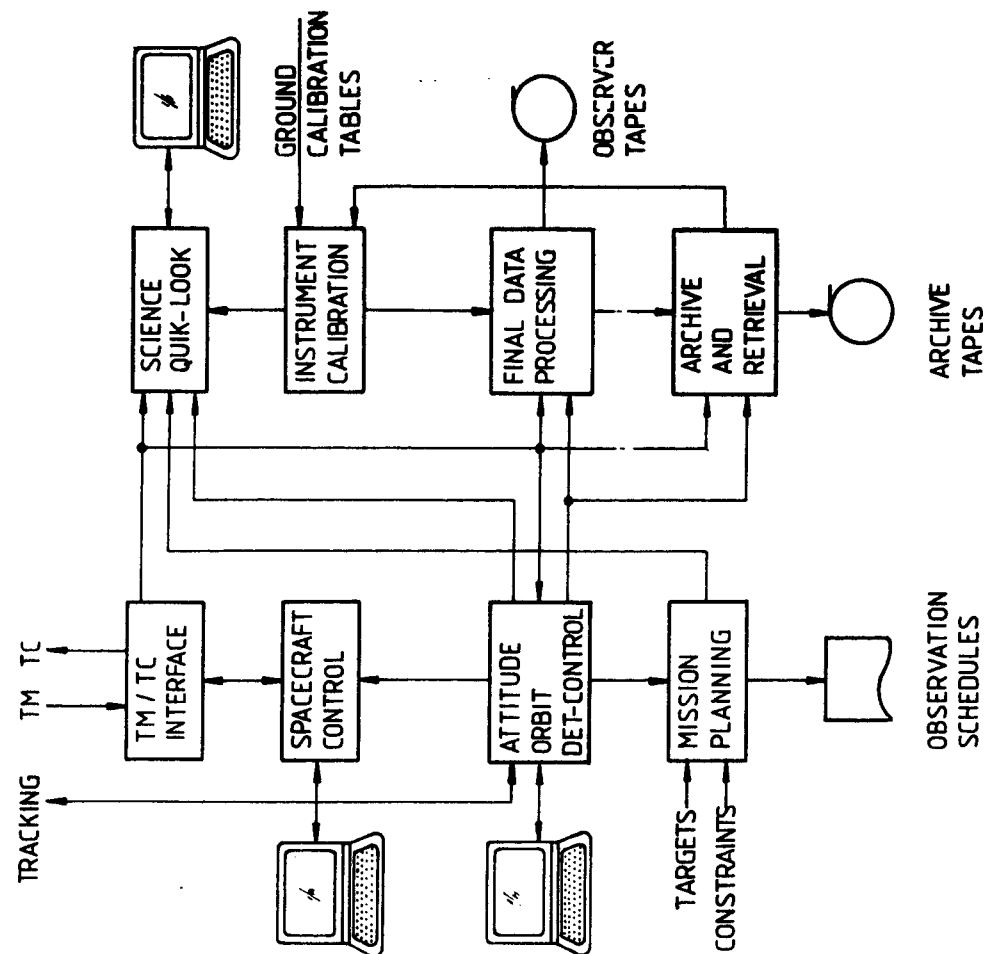


Figure 12.4

FUNCTIONAL BLOCK DIAGRAM
OF GROUND DATA PROCESSING

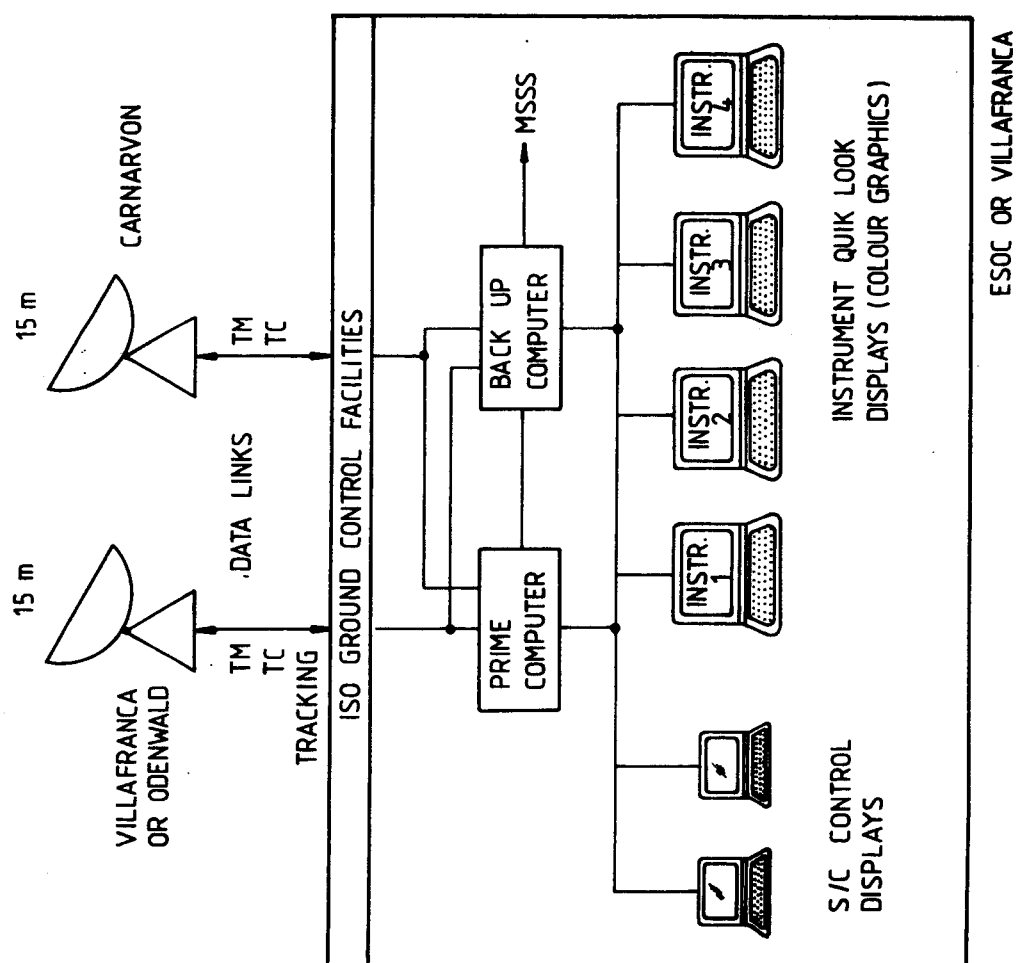


FIG.12.3 GROUND SEGMENT DURING MISSION
OPERATIONS PHASE

Observation Preparation

Guest observers will be able to perform a "dry run" of their observation sequence using a backup set of observatory terminals and appropriate simulation software. This should help to avoid problems during the actual observation session and thus maximise useful observing time. Prior to the actual observation shift, the final list of targets will be checked against constraints taking into account latest orbit and spacecraft status data, and a schedule of observing periods and slew manoeuvres will be prepared. The basic unit of scheduling will be a 10-hour "shift" centred around apogee. During such a shift, possible observation duration will vary between four hours and the full ten hours, depending on the sky co-ordinates of the target.

Since observation periods are usually terminated by the approach of one of the viewing constraints of Sun, Earth or Moon, a time slot with an appropriate safeguard margin must be foreseen to allow slewing to the next target. This slew will in most cases have to be done in several legs, i.e. not along a great circle, in order to avoid constrained regions. Prior to perigee and/or loss of ground station coverage, a slew to a safe (earth avoiding) attitude has to be commanded.

The two daily visibility periods or shifts will alternate between European and Carnarvon coverage.

Conduct of Observation

The observation session will start with the slew of the telescope axis to the required target co-ordinates, using offset pointing with the star tracker on a visible reference star. Nominal sequences of a typical operational orbit are given in figure 9.3.4. The co-ordinates of the target object with respect to the reference star and the reference star co-ordinates will have been verified in advance so that no further checks, eg with finding charts, should be necessary under nominal conditions.

The guest observer will then select his instrument operation modes (instrument selection, filter positions, gain settings, etc), perform any internal calibrations and start collecting his data.

Accumulation of instrument data will be shown on the quicklook display, with basic pre-processing (eg deconvolution, instrument response correction, basic wavelength calibration) performed in real time. With the real time quicklook facility, the observer will be able to immediately detect any unexpected results or anomalies and may terminate the exposure or modify the observing sequence accordingly. Using the same facility, the mapping of extended sources can be controlled by initializing automatic sequences of different offset pointing commands.

For spacecraft safety reasons, the responsibility for vetting and transmitting commands to the satellite will lie with the duty spacecraft controller. The guest observer will be able to communicate his requests through his terminal in a high-level command language. An observatory staff member will always be able to assist during observations.

Final Data Processing

Upon completion of an observation, the scientific data will be subject to standard processing in order to provide the observer with well-defined calibrated output. For this purpose, the data will be corrected for all known instrument errors and attitude and orbit effects, converted to standard units, and annotated with any spacecraft and payload status data necessary to interpret it. Output will be on magnetic tapes in a standard format acceptable to astronomical image processing systems.

Final data scientific reduction and analysis is considered a task of the individual observers and is not planned to be implemented in the observatory data processing system. If computer capacity allows this, the running of user application programs could however be made possible on the backup part of the system. A software environment with standard interfaces, eg STARLINK or MIDAS, could be installed to support this off-line activity. Another off-line activity which will be part of nominal observatory data processing is the regular update of calibration tables by analysis of specifically acquired calibration data and by re-processing of existing observation data.

Archiving

ISO will produce a raw data volume of approximately 2.10^6 Mbits during its lifetime. From experience with IUE, frequent demands can be expected from the user community for copies of portions of raw and processed data. For this reason, a flexible archiving system needs to be installed which allows the easy identification of available data through an efficient indexing and catalogue system, and the fast retrieval of data from storage media.

12.3.3 Data Processing Facilities

The concept chosen for the ISO ground control facility foresees an integrated data processing system supporting both spacecraft control and observatory tasks. This could either be a stand-alone facility in the case of location at Villafranca, or a suitable extension to the existing Multi-Satellite Support System (MSSS) at ESOC (Darmstadt).

Hardware

The core of the data processing hardware will consist of two medium-sized general purpose computers (SEL 32 or VAX 11 or equivalent), or existing MSSS hardware and software supported by special processors for real time image deconvolution. In this configuration, one machine will provide a backup capability for the other applications. Peripheral equipment will therefore be cross-strapped to both machines.

For the observatory support, four identical redundant work stations for interactive control are foreseen, one for each instrument.

These work stations will comprise high-resolution colour graphics terminals combined with keyboard, tracker ball, alphanumeric terminal and hardcopy unit. A high-resolution colour plotter and a high speed line printer could be shared between the two observing stations. Depending on requirements for simultaneous operation of several focal plane instruments, this concept can be modified to provide instrument-specific observing positions.

Software

Spacecraft control software will be modified from existing programmes within MSSS, while for the observatory software, especially the instrument specific parts, support may be required from Principal Investigators. The major software functions of the system are shown in figure 12.4. In addition to mission-specific software, a general image processing and display package will be used, which will be derived from existing image processing software. This software will support tasks like:

- geometric image manipulation;
- matching, differencing, averaging;
- generation of contour maps, histograms, false colour representation, shading and contrast enhancement;
- correlation and filtering of images, frequency domain analysis and convolution with calibration files.

13. MANAGEMENT

13.1 Procurement Policy

The proposed procurement scheme for the spacecraft is to consider the focal plane instrumentation as experiments which are provided by an institute or a consortium of institutes. ESA would be responsible for the overall spacecraft and mission design and would procure the service module and the telescope and cryostat assemblies

The following paragraphs outline the scheme foreseen.

13.2 Scientific Management

13.2.1 Instrument Selection

After approval of the mission, the Agency will issue an Announcement of Opportunity (AO) calling for proposals for the instrument development. The AO will be explicit in terms of the scientific mission, spacecraft resources, technical interfaces, schedule, deliverable items, responsibilities of the parties, observer programme, etc.

Scientific collaborations or individual institutes are expected to respond with proposals describing in detail the design and development of their proposed instrument.

The proposals should describe the management structure within the collaboration and show how responsibilities for the scientific, technical, operational and analysis aspects will be discharged.

Selection of the successful institute will be via the normal procedure of recommendations by the ESA advisory groups and approval by the SPC.

13.2.2 Instrument Development

Following selection of the instrument, the resources allocated to and interfaces of the instrument would be defined prior to the invitation to tender to industry for the spacecraft phase B. These resources and interfaces would be frozen at the end of Phase B.

The development schedule of the instrument is indicated in Figure 13.2. For the instrument, the responsible institute would be required to deliver a structural/thermal model, an electrically functioning engineering model, a flight model and an appropriate set of flight spare units. Special items of mechanical ground support equipment, e.g. attachment and lifting devices, servicing trolleys etc., and electrical checkout equipment including stimuli, recording equipment etc., would also be required.

During the development phase of the instruments the ISO project could conduct, with the Institute, a preliminary design review in the design phase, a critical design review in the early hardware phase and a flight model review.

To support the project, an Science Working Team (SWT) comprising the PIs and the ESA project scientist would be established.

13.3 The Verification Approach

In accordance with the low risk approach outlined in section 7.1.3 the verification programme adopted for ISO is based on the following key features:

- . Ensure adequate design feedback between development models and flight model. This is mainly achieved by
 - completing module development tests before releasing manufacturing of flight models
 - completing test programmes of units/subsystems before their integration into respective module models
 - completing unit qualification before starting unit acceptance and flight model programme.
- . Perform only acceptance test programme on flight models.
- . Make use of the conservatism built in the design to verify the compliance to the specification by analytical methods once they are shown to be, for a comparable risk, more practical and cost effective than tests.
- . Minimize the number of tests at ISO system level when PLM and SVM are mated to minimize the needs for large facilities and resources.

The model philosophy and test programme resulting from the proposed verification approach is summarized in table 13.1 and figure 13.1.

The main features are:

- . Refurbish the SVM structural model into an Engineering Model. As the structural design is very conservative (designed to carry a Payload Module up to 1.8 tons) refurbishment involves very little risk.
- . Develop and test early in the programme the structural and thermal model of the PLM and in function of the test results, decide if a refurbishment is acceptable or if an EM has to be manufactured.

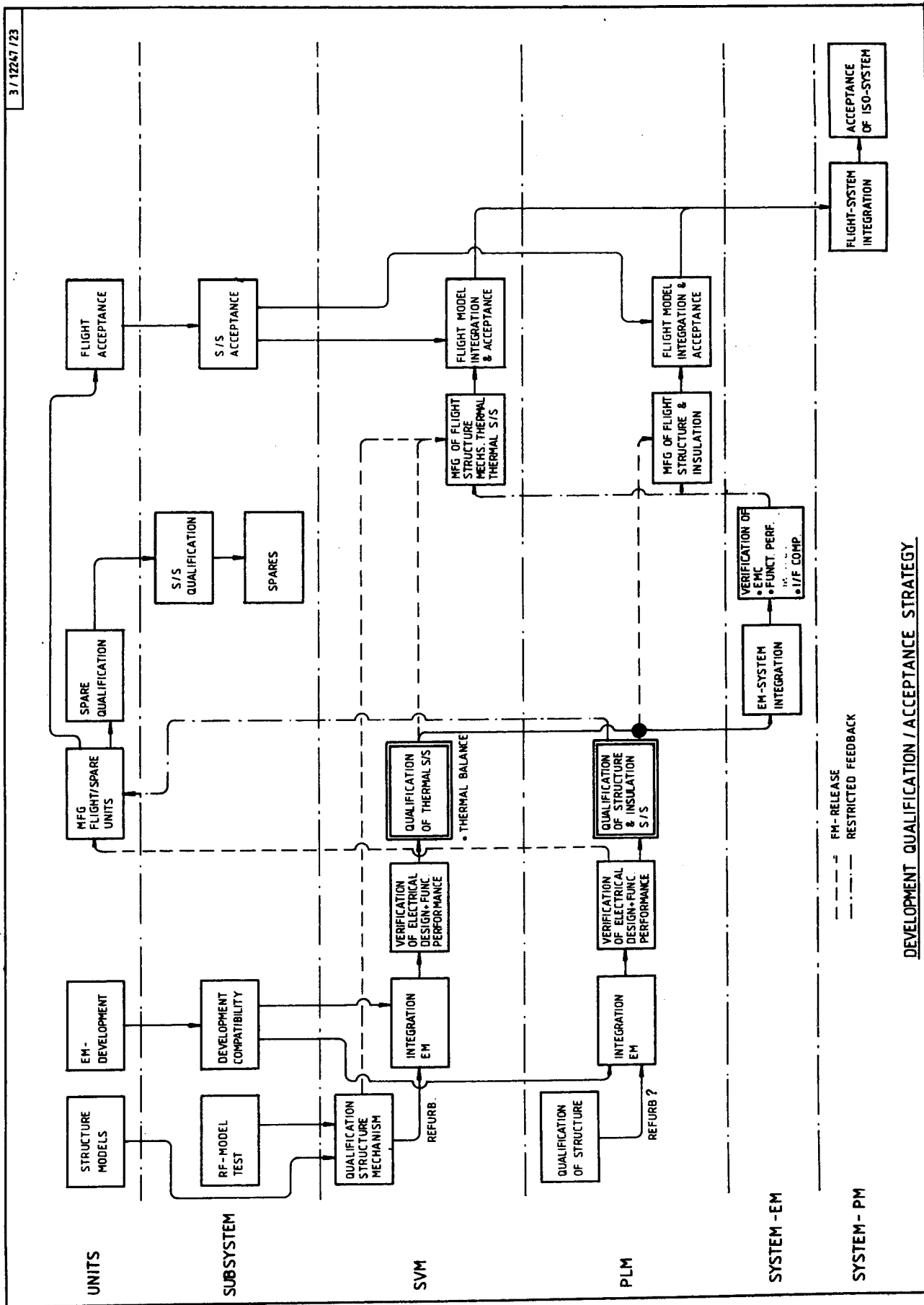
13.4 The ISO Programme Planning

The ISO programme master schedule given in figures 13.2 is based on the approach outlined in section 7.1.3 and on the model philosophy given in section 13. The basic features are:

- A short phase B1 since detailed design data are available at the end of phase A
- The introduction of a pre-phase C during which the PLM structural and thermal model will be developed, manufactured and tested. During this phase the industrial team is maintained at a low level of resources.
- A phasing which allows a proper design feedback between modules avoiding schedule risks and overlaps.

SERVICE MODULE (SVM)	<p>SM</p> <ul style="list-style-type: none"> - Integration - Alignment - Static Load - Alignment - Physical Properties - Vibration (Qual. Sine/Random) - Alignment - Acoustic Noise (Qual.) - Deployment - Shock/Release - Refurbishment 	<p>EM</p> <ul style="list-style-type: none"> - Structure Incoming Inspection - Bonding/Grounding - Subsystems Integration - Initial Alignment - Commissioning Subsystem Software <ul style="list-style-type: none"> . Data Base . Users Test Software . Applications Software - Integrated Subsystem Tests (ISST's) - Leak Measurements - Integrated Module Test (IMT) - Thermal Balance/Solar Sim. 	<p>FM</p> <ul style="list-style-type: none"> - Structure - Bonding/Grounding - Subsystems Integration - Alignment - Commissioning Updated Subsystems software - Integrated Subsystem Tests (ISST's) - Physical Properties - Acceptance Vibration - Integrated Module Test (IMT)
PAYLOAD MODULE (PLM)	<p>STM</p> <ul style="list-style-type: none"> - Integration - Physical Properties - Static Load - Alignment - Vibration - Warm (Sine/Random) - Evacuation/Cooling - Vibration - Cold - Acoustic Noise (Qual.) - Cryostat Tests (Lifetime) - Refurbishment (?) 	<p>EM</p> <ul style="list-style-type: none"> - Integration - EGSE + S/W Tests - Cryostat Tests - Alignment - Integrated Subsystem Tests (ISST's) - Integrated Module Test (IMT) - Temp. + Ground Lifetime Test - Thermal Balance + Cover Release in vacuum - Integrated Module Test (IMT) - Physical Properties 	<p>FM</p> <ul style="list-style-type: none"> - Integration - Cryostat Cooling - Alignment Check - Telescope/Star Tracker - ISST's/IMT - Acceptance Vibration - Alignment Check - Leak Check - Physical Properties
SYSTEM (PLM+SVM)	<p>VERIFICATION</p> <p>by</p> <p>ANALYSIS</p>	<p>EM</p> <ul style="list-style-type: none"> - System Integration - Alignment - Integrated System Test (IST) - Leak - EMC - Antenna check - Vibration (Low Level) - Simplified IST - Compatibility Tests (CTU) (Ground Network) 	<p>FM</p> <ul style="list-style-type: none"> - System Integration - Alignment - Integrated System Test (IST) - Leak - EMC - Antenna Check - Vibration (Sine/Random - Acceptance) - Thermal Vacuum - Integrated System Test (IST) - Alignment - Release/Deployment - Physical Properties - Flight Acceptance

Table 13.1 ISO-Model Philosophy Matrix



UNITS

SUBSYSTEM

SVM

PLM

SYSTEM - EM

SYSTEM - PM

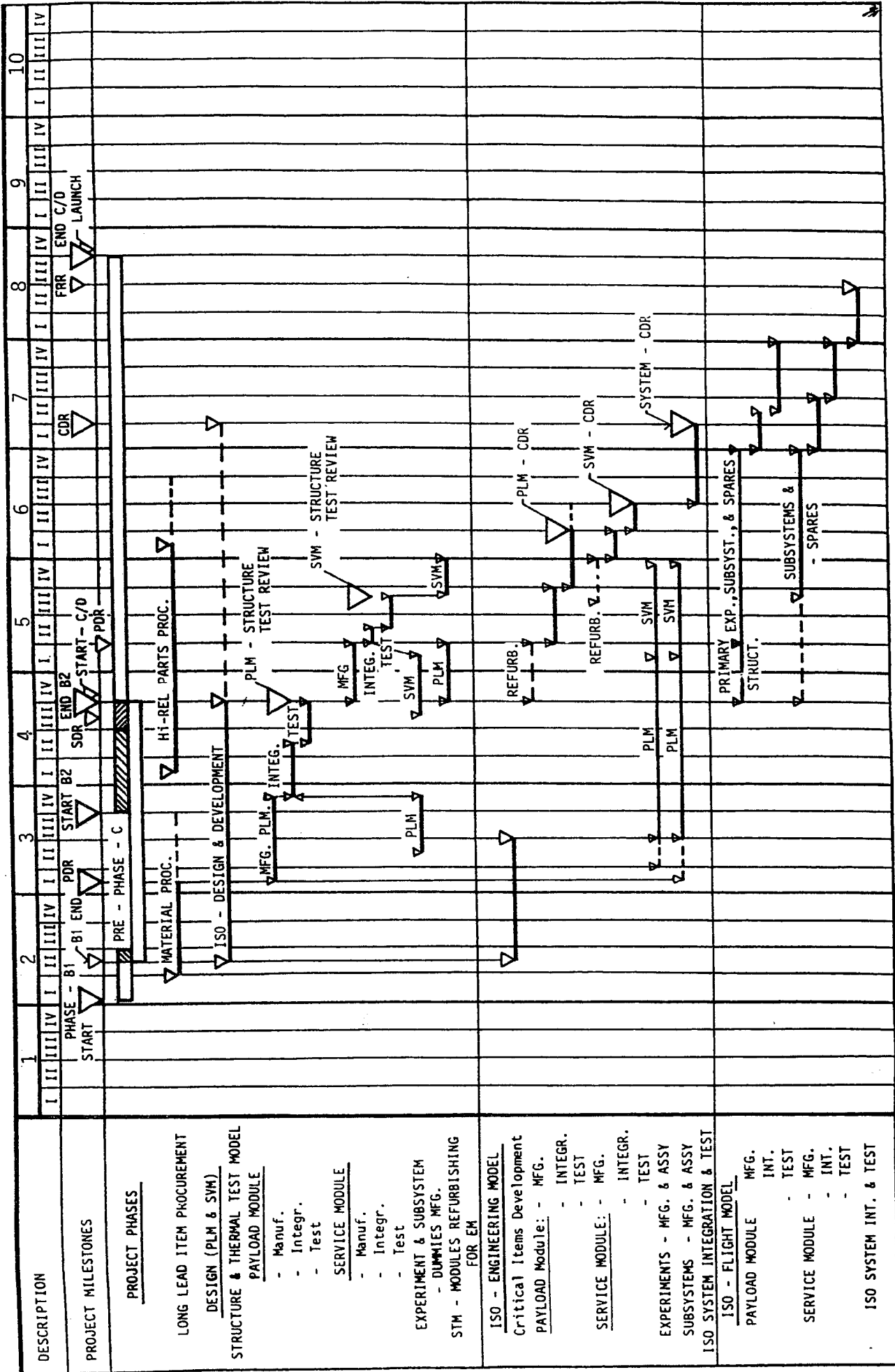


Figure 13.2 I S O PROGRAM MASTER SCHEDULE